ABSTRACT

PHASE NOISE EFFECTS ON OFDM: ANALYSIS AND MITIGATION

by
Songping Wu

Orthogonal frequency division multiplexing (OFDM) is a promising technique which has high spectrum efficiency and the robustness against channel frequency selectivity. One drawback of OFDM is its sensitivity to phase noise. It has been shown that even small phase noise leads to significant performance loss of OFDM. Therefore, phase noise effects on OFDM systems need to be analyzed and methods be provided to its mitigation.

Motivated by what have been proposed in the literature, the exact signal to interference plus noise ratio (SINR) is derived in this dissertation for arbitrary phase noise levels. In a multiple access environment with multiple phase noise, the closed form of bit error rate (BER) performance is derived as a function of phase noise parameters.

Due to the detrimental effects of phase noise on OFDM, phase noise mitigation is quite necessary. Several schemes are proposed to mitigate both single and multiple phase noise. It is shown that, while outperforming conventional methods, these schemes have the performance close to no-phase-noise case. Two general approaches are presented which extend the conventional schemes proposed in the literature, making them special cases of these general approaches. Moreover, different implementation techniques are also presented. Analytical and numerical results are provided to compare the performance of these migitation approaches and implementation techniques.

Similar to OFDM, an OFDM system with multiple antennas, i.e., Multiple Input Multiple Output (MIMO)-OFDM, also suffer severe performance degradation due to phase noise, and what have been proposed in the literature may not be applicable to MIMO-OFDM. Therefore, a new scheme is proposed to mitigate phase noise for

MIMO-OFDM, which provides significant performance gains over systems without phase noise mitigation. This scheme provides a very simple structure and achieves adequate performance with high spectrum efficiency, which makes it very attractive for practical implementations.

PHASE NOISE EFFECTS ON OFDM: ANALYSIS AND MITIGATION

by
Songping Wu

A Dissertation
Submitted to the Faculty of
New Jersey Institute of Technology
in Partial Fulfillment of the Requirements for the Degree of
Doctor of Philosophy in Electrical Engineering

Department of Electrical and Computer Engineering

May 2004

APPROVAL PAGE

PHASE NOISE EFFECTS ON OFDM: ANALYSIS AND MITIGATION

Songping Wu

Dr. Yeheskel Bar-Ness, Dissertation Advisor — Date
Distinguished Professor, Department of Electrical and Computer Engineering, NJIT

Dr. Ali Abdi, Committee Member — Date
Assistant Professor, Department of Electrical and Computer Engineering, NJIT

Dr. Alexander M. Haimovich, Committee Member — Date
Professor, Department of Electrical and Computer Engineering, NJIT

Dr. Zoi-heleni Michalopoulou, Committee Member — Date
Associate Professor, Department of Mathematical Science, NJIT

Dr. Ravi Narasimhan, Committee Member — Date
Assistant Professor, Department of Electrical Engineering, Stanford University

BIOGRAPHICAL SKETCH

Author: Songping Wu

Degree: Doctor of Philosophy

Date: May 2004

Undergraduate and Graduate Education:

- Doctor of Philosophy in Electrical Engineering,
  New Jersey Institute of Technology, Newark, NJ, 2004
- Master of Science in Electrical Engineering,
  Tsinghua University, Beijing, China, 1998
- Bachelor of Science in Electrical Engineering,
  Tsinghua University, Beijing, China, 1996

Major: Electrical Engineering

Presentations and Publications:

Songping Wu and Yeheskel Bar-Ness, "Phase noise mitigation for MIMO-OFDM," *To be sumitted to IEEE Commun. Letter*, 2004.

Songping Wu and Yeheskel Bar-Ness, "OFDM systems in the presence of phase noise: consequences and solutions," *To appear in IEEE Trans. Commun.*, 2004.

Songping Wu and Yeheskel Bar-Ness, "Unified phase noise mitigation approaches in OFDM systems," *To be submitted to IEEE Trans. Wireless Commun.*, 2004.

Songping Wu and Yeheskel Bar-Ness, "On the effect of phase noise on OFDM signals," *To be submitted to IEEE commun. Magzine.*, 2004.

Songping Wu and Yeheskel Bar-Ness, "Computationally Efficient Phase Noise Cancellation Technique in OFDM Systems," *Submitted to Proc. ISSSTA'04*, Sydney, Australia, 2004.

Songping Wu and Yeheskel Bar-Ness, "Multiple phase noise correction for OFDM/SDMA," *Proc. Globecom'03*, San Francisco, California, pp. 1311 –1315, Dec. 2003.

Songping Wu and Yeheskel Bar-Ness, "A new phase noise mitigation method in OFDM systems with simultaneous CPE and ICI correction," *Multi-Carrier Spread-Spectrum for Future Wireless Systems 2003*, Oberpfaffenhofen, Germany, Sep. 2003.

Songping Wu and Yeheskel Bar-Ness, "MC-CDMA performance with multiple phase noise over an uplink correlated rayleigh fading channel," *IST mobile and wireless communications summit 2003*, Aveiro, Portugal, pp. 180 –183, June 2003.

Songping Wu and Yeheskel Bar-Ness, "OFDM channel estimation in the presence of frequency offset and phase noise," *Proc. ICC'03*, Anchorage, Alaska, pp. 3366 –3370, May 2003.

Songping Wu and Yeheskel Bar-Ness, "A phase noise suppression algorithm for OFDM based WLANs," *IEEE Commun. Lett*, vol. 6, pp. 535 –537, Dec. 2002.

Songping Wu and Yeheskel Bar-Ness, "Performance analysis on the effect of phase noise in OFDM systems," *Proc. ISSSTA'02*, Prague, Czech, pp. 133 –138, Sep. 2002.

To my advisor, my friends, my family and people that helped me.

ACKNOWLEDGMENT

It has been my pleasure to be advised by Dr. Yeheskel Bar-Ness, who is an IEEE Fellow and famous in the wireless communications and signal processing field. The extent of his knowledge in wireless communications influenced my research work in so many ways. My future career is sure to benefit. His attitude towards life has taught me many lessons which are especially valuable for a young man who wants to embrace his future.

I am especially grateful to all my committee members, Dr. Ali Abdi, Dr. Alex M. Haimovich, Dr. Zoi-heleni Michalopoulou, and Dr Ravi Narasimhan, for their valuable advice. Their ideas helped improve the quality of this dissertation in many aspects. I am also grateful to my colleagues, Hangjun Chen and Jianming Zhu, at the Center for Communications and Signal Processing Research (CCSPR). The discussions with them were very helpful towards my dissertation work. I extend my thanks to Dr. Ronald S. Kane, Dean of Graduate Studies at New Jersey Institute of Technology, for his helpful advice towards dissertation writings. The support provided to me by National Science Foundation (NSF) under Grant No. CCR-0085846 is gratefully acknowledged.

I am indebted to my wife, Kathy, for her love and encouragement all the way.

TABLE OF CONTENTS

TABLE OF CONTENTS
(Continued)

Chapter **Page**

TABLE OF CONTENTS
(Continued)

Chapter Page

LIST OF TABLES

LIST OF FIGURES

LIST OF FIGURES
(Continued)

Figure **Page**

CHAPTER 1

INTRODUCTION

1.1 Overview

Orthogonal frequency division multiplexing (OFDM) has been widely adopted and implemented in wire and wireless communications, such as digital terrestrial TV broadcasting (dTTB), digital subscriber line (DSL), European high performance local area networks (HIPERLAN) and the IEEE 802.11a standard for wireless local area networks (WLAN) [1–4]. In comparison to single carrier transmission, OFDM is quite effective to eliminate inter-symbol interference (ISI) caused by channel multipath fading while providing high transmission data rate with high spectral efficiency. Moreover, an OFDM receiver becomes relatively simple with a one-tap channel equalizer. Hence, it is very well suited for future high data rate wireless multimedia communications.

The disadvantage of OFDM, however, is its sensitivity to both frequency offset and phase noise. Caused by the frequency difference between the transmitter and the receiver, or by Doppler shift, frequency offset has been thoroughly analyzed and many methods have been proposed for its estimation and correction [5–8]. Unlike frequency offset which is deterministic, phase noise is a random process caused by the fluctuation of the receiver and transmitter oscillators. Phase noise causes leakage of DFT which subsequently destroys the orthogonalities among subcarrier signals, leading to significant performance degradation.

Recent studies have shown that even small phase noise destroys orthogonalities between OFDM subcarrier signals and subsequently gives rise to both common phase error (CPE) and intercarrier interference (ICI), causing significant performance loss [9–15].

1.2 Phase Noise Model

1.2.1 Principle Description

Phase noise $\phi(t)$, generated at both transmitter and receiver oscillators, can be described as a continuous Brownian motion process or a random Wiener process given by

$$\phi(t) = \int_0^t u(t)\, dt \tag{1.1}$$

which has zero mean and variance $2\pi\beta t$, where β denotes the phase noise linewidth, i.e., the frequency spacing between 3-dB points of its Lorentzian power spectral density function [9,11,16]. Furthermore, it can be shown that

$$E\left\{[\phi(t) - \phi(t+\tau)]^2\right\} = 2\pi\beta\,|\tau| \tag{1.2}$$

As a random Wiener process, phase noise has independent Gaussian increments and its power is a monotonically increasing function of time. This indicates that its power could be infinitely large as time increases [16]. However, if restricted to a finite period, phase noise can be modeled as a filtered Gaussian random variable [10,13,14].

To better characterize phase noise, Demir et al. [17] developed a unifying theory using a nonlinear method which proves to be more accurate in describing phase noise. With such method [17, Remark 7.1], $\phi(t)$ is shown to become, asymptotically in time, a Gaussian random process with a constant mean, a variance that increases linearly with time, and the correlation function that satisfies $E[\phi(t)\phi(t+\tau)] = \min\left[E(\phi^2(t)), E(\phi^2(t+\tau))\right]$.

1.2.2 Discrete Phase Noise Model

Consider an N-subcarrier OFDM system with symbol duration T and cyclic prefix length N_g. As indicated in [18], the aforementioned discussion suggests describing

phase noise by a discrete Markov process which, for the nth subcarrier of the mth symbol of an OFDM system, is given by

$$\begin{aligned}\phi_m(n) &= \phi_{m-1}(N-1) + \sum_{i=-N_g}^{n} u\left[m(N+N_g)+i\right] \\ &= \sum_{i=0}^{m(N+N_g)+N_g+n} u\left(i\right) \end{aligned} \tag{1.3}$$

where $u(i)$'s denote mutually independent Gaussian random variables with zero mean and variance $\sigma_u^2 = 2\pi\beta T/N$. In particular, equation (1.3) reduces to $\phi_0(n) = \sum_{i=-N_g}^{n} u\left(i\right)$ for $m = 0$ ($\phi_m(n) = 0$, when $m < 0$).

The correlation function of $\phi_m\left(n\right)$ within the same symbol is shown to be [9,17]

$$\begin{aligned}&E\left[\phi_m\left(n\right)\phi_m^*\left(l\right)\right] \\ &= \frac{2\pi\beta T}{N} \cdot \min\left(m\left(N+N_g\right)+n, m\left(N+N_g\right)+l\right)\end{aligned} \tag{1.4}$$

With OFDM modulation, phase noise modifies the system by multiplying each received signal, in the time domain, by a random rotation factor $e^{j\phi_m(n)}$, whose correlation function, for $n \geq l$, is given by

$$\begin{aligned}&E\left[e^{j\phi_m(n)}e^{-j\phi_m(l)}\right] \\ &= E\left[e^{j\sum_{i=m(N+N_g)+l+1}^{m(N+N_g)+n} u(i)}\right] = \prod_{i=1}^{n-l} \Psi\left(v_i|_{v_i=1}\right)\end{aligned} \tag{1.5}$$

where the characteristic function of the random Gaussian variable $u\left(i\right)$, is shown to be $\Psi\left(v_i\right) = E\left[e^{jv_iu(i)}\right] = e^{-\frac{v_i\sigma_u^2}{2}} = e^{-\pi\beta T v_i/N}$ [19], which further simplifies (1.5) to

$$E\left[e^{j\phi_m(n)}e^{-j\phi_m(l)}\right] = e^{-\pi\beta T(n-l)/N} \tag{1.6}$$

For arbitrary n and l, (1.6) is readily generalized to

$$E\left[e^{j\phi_m(n)}e^{-j\phi_m(l)}\right] = e^{-\pi\beta T|n-l|/N} \tag{1.7}$$

Note that, from (1.3) and (1.4), phase noise is a non-stationary random process with its correlation function changing with time m. Nevertheless, the exponential process of random phase noise, shown in (1.7), is stationary.

1.3 OFDM System Model

1.3.1 OFDM with Phase Noise

Since the effects of phase noise on OFDM systems are of particular interest, perfect frequency and timing synchronizations are assumed. Thus, in the presence of phase noise, the OFDM system model is shown in Fig. 1.1.

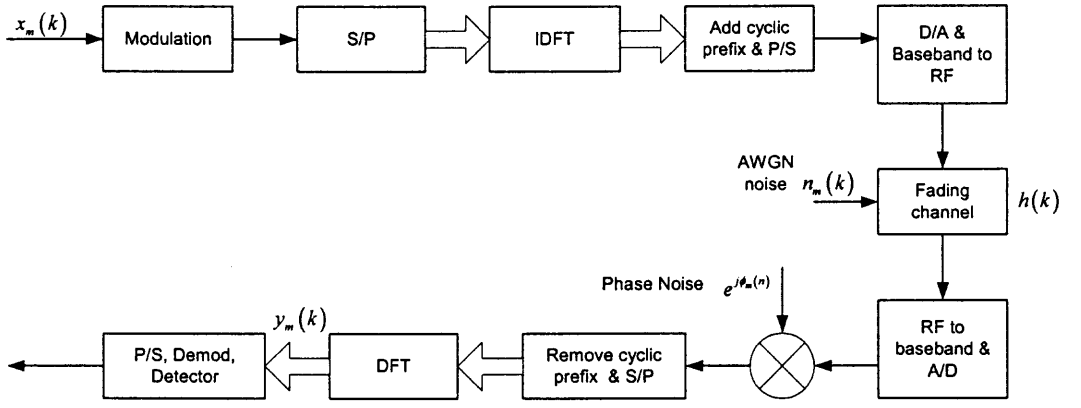

Figure 1.1 OFDM system model in the presence of phase noise

1.3.2 OFDM Transmitter

The principle of OFDM is to transform the incoming data symbol into N low-rate parallel signals $\{x_m(k)\}_{k=0}^{N-1}$, which modulates a set of subcarriers using inverse digital Fourier transform (IDFT) so as to obtain the time-domain signals. A cyclic prefix with length N_g is then added to these time-domain signals to combat inter-symbol interference (ISI) caused by channel multipath fading effects and enables simple channel equalization at the receiver. The resulting baseband signal at the transmitter can then be expressed by

$$s_m(n) = \frac{1}{\sqrt{N}} \sum_{k=0}^{N-1} x_m(k) e^{j2\pi nk/N} \tag{1.8}$$

where n ranges from $-N_g$ to $N-1$.

1.3.3 OFDM Receiver

Due to multipath fading, AWGN and phase noise, the received signal can be written as

$$r_m(n) = e^{j\phi(n)} \left[s_m(n) \otimes \mathcal{F}^{-1}(h(k)) \right] + n_m(n) \tag{1.9}$$

where $\otimes$ and $\mathcal{F}^{-1}(\cdot)$ denote the circular convolution and IDFT respectively while $n(n)$ indicates the AWGN noise with zero mean and variance σ^2. For a high-rate OFDM system, channel is often assumed invariant within a block and the first symbol of each block is used for channel estimation purpose[1]. A typical example is the IEEE 802.11a WLAN standard given in [4]. Therefore, $h(k)$ is not a function of symbol index m as long as these symbols are included within the same block. After removing the cyclic prefix and taking the length-N DFT at the receiver, in terms of (1.9), the received kth subcarrier signal of the mth symbol is expressed by [20, 21]

$$\begin{aligned} y_m(k) &= \mathcal{F}\left[r_m(n)\right] \\ &= x_m(k)h(k)c_m(0) + \underbrace{\sum_{\substack{l=0 \\ l\neq k}}^{N-1} x_m(l)h(l)c_m(l-k)}_{ICI_m(k)} + n_m(k) \end{aligned} \tag{1.10}$$

where $x_m(k)$ and $h(k)$ are the corresponding subcarrier data signal and the channel fading gain in the frequency domain, respectively; $n_m(k)$, which is the DFT of $n_m(n)$, denotes the AWGN noise in the frequency domain with zero mean and variance

[1] We thereby assume invariant channel within an OFDM block in the context of the whole dissertation.

σ^2. The transmitted signals $x_m(k)$ are assumed to be mutually independent with $E\left[|x_m(k)|^2\right] = \varepsilon_x$, while the energy of the channel gain $h(k)$ is normalized to unity, namely $E\left[|h(k)|^2\right] = 1$. Finally $c_m(p)$ is given by

$$c_m(p) = \frac{1}{N}\sum_{n=0}^{N-1} e^{j2\pi np/N + j\phi_m(n)} \tag{1.11}$$

Note that, in terms of (1.11), $c_m(p)$ is actually the IDFT of $e^{j\phi_m(n)}$ with $c_m(p) = c_m(p \bmod N)$.

1.3.4 Phase Noise Effects

Equation (1.10) suggests that the received signal $y_m(k)$ is the weighted sum of $x_m(k)h(k)$ plus AWGN noise, wherein the weighting coefficients are denoted by $\{c_m(p)\}_{p=0}^{N-1}$. Phase noise destroys orthogonalities among OFDM subcarrier signals and leads to two detrimental effects:

1. Common phase error (CPE) denoted by $c_m(0)$, which indicates the phase rotation of the desired signal;

2. Intercarrier interference (ICI) represented by the second term of (1.10) as a function of $\{c_m(p)\}_{p=1}^{N-1}$, which depicts the interference on the desired subcarrier signal by all the other subcarrier signals of the same OFDM symbol.

The effects of phase noise on OFDM signals are illustrated in Fig. 1.2, where phase noise corrupts the 16-QAM constellations with both CPE and ICI. It's shown that phase noise forces the desired signal into a wrong decision area, and worsens the BER performance accordingly. As indicated in [22], when phase noise variance is of the order of 10^{-1}, phase noise mainly contributes to CPE which plays a more important role in system performance compared with ICI, while for large phase noise, ICI becomes the major impairment on the system performance.

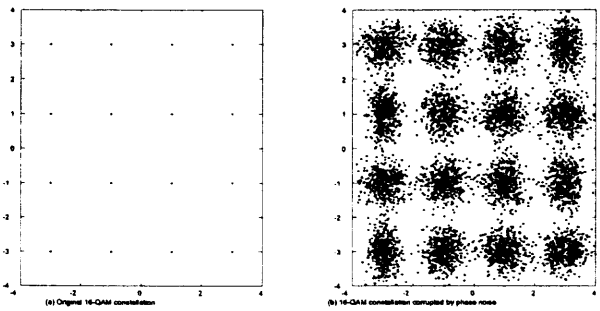

Figure 1.2 Phase noise effects on 16-QAM modulated OFDM signals (a) original 16-QAM constellations (b) 16-QAM constellations corrupted by phase noise

1.4 Conclusions

Both effects of phase noise lead to significant performance loss of OFDM systems, and consequently raise interests in two aspects.

First, one would like to know how the performance of an OFDM system is related to phase noise, and in particular, understand the system behavior as a function of various parameters, such as phase noise, number of subcarriers, transmission data rate etc., for both single-user and multi-user cases.

Second, there have been some methods in the literature for mitigating phase noise. It's of interest to propose new schemes which further improve the system performance. Extension of such schemes into the multi-user case is also desirable since mitigation methods have never been proposed for the case of multiple phase noise.

These two issues will be our main tasks throughout this dissertation.

CHAPTER 2

PERFORMANCE ANALYSIS OF OFDM SYSTEMS IN THE PRESENCE OF PHASE NOISE

2.1 Introduction

Phase noise causes leakage of DFT which subsequently destroys the orthogonalities among subcarrier signals, causing both CPE and ICI. CPE results in signal phase rotation which stays invariant within an OFDM symbol, while ICI introduces interferences to each subcarrier of a certain symbol from all the other subcarriers of that symbol and therefore exhibits noise-like characteristics.

Phase noise in OFDM systems has been analyzed in many papers [9–15]. The original work done in [9] has successfully derived an expression of OFDM system degradation in a closed form, but only valid for small phase noise and large number of subcarriers. In [10] and [12], the characterization of phase noise and its effects on OFDM have also been carefully studied and the BER performance has been further analyzed. In [15] a different approach was proposed that has provided the upper and lower bounds on signal to noise plus interference ratio (SINR). In this approach, by deriving a compact form for SINR bounds, it was easy to show the dependence of OFDM system performance on some of its critical parameters, such as phase noise linewidth and number of subcarriers etc.. Nevertheless, the analytical results in [10, 12, 15] have assumed that phase noise variance is much less than unity, and are only suitable for AWGN channels even though some simulation results has been provided over multipath fading channels. On the other hand, in [11], the robustness of modulation methods to phase noise has been studied in a general OFDM system. The effect of phase noise bandwidth to subcarrier spacing ratio on system performance, has been analyzed in [13] and further extended in [14] to include the effect of the number

of subcarriers on system performance both with and without phase noise correction. The approaches in [11, 13, 14], however, do not provide, even for AWGN channels, a closed form analytical result that show the exact quantitative relations between various parameters of an OFDM system and its performance; therefore computer simulation was necessary to illustrate these relations.

In [21], we have derived the exact SINR expression in a closed form for arbitrary phase noise level and various numbers of OFDM subcarriers. SINR is expressed as a function of various critical system parameters and provides a quantitative understanding of how system behavior changes with a certain parameter. This enables one to determine under which condition phase noise can be treated as small and consequently leads to adequate mitigations; and what are the proper parameter settings for a specific OFDM system which provides adequate performance levels in the presence of phase noise .

The chapter is organized as follows. In Section 2.2, the exact performance analysis of the phase noise effects is provided with arbitrary phase noise level and number of subcarriers; By introducing SINR in a closed form in Section 2.3, OFDM performance is precisely described as a function of various system parameters in a multipath fading environment. In Section 2.4, the small phase noise assumption is given and some approximation results are obtained which fit well with those in the literature. Simulation results are provided in Section 3.5 to illustrate the effectiveness of the derived expression in system evaluation. This chapter is concluded in Section 3.6.

2.2 Exact SINR Expression

Many approaches of system analysis in the literature are based on small phase noise levels and large number of subcarriers. Although this assumption may be true in practice, a thorough and exact evaluation without such restrictions will not only

extend those analysis, but also provide an in-depth insight of phase noise effects on the actual system performance by introducing the latter as a function of critical system parameters. In particular, with such exact analysis, it's possible to determine what is an acceptable level of phase noise for a certain OFDM system and how it can be designed to avoid severe degradation in the presence of such noise. Therefore in our work, we assume a general OFDM system where phase noise variance is not necessarily much less than unity and the number of subcarriers is not necessarily very large. Since SINR is a very important indicator of system performance, its exact expression will be found and used in our analysis.

From (1.10), SINR can be given by

$$\Gamma = \frac{\varepsilon_x E[|c_m(0)|^2]}{E[|ICI_m(k)|^2] + \sigma^2} \tag{2.1}$$

where, as described in Section 1.3.3, the conclusion $E\left[|h(k)|^2\right] = 1$ is used. It is also assumed that the OFDM subcarrier signals $\{x_m(k)\}_{k=0}^{N-1}$ are mutually independent random variables with zero mean and variance ε_x. From the definition in (1.10), we have

$$E[|ICI_m(k)|^2] = \varepsilon_x \sum_{p=1}^{N-1} E\left[|c_m(p)|^2\right] \tag{2.2}$$

Note that, for a slow fading channel as described in Section 1.3.3, given $c_m(0)$ and $h(k)$, one can see from (2.1) and (2.2) that the SINR expression has the same form as the one we have obtained [15] for AWGN channels, provided that the transmitted signals are independent and the energy of channel response is normalized to unity. From Appendix A, the energy of $c_m(p)$ is given by (A.7)

$$\begin{aligned} & E\left[|c_m(p)|^2\right] \\ = \; & \frac{1}{N^2}\left\{2\,\mathrm{Re}\left(\frac{d_p^{N+1} - (N+1)d_p + N}{(d_p-1)^2}\right) - N\right\} \end{aligned} \tag{2.3}$$

where $d_p = e^{j\frac{2\pi p}{N} - \frac{\pi\beta}{R}}$, with $R = N/T$ denoting the transmission data rate. Equation (2.3) shows the dependence of the energy of $c_m(p)$ on phase noise linewidth β, number of subcarriers N and transmission data rate R. Substituting (2.3) into (2.2) yields

$$\begin{aligned} & E[|ICI_m(k)|^2] \\ = & \frac{\varepsilon_x}{N^2} \sum_{p=1}^{N-1} \left\{ 2\,\mathrm{Re}\left(\frac{d_p^{N+1} - (N+1)d_p + N}{(d_p - 1)^2} \right) - N \right\} \end{aligned} \tag{2.4}$$

In light of the definition of d_p, we have $d_p^* = d_{N-p}$, with which it can be shown that the sum of $\frac{d_p{}^{N+1} - (N+1)d_p + N}{(d_p-1)^2}$ in (2.4) is real, hence

$$\begin{aligned} & E[|ICI_m(k)|^2] \\ = & \frac{\varepsilon_x}{N^2} \sum_{p=1}^{N-1} \left\{ 2\frac{d_p^{N+1} - (N+1)d_p + N}{(d_p - 1)^2} - N \right\} \end{aligned} \tag{2.5}$$

Substituting (2.3) and (2.5) into (2.1), we obtain the exact SINR expression,

$$\Gamma = \frac{2\frac{d_0^{N+1} - (N+1)d_0 + N}{(d_0-1)^2} - N}{\sum_{p=1}^{N-1} \left\{ 2\frac{d_p{}^{N+1} - (N+1)d_p + N}{(d_p-1)^2} - N \right\} + N^2/\gamma_s} \tag{2.6}$$

where $\gamma_s = \varepsilon_x/\sigma^2$ denotes the signal to noise ratio per subcarrier. As shown in next section, both (2.3) and (2.6) indicate that, in the presence of phase noise, several parameters affect OFDM system performance, resulting in severe performance degradation which is intolerable in practice. In case of perfect phase synchronization, $c_m(p)$ becomes Dirac delta function, i.e., $c_m(p) = 0$ for $p \neq 0$, and the SINR expression of (2.6) reduces to SNR, i.e., $\Gamma = \gamma_s$.

2.3 Phase Noise Effects

In the presence of phase noise, equation (2.6) shows that SINR is a function of various system parameters, β, N, T, γ_s and their corresponding ratios. These relations are separately depicted in Fig. 2.1-2.5.

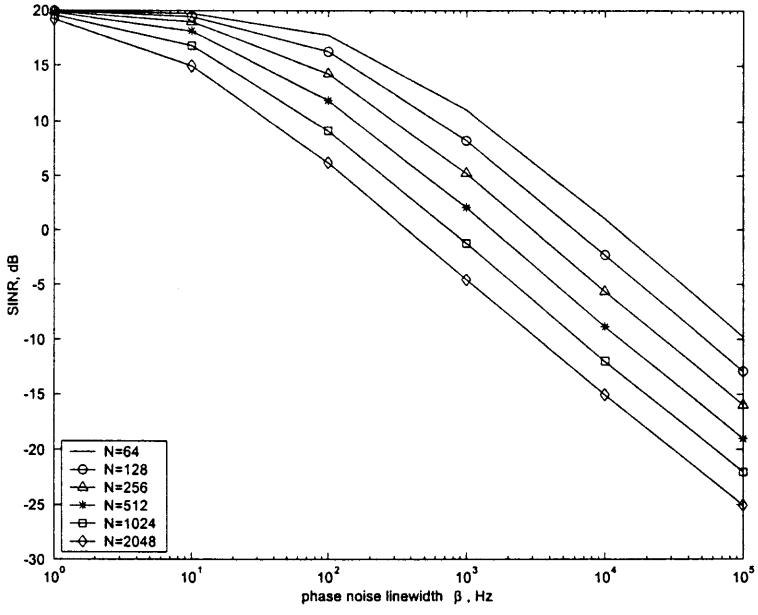

Figure 2.1 The effect of phase noise linewidth on system performance, where SNR=20dB and $R = 10^6$ samples/s

1) It is well known that OFDM system performance with imperfect oscillators, is strongly dependent on phase noise linewidth β [14]. As shown in Fig. 2.1, the larger β, the worse is SINR, degrading logarithmically linear as a function of phase noise linewidth β for $\beta \geq 10^2$ Hz. Hence, as we stated earlier, the best way to eliminate the detrimental effects of phase noise is to improve the oscillator stability and thus decrease the phase noise linewidth.

2) It's quite straightforward to see that larger number of subcarriers N leads to worse system performance due to the smaller subcarrier spacing distance, hence more sensitive to phase noise. In particular, Fig.2.2 suggests that, when β/R ratio is of the order of 10^{-3} or less, doubling N always causes about 3 dB loss of SINR for

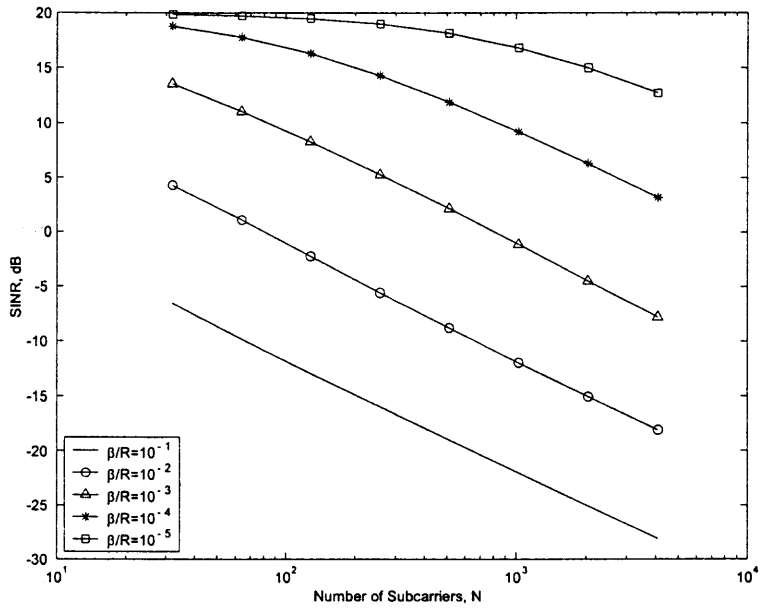

Figure 2.2 The effect of number of subcarriers N on SINR, where SNR=20dB

all N values. This implies that, when β/R is below a certain level, SINR becomes inversely proportional to the number of subcarriers N.

3) Higher transmission data rate R results in better system performance. In fact, the transmission data rate to phase noise linewidth ratio R/β is of our interest. Fig. 2.3 shows that SINR has a limiting low value for small R/β regardless of SNR values. This can also be verified from (2.6) by letting R/β approach zero, i.e.,

$$\Gamma|_{R/\beta=0} = \frac{\gamma_s}{(N-1)\gamma_s + N} \tag{2.7}$$

In particular, for very large SNR, or γ_s, the limit of (2.7) is readily approximated as $1/(N-1)$. This suggests that for large phase noise (thus low R/β), high SNR does not help the performance, as in this case, the ICI caused by phase noise is dominant over AWGN noise. Therefore, a well designed system should have a reasonable R/β ratio leading to adequate performance. In particular, (2.6) shows that SINR becomes SNR when R/β increases without limit, i.e.,

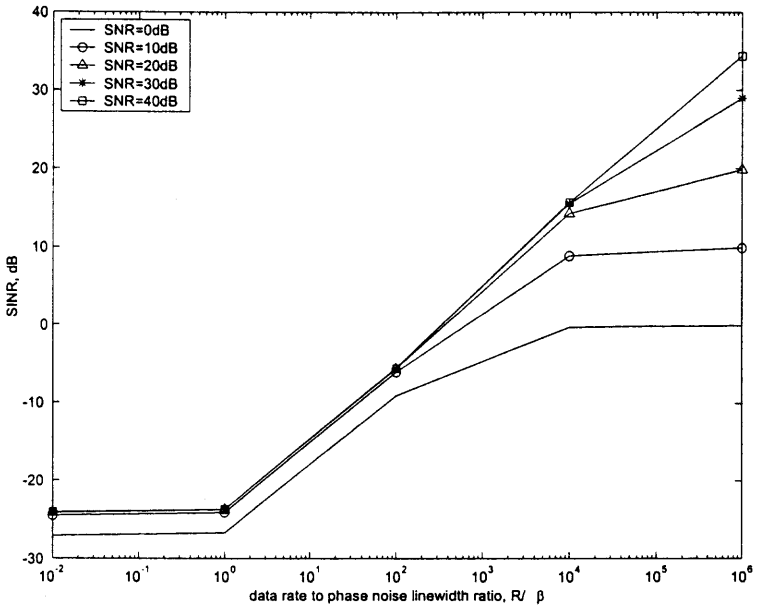

Figure 2.3 SINR as a function of R/β, where N=256

$$\Gamma|_{R/\beta=\infty} = \gamma_s \tag{2.8}$$

This makes sense by noticing that when R/β goes to infinity, the system is equivalent to one without phase noise.

4) From (2.6), SINR is strongly dependent on $d_p = e^{j\frac{1}{N}(2\pi p - \frac{\pi\beta N}{R})}$, depicted in Fig. 2.4. For high data rate R, when β is very small in comparison to the subcarrier spacing R/N, i.e., $\beta N/R$ is of the order of 10^{-5} or less, phase noise becomes negligible and it is equivalent to non-phase-noise case. In fact, when $\beta N/R$ is between 10^{-5} and 10^{-2}, phase noise is small and thus effective schemes are available for its mitigation.

5) Higher SNR leads to the better performance in the presence of phase noise. But systems with high SNR are more sensitive to phase noise, as shown in Fig. 2.5. For high phase noise levels with $\beta N/R \geq 1$, SINR degradation exceeds the value of SNR itself. This implies that the ICI overwhelms the desired signals. In particular, if we use phase noise mitigation methods based on CPE estimation, as indicated in [14],

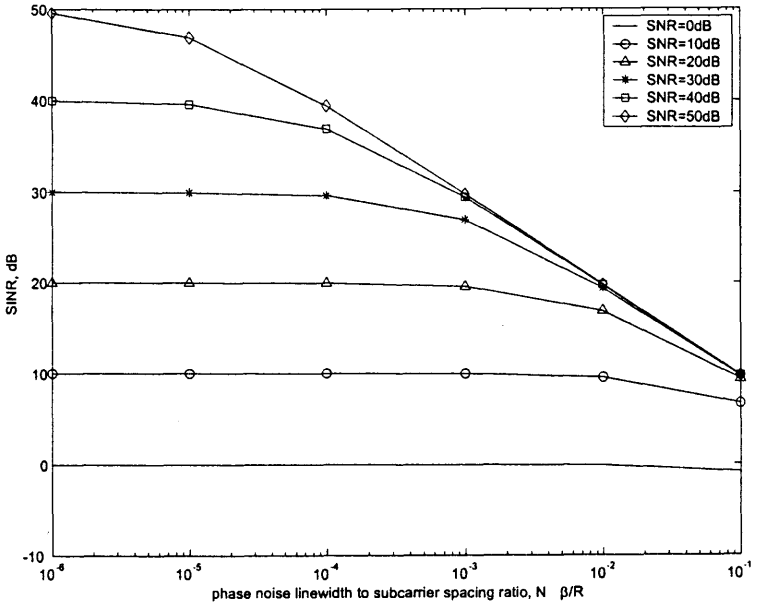

Figure 2.4 SINR as a function of phase noise linewidth to subcarrier spacing ratio $\beta N/R$

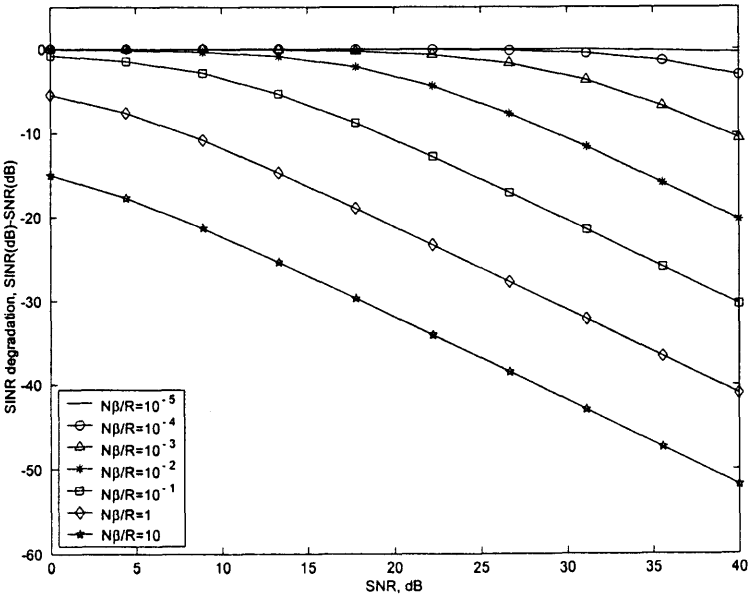

Figure 2.5 SNR as a function of SINR degradation

this does not improve or even makes the performance worse with high phase noise levels. It can be seen from Fig. 2.5 that, When $10^{-2} \leq \beta N/R \leq 1$, though system loss does not exceed the value of SNR, it is pretty high, e.g., SINR degrades 20dB for $\beta N/R = 10^{-1}$ when SNR equals 30dB. In this case, phase noise correction can be applied but performance requirement may not be guaranteed.

2.4 Small Phase Noise Approximation

In case of small phase noise, the SINR expression of OFDM systems becomes simpler than that in (2.6). In the literature, small phase noise condition was presented by either the absolute value of phase noise or the phase noise variance which is much less than unity. The former definition is more strict than the latter, and is actually a special case of the latter. In order to distinguish these two definitions, the former is referred to as *small phase noise* while the latter as *small phase noise variance.*

2.4.1 Small Phase Noise

Phase noise is small when its absolute value is much less than unity, namely, $|\phi_m(n)| \ll 1$. With this definition, the approximation $e^{j\phi_m(n)} \approx 1 + j\phi_m(n)$ holds [10, 13]. Applying this approximation to $c_m(p)$, we have [15]

$$\begin{aligned} e^{-j\phi_m(0)} c_m(0) &= \frac{1}{N} \sum_{n=0}^{N-1} e^{j[\phi_m(n) - \phi_m(0)]} \\ &\simeq 1 + \frac{j}{N} \sum_{n=0}^{N-1} (N-n)\, u(n) \end{aligned} \tag{2.9}$$

and for $p \neq 0$

$$\begin{aligned} e^{-j\phi_m(0)} c_m(p) &= \frac{1}{N} \sum_{n=0}^{N-1} e^{j[\phi_m(n) - \phi_m(0)] + j2\pi pn/N} \\ &\simeq 1 + \sum_{n=0}^{N-1} u(n) \sum_{i=n}^{N-1} e^{j2\pi pi/N} \end{aligned} \tag{2.10}$$

Then in terms of (2.9) and (2.10), after some algebraic manipulations, we have, for large N, [15]

$$\begin{aligned} E\left[|c_m(0)|^2\right] &= E\left[\left|e^{-j\phi_m(0)}c_m(0)\right|^2\right] \\ &= E\left[\left|1+\frac{j}{N}\sum_{n=0}^{N-1}(N-n)\,u(n)\right|^2\right] \\ &= 1+\frac{2\pi\beta T}{3} \end{aligned} \tag{2.11}$$

and

$$\begin{aligned} E\left[|c_m(p)|^2\right] &= E\left[\left|e^{-j\phi_m(0)}c_m(p)\right|^2\right] \\ &= E\left[\left|1+\sum_{n=0}^{N-1}u(n)\sum_{i=n}^{N-1}e^{j2\pi pi/N}\right|^2\right] \\ &= \frac{\pi\beta T}{N^2\sin^2(p\pi/N)} \end{aligned} \tag{2.12}$$

where β is defined in Section 1.2.1 as the two-sided 3dB linewidth[1]. Substituting (2.11) and (2.12) into the definition of the SINR (2.1) yields

$$\Gamma_1 = \frac{3R/N+2\pi\beta}{\frac{3\pi\beta}{N^2}\sum_{m=1}^{N-1}\frac{1}{\sin^2(m\pi/N)}+\frac{3R}{N}/\left(\frac{\varepsilon_x}{\sigma^2}\right)} \tag{2.13}$$

In terms of the inequalities

$$\sum_{p=1}^{N/2-1}\frac{2}{(p\pi/N)^2}+1 \le \sum_{p=1}^{N-1}\frac{1}{\sin^2(p\pi/N)} \le \sum_{p=1}^{N/2-1}\frac{2}{(2p/N)^2}+1$$

the corresponding upper and lower bounds of SINR were further derived in [15], as

$$\Gamma_{1\_upper} = \frac{3R/N+2\pi\beta}{\frac{6\beta}{\pi^2}\sum_{p=1}^{N/2-1}\frac{1}{(p\pi/N)^2}+\frac{3\pi\beta}{N^2}+\frac{3R}{N}/\left(\frac{\varepsilon_x}{\sigma^2}\right)} \tag{2.14}$$

[1]Phase noise linewidth β is defined as the one-sided 3dB linewidth in [15]. Due to this, equation (2.11) and (2.12) are different from the references by a factor of two.

and

$$\Gamma_{1\_lower} = \frac{3R/N + 4\pi\beta}{\frac{\pi^3\beta}{8} + \frac{3\pi\beta}{N^2} + \frac{3R}{N}/\left(\frac{\varepsilon_x}{\sigma^2}\right)} \tag{2.15}$$

2.4.2 Small Phase Noise Variance

Small phase noise can also be interpreted as phase noise whose variance is much less than unity. In other words, $N\sigma_u^2 = 2\pi\beta T = 2\pi\beta N/R$ is much less than unity.

In this case, equation (2.6) can be further simplified. Using the approximation $e^x \approx \sum_{k=0}^{3} \frac{1}{k!}x^k$ for small x with $x = -\sigma_u^2/2$ and $x = -(N+1)\sigma_u^2/2$, respectively, equation (2.3) further yields (see Appendix B for details)

$$\begin{aligned} & E\left[|c_m(0)|^2\right] \\ = \; & 1 - \frac{(N+1)(N+2)}{6N}\sigma_u^2 \end{aligned} \tag{2.16}$$

For large subcarrier number N, (2.16) becomes

$$E\left[|c_m(0)|^2\right] = 1 - \frac{\pi\beta N}{3R} \tag{2.17}$$

Considering the difference of phase noise linewidth β definition in [9] (one-sided linewidth) and in the Section 1.2.2 of this dissertation (two-sided linewidth), the result of (2.17) is exactly the same as that derived in [9]. In Appendix B, equation (B.5) further shows that the total energy of all phase noise components $c_m(p)$ is equal to unity, from which, together with (2.2) and (2.17), it follows that

$$E[|ICI_m(k)|^2] = \frac{\pi\beta N\varepsilon_x}{3R} \tag{2.18}$$

Substituting (2.17), (2.18) into (2.1), we end up with

$$\Gamma_2 = \frac{1 - \frac{\pi\beta N}{3R}}{\frac{\pi\beta N}{3R} + \frac{1}{\gamma_s}} \tag{2.19}$$

Remark 1 *It's quite straightforward to see that small phase noise in Section 2.4.1 always leads to small phase noise variance as defined in Section 2.4.2, but the converse is not true. That is, small phase noise variance is a necessary condition of small phase noise. In other words, the discussion in Section 2.4.2 is more general than that in Section 2.4.1. Hence, the results in Section 2.4.1 are also applicable for the condition held in Section 2.4.2.*

Remark 2 *In Section 2.4.1, the approximation was made by dropping those high-order terms, which are random and may not be zero mean. Moreover, it occurred before the ensemble average. Therefore, the ensemble average could possibly accumulate the errors caused by the approximation. In particular, the energy of* $c_m(0)$ *should always be less than unity while in (2.11) it was derived to be a little larger than unity, due to the approximation error spread after ensemble average. Whereas, the approximation in Section 2.4.2 was carried on after the calculation of statistics has been done and therefore does not give rise to such a problem. Hence, the derived SINR expression in Section 2.4.1 could be less accurate than that in Section 2.4.2.*

In summary, the derived SINR form in Section 2.4.2 is more compact than that in Section 2.4.1 and more suitable in many applications with its relatively lower requirement on phase noise levels, while the upper and lower bounds given in Section 2.4.1 is specially useful in designing an OFDM system in the presence of small phase noise.

2.5 Conclusions

In this chapter, the phase noise effects on OFDM signals have been carefully analyzed. The derived exact closed-form SINR expression has provided an in-depth insight of

phase noise effects on the actual system performance by introducing the SINR as a function of critical system parameters, such as phase noise linewidth β, number of subcarriers N, duration of symbol period T, and SNR γ_s. It has been further demonstrated that the derived SINR expression can be further simplified by introducing either small phase noise assumption, or the assumption of small phase noise variance. the upper and lower SINR bounds have been derived for the case of small phase noise; and with small phase noise variance, it has been shown that the simplified result using suitable approximation coincides with what has been done in the literature.

CHAPTER 3

PHASE NOISE MITIGATION

3.1 Introduction

Due to its severe effects on OFDM system performance, phase noise mitigation should be considered in practice. As introduced in the previous chapter, there is no guarantee of the effectiveness of any mitigation schemes in case of large phase noise. In fact, system performance with large phase noise may not be improved and, in many cases, become even worse after phase noise mitigation. Nevertheless, it was shown in the literature [10, 20, 23], that mitigation is quite effective for small phase noise levels (phase noise variance is much less than unity, or more specifically, as we discussed earlier, $\beta N/R$ is of the order of 10^{-2} or less).

To compensate for phase noise, several methods have been proposed in [10, 13, 20, 23, 24] and references therein. These methods can be categorized into time-domain [10, 24] and frequency-domain approaches [13, 20, 23].

Time domain approaches aim to eliminate the multiplicative phase noise before applying digital Fourier transform (DFT) at the receiver. This can be achieved by extracting a single pilot subcarrier signal from each OFDM symbol to drive a phase lock loop (PLL) for phase noise mitigation [10]. Despite its low cost, this method requires a special pilot pattern with pilots inserted in the middle of the bandwidth which is not feasible in practice. Another time-domain method proposed in [24] interprets time domain phase noise using orthogonal transforms (e.g., discrete cosine transform (DCT)), and mitigates phase noise by means of the recovery of DCT-based real-value waveforms. This method is quite effective when dealing with linear phase shift, but may not be spectrally efficient in case of random phase noise, as it requires

a large number of pilot signals for adequate performance. More importantly, in case of fading channels, the effectiveness of this method has never been examined.

Frequency domain methods requires post-DFT processing which corrects CPE and/or ICI. This proves to be feasible in practice regardless of pilot patterns or channel environments. Hence, it is of our interest to study the performance of various methods in the frequency domain. A conventional frequency domain method, as introduced in [13,23] and references therein, directly compensates for CPE or its phase. However, this method has some drawback as it neglects ICI, the important contribution of phase noise. Therefore, it is possible to further suppress phase noise by considering both the CPE and ICI.

This chapter is organized as follows. Section 3.2 presents the conventional CPE correction (CPEC) method, which is then extended to a new phase noise suppression (PNS) algorithm in Section 3.3 by estimating CPE and approximating ICI as additive noise to achieve the minimum mean square error (MMSE) for signal detection. In Section 3.4, an alternative approach is proposed, which, with the estimates of phase noise parameters, directly compute the values of both CPE and ICI and cancel them accordingly. Numerical results are presented in Section 3.3 and 3.4 to demonstrate the effectiveness of the proposed methods in comparison to the conventional methods. This chapter is concluded in Section 3.5.

3.2 Conventional CPE Correction (CPEC) Method

The conventional CPE correction (CPEC) method was introduced in [23] where the phase of CPE is estimated and compensated for. This approach is feasible since for small phase noise, the effect of CPE amplitude can thus be neglected as it is approximately unity. Nevertheless, as reported in [20], directly estimating CPE saves computational complexity needed for extracting its phase from pilot signals, and results in an improved estimation accuracy and hence better receiver performance.

Let $\acute{n}_m(k)$ denote ICI plus AWGN noise term $\sum_{\substack{l=0 \\ l\neq k}}^{N-1} x_m(l)h(l)c_m(l-k)+n_m(k)$ of (1.10). Equation (1.10) is then rewritten as

$$y_m(k) = x_m(k)h(k)c_m(0) + \acute{n}_m(k) \tag{3.1}$$

In the sequel, we use the estimate of $c_m(0)$ obtained by [20]

$$\begin{aligned} & \hat{c}_m(0) \\ = & \arg\min_{c_m(0)} \sum_{k\in P} \|y_m(k) - x_m(k)h(k)c_m(0)\|^2 \\ = & \frac{\sum_{k\in P} y_m(k)x_m^*(k)h^*(k)}{\sum_{k\in P} |x_m(k)h(k)|^2} \end{aligned} \tag{3.2}$$

where P represents the set of N_p pilot signals. Channel fading gain $h(k)$ can be obtained via OFDM channel estimation [25] using the preamble of the transmitted block,

$$y_0(k) = x_0(k)h(k)c_0(0) + \acute{n}_0(k) \tag{3.3}$$

with $c_0(0)$ denoting CPE from the preamble symbol. Equation (3.3) implies that, in the presence of phase noise, channel estimation actually gives $\hat{h}(k)$, the estimate[1] of $h(k)c_0(0)$, indicating an increase of channel estimation errors. Correspondingly, when using the channel estimate $\hat{h}(k)$ to estimate $c_m(0)$ in (3.2), it yields the estimate of $c_m(0)/c_0(0)$, which compensates, to some extent, for extra channel estimation errors caused by phase noise. From this standpoint, CPE estimation is not only used to correct phase rotation error, but also helps reduce extra channel estimation errors introduced by random phase noise.

[1]Hereinafter, the superscript $\hat{}$ is used to indicate the estimation results.

The detected data bit $\hat{x}_m(k)$ can be obtained from the CPE-corrected signal

$$\hat{x}_m(k) = \hat{c}_m^{-1}(0) y_m(k) \tag{3.4}$$

3.3 Phase Noise Suppression (PNS) Algorithm

The performance improvement of the CPEC method is limited as it uses CPE only. As shown in (1.10), the performance loss of OFDM systems is caused by CPE and ICI, both of which should be considered for phase noise mitigation. Accordingly, this approach would yield better performance in comparison to CPEC. In other words, we may choose to minimize the mean square error (MSE) of the detected signal or equivalently, use the MMSE equalization technique [20], which suppresses both CPE and ICI caused by phase noise. This algorithm is termed as phase nosie suppression (PNS).

The MMSE criterion requires to find an optimal coefficient $g_m(k)$ as follows

$$\min_{g_m(k)} E\left[|x_m(k) - g_m(k) y_m(k)|^2\right] \tag{3.5}$$

As mentioned earlier, in terms of (1.10) and (3.1), we note that $\acute{n}_m(k)$ in (3.1) indicates the sum of ICI and AWGN noise. For small phase noise, the ICI term can be approximated as a Gaussian random with zero mean and variance shown in (2.18) equal to $\frac{\pi N \beta \varepsilon_x}{3R}$. Since ICI is independent of AWGN noise $n_m(k)$, $\acute{n}_m(k)$ in (3.1) is also Gaussian distributed with zero mean and variance

$$\sigma_{\acute{n}}^2 = \frac{\pi N \beta \varepsilon_x}{3R} + \sigma^2 \tag{3.6}$$

Given the knowledge of $c_m(0)$ and $h(k)$, the optimal $g_m(k)$, in terms of (3.5) and (1.10), is shown to be

$$\begin{aligned} & g_m(k)|_{c_m(0),h(k)} \\ = & \frac{c_m^*(0)h^*(k)}{|c_m(0)h(k)|^2 + \sum_{p=1}^{N-1} E\left[|c_m(p)|^2\right] + \sigma^2/\varepsilon_x} \\ = & \frac{c_m^*(0)h^*(k)}{|c_m(0)h(k)|^2 + \{E[|ICI_m(k)|^2] + \sigma^2\}/\varepsilon_x} \end{aligned} \tag{3.7}$$

which gives the data decision

$$\hat{x}_m(k) = g_m(k)|_{c_m(0),h(k)} \cdot y_m(k) \tag{3.8}$$

Since OFDM channel estimation has been considered in many papers, e.g., [25] and [26], channel frequency response $\{h(k)\}_{k=1}^N$ are assumed known in this dissertation. However, for the complete solution of (3.7), the CPE term $c_m(0)$ has to be estimated.

Minimizing the cost function $\sum_{k\in S_P} |y_m(k) - c_m(0)h(k)x_m(k)|^2$, leads to the estimate

$$\hat{c}_m(0) = \frac{y_m(k)h^*(k)x_m^*(k)}{\sum_{k\in S_p} |h(k)x_m(k)|^2} \tag{3.9}$$

where S_P denotes the set of pilot signals.

The ICI plus noise energy in (3.7) can be pre-calculated using (2.5) if we have *a prior* knowledge of both AWGN and phase noise statistics. In this case, the optimal coefficient $g_m(k)$ is obtained towards data equalization. However, in case of unknown noise statistics, it is required to estimate the ICI plus AWGN noise energy from received signals. The approximation of (2.18) illustrates that, for small phase noise, ICI energy is constant within a symbol, which implies that we can possibly estimate the ICI plus noise energy using pilot subcarriers. If these specific pilot subcarriers carry null data at the transmitter, we can readily see from (1.10) that, after DFT at the receiver, we will find nothing except ICI plus noise on these subcarriers. This

suggests the possible usage of these subcarriers for ICI plus noise energy estimation. The estimator is therefore expressed by

$$\sigma^2_{ICI+noise} = \frac{1}{N_I} \sum_{k \in S_I} |y_m(k)|^2 \tag{3.10}$$

where S_I and N_I denote the set and number of these pilot subcarriers, respectively, used for energy estimation. Note that S_I is different from pilot set S_P which is used for CPE correction and can not be null. It is worth mentioning that transmitting extra pilot signals for ICI plus noise energy estimation will decrease the spectral efficiency, and it is not suitable especially when bandwidth is precious, e.g., IEEE 802.11a standard [4].

3.3.1 Practical Considerations for PNS Algorithm

It's important to examine how to implement the PNS algorithm and what performance it would present. Naturally for this, the IEEE 802.11a WLAN standard is of interest since it is based on OFDM technique.

The data structure of IEEE 802.11a standard is shown in Fig. 3.1. In this standard, the data packet consists of the preamble and the data. The preamble includes short and long pilots which are used, e.g., for synchronization, frequency offset and channel estimation, while the data part of the packet is OFDM modulated. Each OFDM data symbol contains $N = 64$ subcarrier signals, including the data set S_D with $N_D = 48$ subcarrier signals, the pilot set S_P with $N_P = 4$ subcarrier signals, and the null set S_N with $N_N = 12$ subcarrier signals. It is assumed that channel frequency response is known within the whole packet as it can be estimated using the preamble.

It has been shown in (2.5) that the self-correlation (or the energy) of the ICI term is not a function of time m or the subcarrier index k. For small phase noise

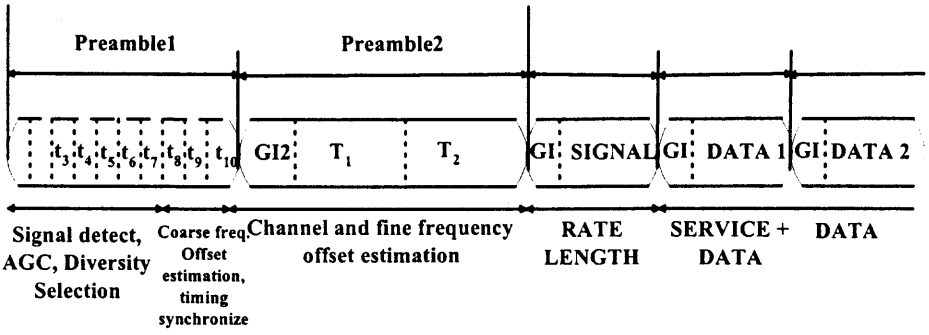

Figure 3.1 The data structure of IEEE 802.11a WLANs

approximation, this expression is further simplified as (2.18). However, considering the existing null subcarriers on each OFDM symbol of IEEE 802.11a standard, (2.18) is modified to [20]

$$\begin{aligned} E[|ICI_m(k)|^2] &= \frac{\pi\beta T\left(N-N_N\right)\varepsilon_x}{3N} \\ &= \frac{\pi\beta\left(N-N_N\right)\varepsilon_x}{3R} \end{aligned} \tag{3.11}$$

And so is the variance of $\acute{n}_m(k)$ in (3.6), namely

$$\sigma_{\acute{n}}^2 = \frac{\pi\beta\left(N-N_N\right)\varepsilon_x}{3R} + \sigma^2 \tag{3.12}$$

Due to the fact that in IEEE 802.11a standard, only $N_P = 4$ pilots are available for the CPE estimator (3.9), one may argue that (3.9) may not be accurate with so few numbers of pilot symbols. In order to improve the estimation accuracy, initially $c_m(0)$ is estimated using (3.9); then, after equalization and detection, decision is fed back for further enhancement of the performance of (3.9) using[2]

$$\check{c}_m(0) = \gamma\grave{c}_m(0) + (1-\gamma)\,\acute{c}_m(0) \tag{3.13}$$

[2]The estimator of PNS is indicated by the superscript $\check{c}$ in order to distinguish it from that of CPEC, where the estimation result is denoted by $\hat{c}$.

where γ is the forgetting factor, and $\grave{c}_m(0)$ and $\acute{c}_m(0)$ take the same form as (3.9), but use the pilot set S_P and the data set S_D from decision feedback, respectively.

Note that the ICI energy given in (3.12) can be different for $k \in S_N$, i.e., for the null subcarriers which acts as the guard band, since the analog bandpass filter before RF down conversion will color the AWGN noise within these subcarriers, but would hardly affect the ICI term caused by phase noise within these subcarriers. This is because phase noise occurs mainly due to the receiver oscillator after RF down conversion, rather than that caused by the transmitter oscillator.

Remark 1 *The analog filter increases the estimation error of the estimator (3.10). The question is that if this extra estimation error is tolerable? First, the ICI plus noise energy, derived in (3.10), is independent of subcarrier index; Second, in spite of the colored noise due to the analog bandpass filter, for sufficiently high signal to noise ratio (SNR), the ICI term at the null subcarriers is dominant over the noise. Therefore, despite the existence of the colored noise, the estimation of ICI plus noise energy of null subcarriers can be used to approximate that of data subcarriers and hence used in the MMSE equalizer of (3.7).*

Based on the discussion above, the proposed post-FFT PNS algorithm is described by the following steps:

1) Obtain the estimate of CPE by (3.9) as well as the estimate of ICI plus noise energy by (3.10);

2) Use (3.7) to calculate the equalizer coefficients for N samples of each symbol, where the unknown parameters are replaced by the estimated values from step 1;

3)Use (3.8) to get the estimated signals for data detection. Decision feedback is used to update the estimate of by implementing (3.13).

4)Repeat steps 1-3 for all data symbols.

3.3.2 Normalized MMSE (NMMSE) for PNS Algorithm

In terms of (3.7), the estimate of the desired signal can be written as

$$\begin{aligned} & \hat{x}_m(k) = g_m(k) y_m(k) \\ = & \frac{\varepsilon_x c_m^*(0) h^*(k) y_m(k)}{|c_m(0)h(k)|^2 \varepsilon_x + \varepsilon_x \sum_{p=1}^{N-1} E\left[|c_m(p)|^2\right] + \sigma^2} \end{aligned} \tag{3.14}$$

Substituting (3.7) into $E\left[|x_m(k) - g_m(k)y_m(k)|^2\right]$ yields the minimum MSE (MMSE) conditional on $c_m(0)$ and $h(k)$, namely

$$\begin{aligned} & MMSE|_{c_m(0),h(k)} \\ = & \frac{\left\{\varepsilon_x \sum_{p=1}^{N-1} E\left[|c_m(p)|^2\right] + \sigma^2\right\} \varepsilon_x}{|c_m(0)h(k)|^2 \varepsilon_x + \varepsilon_x \sum_{p=0}^{N-1} E\left[|c_m(p)|^2\right] + \sigma^2} \end{aligned} \tag{3.15}$$

Then the normalized MMSE (NMMSE) is defined as

$$\begin{aligned} NMMSE &= \frac{1}{\varepsilon_x} MMSE|_{c_m(0),h(k)} \\ &= \frac{\varepsilon_x \sum_{p=1}^{N-1} E\left[|c_m(p)|^2\right] + \sigma^2}{\varepsilon_x \sum_{p=0}^{N-1} E\left[|c_m(p)|^2\right] + \sigma^2} \end{aligned} \tag{3.16}$$

where $|c_m(0)h(k)|^2$ is approximated by its expectation $E\left[|c_m(0)h(k)|^2\right]$, and therefore removed the conditions on $c_m(0)$ and $h(k)$. It gives rise to the average unconditional NMMSE. The independence between $c_m(0)$ and $h(k)$ was assumed in deriving (3.16). The numerator in (3.16) gives the energy of ICI plus AWGN noise while the denominator indicates the entire energy of the received signal after DFT. Moreover, for the PNS scheme, the assumption of small phase noise and large N results in (2.17) and (2.18), which further yield

$$
\begin{aligned}
NMMSE &= 1 - \frac{E\left[|c_m(0)|^2\right]}{1+\sigma^2/\varepsilon_x} \\
&= 1 - \left(1+\frac{1}{\gamma_s}\right)^{-1}\left(1-\frac{\pi\beta N}{3R}\right) \qquad (3.17)
\end{aligned}
$$

Equation (3.17) suggests that, in case of small phase noise, NMMSE can be expressed as a simple function of the phase noise linewidth to subcarrier spacing ratio $\beta N/R$ and SNR γ_s. It further shows that either decreasing $\beta N/R$ or increasing γ_s will reduce the residual MMSE and subsequently enhance receiver performance. This conclusion coincides with what have been found in Section 2.3. Fig. 3.2 illustrates how NMMSE is related to $\beta N/R$ and γ_s. With smaller $\beta N/R$ which indicates better frequency and phase synchronization, SNR has a dominant effect on NMMSE. In case $\beta N/R$ is of the order of 10^{-4} or less, NMMSE decreases almost linearly with SNR, and the effects of phase noise is negligible. Larger $\beta N/R$, however, results in more errors that overwhelms the positive effects of high SNR over NMMSE, as indicated by the inevitable error floor in Fig. 3.2 even after phase noise mitigation.

3.3.3 Numerical Results

The PNS algorithm is evaluated for a normalized frequency-selective Rayleigh fading channel by Monte Carlo trials. Six multiple radio paths have been chosen for simulation. 16 QAM, which is more sensitive to phase noise than MPSK, is used in the simulation to evaluate the performance of the PNS algorithm under the modulation. Phase noise is simulated using an independent Gaussian increment between adjacent subcarrier signals as proposed in [16]. Channel impulse response remains static within an OFDM block (or frame) but varies independently from block to block. In computer simulations, two cases are studied as shown in Table 3.1.

In case 1, pilots are required for both CPE and ICI and evenly interpolated into OFDM symbols, while case 2, which is based on IEEE 802.11a standard, has no pilots

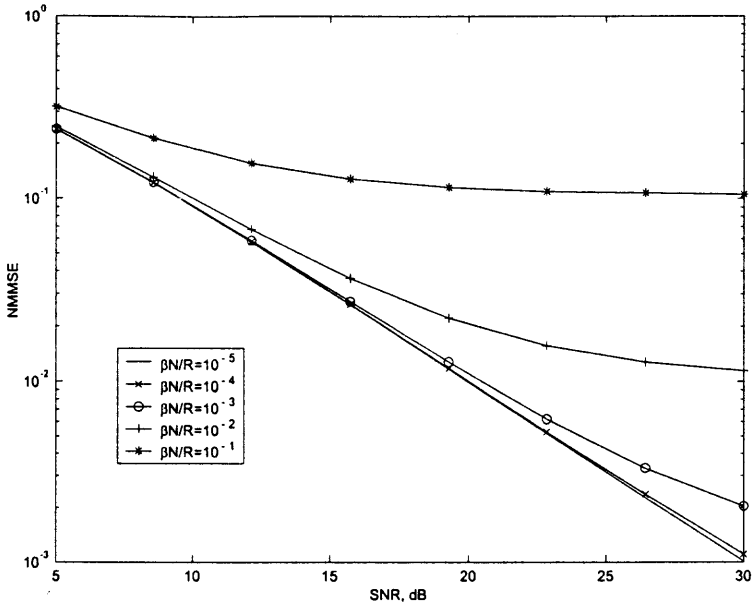

Figure 3.2 Normalized MMSE for a 1024-subcarrier system with different $\beta N/R$ values

for ICI. Decision feedback is only required in case 2. The theoretical values of c_m (0) and σ_n^2 based on (1.11) and (3.12) are calculated to examine the effectiveness of the proposed algorithm. Simulations results with the PNS algorithm are compared with the theoretical calculation as well as with the result obtained for the CPE estimation algorithm of [23].

Fig. 3.3-3.4 obtained with case 1 show the catastrophic effects of phase noise on SER performance when no correction is applied. The CPE estimation and correction helps improve the system performance, but exhibits an error floor at high SNRs as it does not consider ICI. The proposed PNS algorithm outperforms the CPE estimation scheme, both in general OFDM and IEEE 802.11a systems, by considering ICI and minimizing the overall errors. The theoretical curve indicated in this figure is based on the theoretical calculation of $\sigma^2_{ICI+noise}$ with *a prior* knowledge of AWGN and phase noise statistics. It is worth mentioning that the simulation result of the PNS algorithm coincides very well with the theoretical calculation (both curves are almost

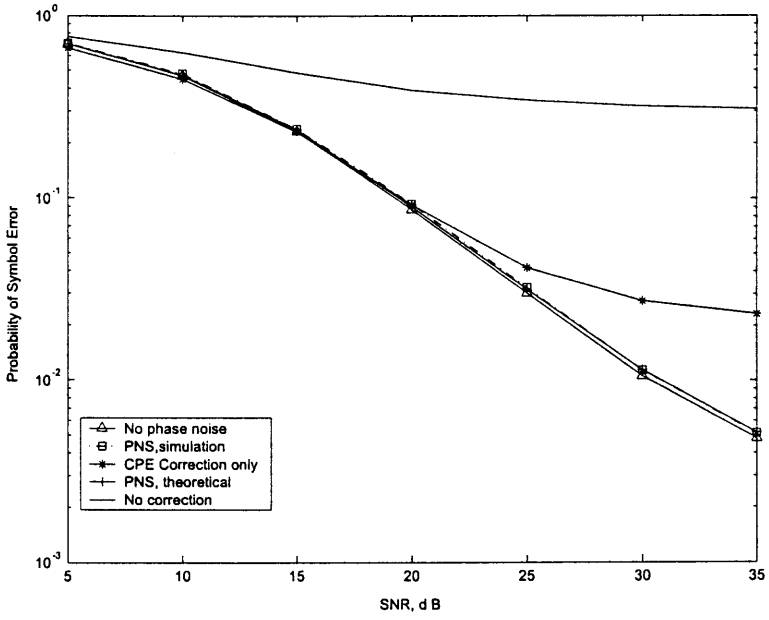

Figure 3.3 PNS performance versus phase noise variance for a general 1024-subcarrier OFDM system, with 16QAM, $2\pi\beta T = 0.0384$ rad^2

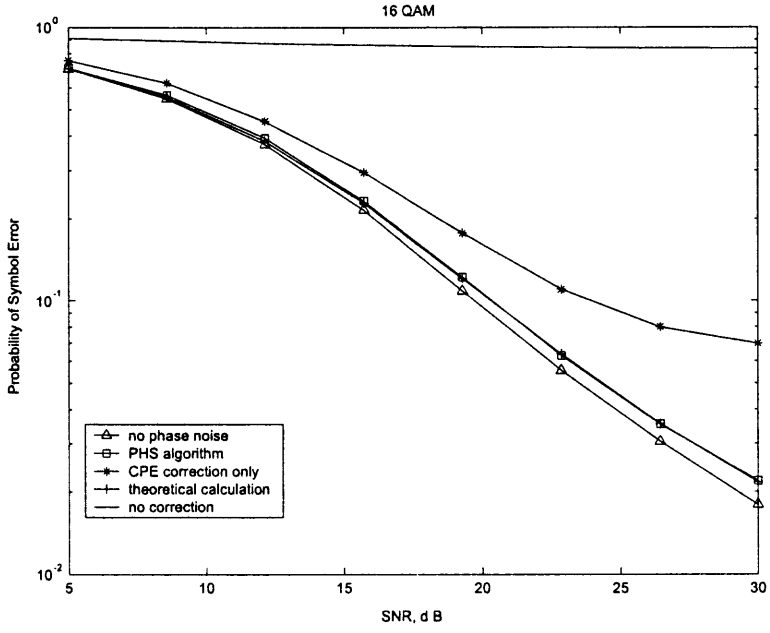

Figure 3.4 PNS performance for IEEE 802.11a WLANs, with 16QAM and $2\pi\beta T = 0.0384\ rad^2$

Table 3.1 Simulation parameters for the PNS algorithm

	Case 1	Case 2(802.11a)
No of Subcarriers(N)	1024	64
No of CPE Pilots(N_P)	32	4
No of ICI Pilots(N_I)	32	0
No of Guard Band Subcarriers(N_N)	64	12

identical). This suggests the effectiveness and capability of the proposed scheme in a general OFDM system.

Fig. 3.5 depicts the SER performance of the proposed scheme as a function of phase noise variance, showing that it always outperforms CPEC. Moreover, the PNS scheme has approximately the same performance as no-phase-noise case with phase noise variance less than 10^{-2}. Since such a requirement for small phase noise can practically be met in many cases, the proposed PNS scheme is thus suitable for practical applications.

Fig. 3.5-3.6 suggest that the proposed PNS algorithm always outperforms the CPEC for different phase noise levels. It's well known that the variance of phase noise is usually much less than unity in many applications. From these figures, when the phase noise variance decreases, the PNS performance approaches the non-phase-noise case by minimizing the overall mean square error. It has the similar performance with the non-phase-noise case when the phase noise variance is less than 10^{-3}.

3.4 Simultaneous CPE and ICI Correction (SCIC)

3.4.1 Maximum-Likelihood Estimation (MLE) of $c_m(p)$

The previous section has shown that, PNS improves the system performance by suppressing both interference and AWGN noise using MMSE technique. As we

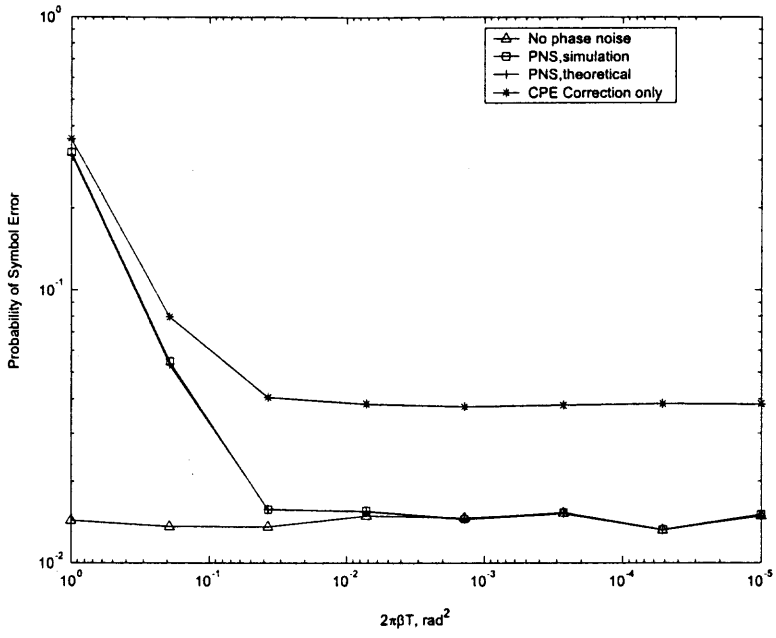

Figure 3.5 PNS performance versus phase noise variance for a general 1024-subcarrier OFDM system, with 16QAM

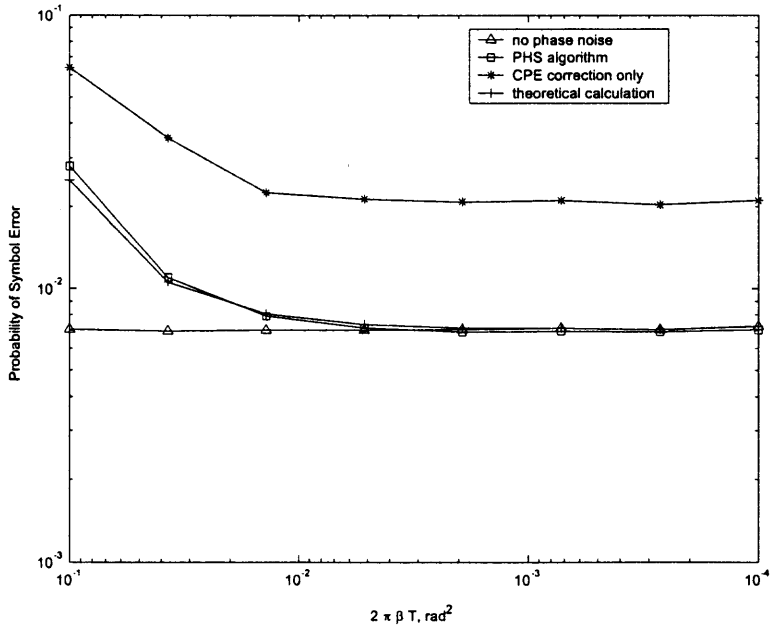

Figure 3.6 PNS performance versus phase noise variance for IEEE 802.11a WLANs, with 16QAM

learned from DS-CDMA systems, parallel interference cancellation (PIC) or sucessive interference cancellation (SIC) performs better than MMSE when dealing with interference. Hence, rather than suppressing interference, a new method is proposed to estimate CPE and ICI simultaneously and cancel them accordingly. The basic idea is to obtain the estimates of $\{c_m(p)\}_{p=0}^{N-1}$, which are the corresponding DFT output of time-domain phase noise $\left\{e^{j\phi_m(n)}\right\}_{n=0}^{N-1}$, serving as the weighting coefficients of CPE and ICI as in (1.10). The question is that how to estimate the entire set of $\{c_m(p)\}_{p=0}^{N-1}$ in order to compute and remove both CPE and ICI. This method is termed as simultaneous CPE and ICI correction (SCIC).

We start by rewriting (1.10) as

$$\underbrace{\begin{pmatrix} y_m(0) \\ y_m(1) \\ \vdots \\ y_m(N-1) \end{pmatrix}}_{\mathbf{y}} = \underbrace{\begin{pmatrix} \mathbf{w}_0 & \mathbf{w}_1 & \cdots & \mathbf{w}_{N-1} \end{pmatrix}}_{\mathbf{W}} \cdot \underbrace{\begin{pmatrix} c_m(0) \\ c_m(1) \\ \vdots \\ c_m(N-1) \end{pmatrix}}_{\mathbf{c}} + \underbrace{\begin{pmatrix} n_m(0) \\ n_m(1) \\ \vdots \\ n_m(N-1) \end{pmatrix}}_{\mathbf{n}} \tag{3.18}$$

where $\mathrm{w}_k = \begin{pmatrix} a_k & \cdots & a_{N-1} & a_0 & \cdots & a_{k-1} \end{pmatrix}^T$ with $a_k = x_m(k)h(k)$, $k = 0, 1, ..., N-1$. Note that any w_k with $k \neq 0$ is a left circular shift of w_0.

Our aim is to recover the weighting coefficient vector $\mathbf{c}$ from the received signal vector $\mathbf{y}$. Given the knowledge of channel and transmitted signals, $\mathbf{W}$ is deterministic and known. Moreover, conditioned on $\mathbf{c}$, $\mathbf{y}$ is an N-dimensional Gaussian random variable vector with mean $\mathbf{Wc}$ and covariance matrix $\sigma^2\mathbf{I}$ with $\mathbf{I}$ denoting

identity matrix. Its conditional probability distribution function is given by $p(\mathbf{y}|\mathbf{c}) = \frac{1}{(2\pi\sigma^2)^{\frac{N}{2}}} \exp\left[-\frac{(\mathbf{y}-\mathbf{Wc})^H(\mathbf{y}-\mathbf{Wc})}{2\sigma^2}\right]$. In order to estimate vector $\mathbf{c}$, we choose the MLE method, which asymptotically achieves Cramer-Rao lower bound (CRLB) by minimizing the conditional probability distribution function $p(\mathbf{y}|\mathbf{c})$ [27]. In additive white Gaussian noise $\mathbf{n}$, this is equivalent to minimizing the squared Euclidean distance

$$\check{\mathbf{c}}=\arg\min_{\mathbf{c}} \|\mathbf{y}-\mathbf{Wc}\|^2$$

which leads to

$$\begin{aligned} \check{\mathbf{c}} &= (\mathbf{W}^H\mathbf{W})^{-1}\mathbf{W}^H\mathbf{y} \\ &= \mathbf{W}^{-1}\mathbf{y} \end{aligned} \tag{3.19}$$

To solve (3.19), we have to know the matrix $\mathbf{W}$, which requires the knowledge of the channel and the transmitted signals. The former can be estimated using the preamble of each block, as discussed in Section 1.3.3. Since it is impractical to use all transmitted subcarrier signals as pilots, the tentative decision output $\hat{x}_m(k)$ of (3.4) after CPEC can be taken as the approximation of transmitted signals towards the solution of (3.19). Finally, we obtain the estimate of $\mathbf{W}$, whose entries are replaced by $a_k = \hat{x}_m(k)\hat{h}(k)$. Note that with random channel fading gains and carefully chosen pilot patterns, $\mathbf{W}$ may not be singular. Therefore the inverse of $\mathbf{W}$ or $\mathbf{W}^H\mathbf{W}$ is feasible.

Equation (3.18) can be further rewritten as

$$\mathbf{y} = c_m(0)\mathbf{Hx} + \mathbf{W}^1\mathbf{c}^1 + \mathbf{n} \tag{3.20}$$

where $\mathbf{W}^1\mathbf{c}^1$ indicates the ICI vector produced by random phase noise, with $\mathbf{W}^1$ and $\mathbf{c}^1$ denoting matrix $\mathbf{W}$ without the first column and vector $\mathbf{c}$ without the first entry, respectively; $\mathbf{H} = diag(h(0), ..., h(N-1))$ and $\mathbf{x} = \begin{pmatrix} x_m(0) & \cdots & x_m(N-1) \end{pmatrix}^T$.

Therefore, subtracting ICI from the received signal leads to

$$\mathbf{y}^s = \mathbf{y}\text{-}\mathbf{W}^1\breve{\mathbf{c}}^1 \tag{3.21}$$

The "ICI-cancelled" signal vector y^s is then compensated for its CPE error and yields the phase noise mitigated signals

$$\begin{aligned} \mathbf{y}^{sc} &= \breve{c}_m^{-1}(0)\mathbf{y}^s \\ &= \breve{c}_m^{-1}(0)\left(\mathbf{y}\text{-}\mathbf{W}^1\breve{\mathbf{c}}^1\right) \end{aligned} \tag{3.22}$$

where $\breve{c}_m(0)$, the first entry of vector $\breve{\mathbf{c}}$, denotes the estimate of CPE. After phase noise mitigation as described in (3.22), data are used for channel equalization and detection.

3.4.2 Computation Complexity Reduction

The method proposed in this section requires the inverse operation of $\mathbf{W}$, hence it can be more complex than CPEC or PNS. Reduction of computational complexity can be achieved by estimating only a subset of $\mathbf{c}$, e.g., the first L entries with $L < N$, denoted by c_r. In this case, the estimated c_r still has the same form of (3.19), namely,

$$\breve{\mathrm{c}}_r = (\mathbf{W}_r^H\mathbf{W}_r)^{-1}\mathbf{W}_r^H\mathbf{y} \tag{3.23}$$

where $\mathbf{W}_r$ is an $N \times L$ matrix which comprises L column vectors of $\mathbf{W}$ corresponding to vector c_r. Accordingly, computational complexity is reduced. It follows that the performance with this simplified version degrades in comparison to the original approach due to the trade-off between performance and computational efficiency. Nevertheless, we show via simulation that the resultant performance loss is quite tolerable even with small L, e.g., $L = N/4$.

3.4.3 Numerical Results

Numerical results given in this section demonstrate the effectiveness of the new approach. An uncoded OFDM system is chosen with symbol size $N = 64$. A Rayleigh fading channel consisting of six multiple paths is assumed in the simulation. To eliminate ISI caused by channel frequency selectivity, a cyclic prefix, larger than channel maximum delay spread, is added to the beginning of each OFDM symbol. As usual, the first symbol of each OFDM block is used for channel estimation. Each subcarrier signal is 16-QAM modulated. N_p pilot subcarrier signals are evenly distributed within a symbol for conventional CPEC in (3.2).

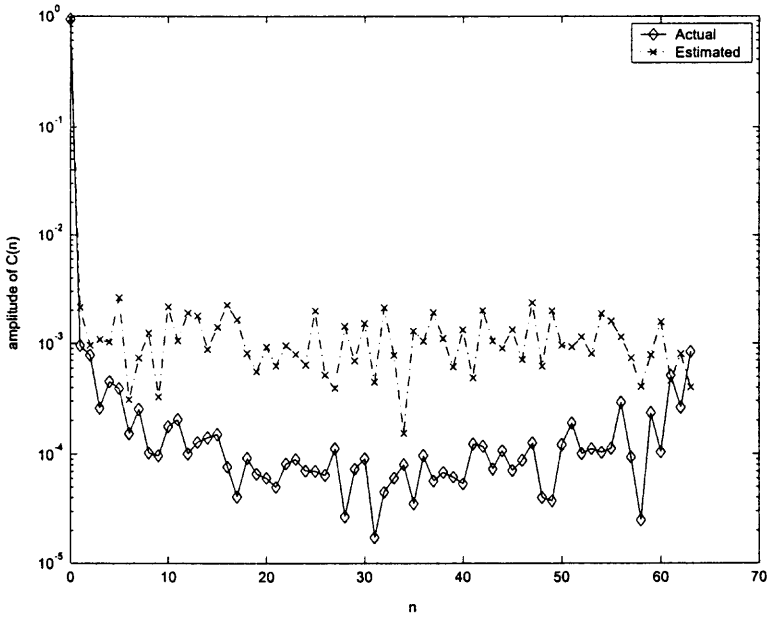

Figure 3.7 Comparison between the actual and estimated amplitudes of $\{c_m(p)\}_{p=0}^{N-1}$, with SNR=10dB, $N_p = 4$.

Simulation results are presented in Fig. 3.7-3.10, which provide a clear insight into the role of phase noise on SER performance and the effectiveness of different phase noise mitigation approaches.

We show in Fig. 3.7-3.8 the actual versus estimated values of parameters, including weighting coefficients $\{c_m(p)\}_{p=0}^{N-1}$, CPE (its real and imaginary parts) and

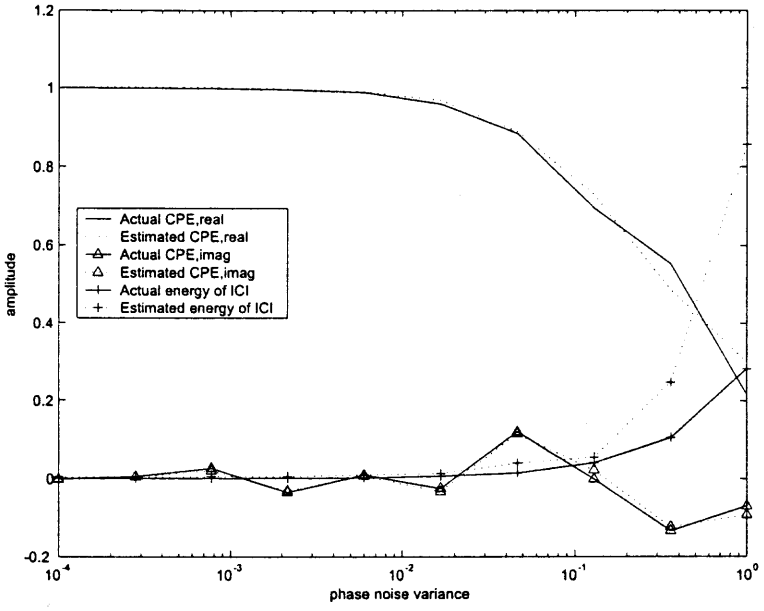

Figure 3.8 Actual and estimated values of CPE and ICI versus phase noise variance, SNR=10dB, $N_p = 4$

the energy of ICI. Fig. 3.7 suggests that, both curves of the actual and estimated CPE (or $c_m(0)$), stay close, while the amplitudes of estimated $c_m(n)$,with $n \in [10, 60]$, are of the order of 10^{-4}, in comparison to their actual values of the order of 10^{-3}, exhibiting some estimation errors.

Fig. 3.8 shows that, for different phase noise levels, both real and imaginary parts of the estimated CPE consistently match the actual values. The energy of the estimated ICI, based on the weighting coefficients $\{c_m(p)\}_{p=1}^{N-1}$, approaches that of the actual value for phase noise variance less than 10^{-1}. For large phase noise, the estimation accuracy is no longer guaranteed. However, as in practice the phase noise variance does not exceed 10^{-1}, this suggests the robustness of the proposed method to phase noise.

Fig. 3.9 shows the SER performance as a function of SNR when the number of pilots N_p is equal to 4 (as in IEEE 802.11a WLAN standard [4]). Not surprisingly, the proposed method, which directly corrects CPE and cancel ICI, significantly

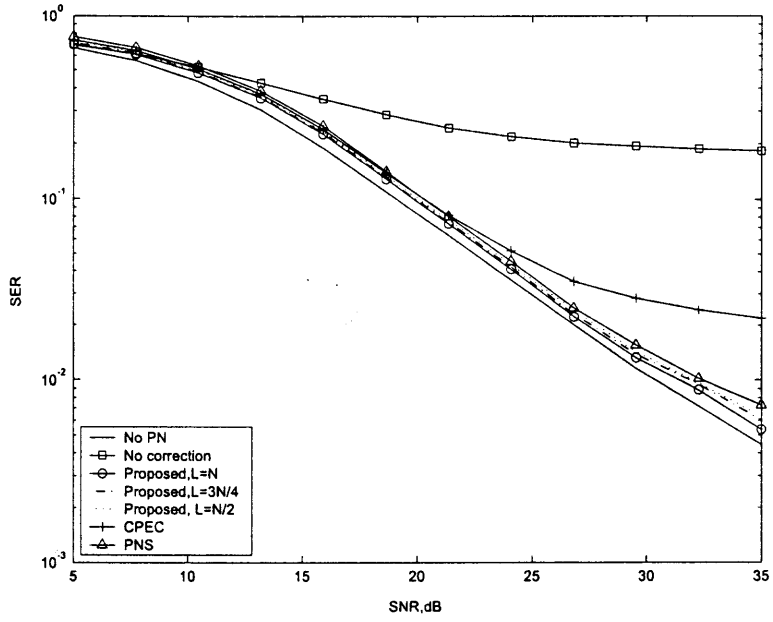

Figure 3.9 SER performance with phase noise variance equal to 0.01 and number of pilots $N_p = 4$.

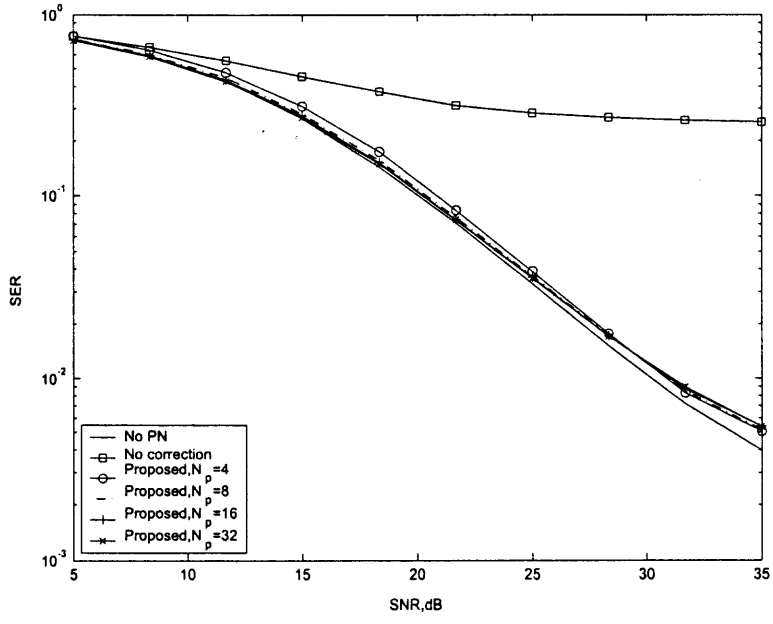

Figure 3.10 SER performance versus SNR with different number of pilots N_p, where $L = N$

improves the receiver performance. It can be seen that it is even better than PNS for high SNRs. Parameter settings $L = N/2$ and $L = N/4$ simplify the proposed method and significantly reduce the computational complexity, but still lead to some performance improvement comparable to PNS. Therefore, the scheme presented in this dissertation, with some modification, is highly competent with respect to computation and performance, and therefore is a good alternative to our previous PNS method.

We also note from Fig. 3.9 that, there is still some performance gap between this new approach and no-phase-noise case. Therefore, it is interesting to examine the performance of this method with different number of pilots N_p. Fig. 3.10 shows that, when number of pilots N_p increases, the performance gap decreases, indicating some performance improvement. Whereas, this improvement is never significant even if we use half of bandwidth as pilots, i.e., $N_p = 32$. This is mainly because $N_p = 4$ leaves quite small performance gap (up to 0.5 dB) between the proposed method and no-phase-noise case. Hence, $N_p = 4$ (occupying 6.25% bandwidth) is enough in all cases, implying the high spectral efficiency of this new approach with sufficient performance.

3.5 Conclusions

OFDM suffers severe performance degradation in the presence of phase noise. Different methods have been proposed in the literature to correct phase noise either in the time domain or in the frequency domain. Time-domain approaches usually have some impractical assumptions on pilot patterns or channel environments, making frequency-domain approaches preferable in practice. Conventional frequency-domain methods which emphasize CPE correction was further enhanced by the PNS algorithm proposed in [20] using the estimate of ICI plus noise energy to minimize the mean square error.

The theoretical analysis has been provided which is followed by the implementations of PNS algorithm in IEEE 802.11a WLAN standard. The theoretical analysis has been further confirmed by computer simulations.

To complement the work in [20], in the presence of channel estimation errors, an alternative approach has been proposed for simultaneous CPE and ICI correction, which first estimates a set of weighting coefficients that are the DFT of time-domain phase noise; then use them to correct and cancel CPE and ICI respectively. In order to reduce computational complexity, the proposed method has further been simplified by estimating only a subset of those coefficients. Numerical results have been provided to demonstrate the potential of this new approach and its simplified version with the performance close to PNS.

When comparing two proposed phase noise mitigation methods, namely, PNS and simultaneous CPE and ICI cancellation method, we notice that both methods have the same spectral efficiency. The advantage of the simultaneous CPE and ICI cancellation method is its performance improvement over PNS, as it estimates each weighting coefficients to calculate and cancel CPE and ICI. while PNS only treats ICI as additive noise. The advantage of PNS, however, is its lower computational complexity with little performance loss in comparison to the simultaneous CPE and ICI cancellation method. Even with the simplified version, the computation of the simultaneous CPE and ICI cancellation method is still more complex than that of PNS. This implies that PNS is quite simple yet effective which makes it very attractive for most real-time applications since it aims to minimizes the mean square error and has the performance close to the no-phase-noise case. On the other hand, the proposed method is suitable for the cases where performance is very crucial while computational cost is less important.

CHAPTER 4

MULTIPLE PHASE NOISE ANALYSIS AND MITIGATION IN MULTI-USER OFDM SYSTEMS

4.1 Introduction

The effects of phase noise on OFDM systems have been discussed in the previous chapters. Although it was not explicitly stated, the previous analysis and the proposed schemes are particularly applied to the single user case with single phase noise. In a multi-user OFDM system, e.g., multi-carrier code division multiple access (MC-CDMA), or orthogonal frequency division multiple access (OFDMA), the simultaneous access of multiple users gives rise to multiple phase noise (MPN), which is of interest. As with the single phase noise case, this problem has two aspects: its effects on the multi-user systems, and what is needed for its mitigation.

We begin our analysis with a MC-CDMA system, which, by implementing OFDM technique, is also sensitive to phase noise [22]. To the best of this author's knowledge, past work that has been done on phase noise has never considered MPN. However, this phenomenon occurs in a multiple access environment. Therefore, we analyze, in the chapter, the effects of MPN on MC-CDMA systems and derive the closed-form BER expression with correlated channel fading. Following the understandings of MPN, we discuss its mitigation in a multiple access environment and propose a new MPN correction scheme.

The organization of this chapter is as follows. Section 4.2 gives the MC-CDMA system model with MPN over a correlated fading channel, which is followed by the derivation of the closed-form BER expression. Numerical results are provided to further explain the analytical results we obtain. MPN mitigation is discussed in

Section 4.3 with multiple receive antennas. As such, spatial diversity is exploited to help the performance of the proposed MPN mitigation method.

4.2 Effects of Multiple Phase Noise

The performance of a MC-CDMA system, in the presence of frequency offset and phase noise, was evaluated in [22], where analytical results are given only for single-user case and downlink MC-CDMA systems. This work was partially extended to an uplink MC-CDMA system in [28] where only single frequency offset was considered.

We consider an uplink MC-CDMA system with phase noise and Rayleigh fading environment, wherein multiple users give rise to MPN which are mutually independent In practice, channel fading gains on different subcarriers of the same OFDM symbol are generally correlated and thus we assume correlated fading channel throughout this chapter. Therefore our goal is to derive an expression for average bit error rate (BER) of uplink MC-CDMA systems with the impact of MPN over a correlated fading channel.

4.2.1 System Model

A time synchronous MC-CDMA system with K active users and N subcarriers is present with BPSK modulation. Phase noise is usually caused by the oscillators both at the transmitter and the receiver, but we will assume it to occur only at the transmitter (mobile station) for the uplink communications, since the oscillator of the receiver (base station) is quite stable, due to possibly higher cost [22]. Based on the principle of MC-CDMA [29], the transmitted baseband signal for user k can be expressed by

$$s_k(t) = \sum_{m=-\infty}^{\infty} \sum_{n=0}^{N-1} \left\{ x_k(m) c_{k,n} u\left(t - mT_b\right) e^{j[2\pi f_n t + \phi_k(t)]} \right\} \tag{4.1}$$

where $x_k(m)$ and $c_{k,n}$ denote the kth user's mth data bit and the nth chip of the ith user's binary signature sequence respectively. With T_b, $u(t)$ and $f_n = n/T_b$ denoting the bit duration, the rectangular window defined on $[0,T_b)$ and the nth subcarrier frequency, respectively. Phase noise $\varphi_k(t)$ of the kth transmitter is defined by a continuous Brownian motion process with zero mean and variance $2\pi\beta_k t$ with β_k denoting the two-sided phase noise linewidth of the oscillator at the kth transmitter. After passing through the channel, the received signal can thus be given by

$$r(t) = \sum_{k=1}^{K} s_k(t) \otimes h_k(t) + n(t) \tag{4.2}$$

where $\otimes$ denotes the convolutional operation while $h_k(t)$ and $n(t)$ denotes the kth user's channel impulse response and the AWGN noise with zero mean and variance σ_n^2, respectively. $\{h_k(t)\}_{k=1}^{K}$ are assumed mutually independent for different users, which makes sense for the uplink communications.

4.2.2 Performance Analysis

With a coherent correlation receiver, we consider the maximum ratio combining (MRC) technique with the combing coefficients $g_{k,n} = c_{k,n}h_{k,n}^*$. For BPSK, the real part of some received signal is of concern since the decision is based on it; and from (4.2) and (4.1), after Fourier transform and MRC, we have the 0th data bit of user i

$$\begin{aligned} R_i &= \mathrm{Re}\left\{\sum_{j=0}^{N-1} g_{i,j}\frac{1}{T_b}\int_0^{T_b} r(t)e^{-j2\pi f_j t}dt\right\} + \eta \\ &= \sum_{j=0}^{N-1}\sum_{n=0}^{N-1}\sum_{k=1}^{K}\left\{x_k c_{i,j}c_{k,n}\left|h_{i,j}^* h_{k,j}p_{k,n-j}\right|\right. \\ &\quad \left.\cdot\cos\varphi\right\} + \eta \\ &= A_i + I_{i1} + I_{i2} + I_{i3} + \eta \end{aligned} \tag{4.3}$$

where η is the real AWGN noise with zero mean and variance $\sigma_n^2/2$; $h_{k,j}$ is the Fourier transform of $h_k(t)$, denoting the channel fading gain on the jth subcarrier of user k[1]. A_i denotes the desired signal of user i. I_{i1} denotes multiple access interference (MAI) while both I_{i2} and I_{i3} are the intercarrier interference terms (ICI), caused by MPN. φ is the phase of the item $h_{i,j}^* h_{k,j} p_{k,n-j}$.

In (4.3), random phase noise $\varphi_k(t)$ of user k results in, on the nth subcarrier, $p_{k,n} = \frac{1}{T_b}\int_0^{T_b} e^{j(2\pi nt/T_b + \varphi_k(t))}dt$, which has the mean and the autocorrelation, respectively [22]

$$E\left[p_{k,n}\right] = \frac{1 - e^{-v_k}}{v_k - j\omega_n} \tag{4.4}$$

$$E\left[|p_{k,n}|^2\right] = 2\frac{v_k^3 - v_k^2 + \omega_n^2(1+v_k) + e^{-v_k}\left(v_k^2 - \omega_n^2\right)}{\left(v_k^2 + \omega_n^2\right)^2} \tag{4.5}$$

where $\omega_n = 2n\pi$ and $v_k = \pi\beta_k T_b$, with the phase noise linewidth to subcarrier spacing ratio (PNLSSR) denoted by $\beta_k T_b$[2].

1. A_i is obtained in (4.3) by letting $k = i$ and $j = n$;

$$A_i = \mathrm{Re}\left[p_{i,0}\right] x_i \sum_{n=0}^{N-1} |h_{i,n}|^2 \tag{4.6}$$

$p_{i,0}$ is the average of $e^{j\phi_i(t)}$ over the period T_b. Define $r_i = \frac{1}{2}\sum_{n=0}^{N-1} |h_{i,n}|^2$. Equation (4.6) is rewritten as

$$A_i = 2x_i \,\mathrm{Re}\left[p_{i,0}\right] r_i \tag{4.7}$$

[1]For the sake of simplicity, we drop the time index m for the rest of this chapter as we focus on the time epoch $m = 0$. For example, we write $R_i(0)$ and $a_k(0)$ as R_i and a_k, respectively.
[2]Sometimes it is also termed normalized phase noise linewidth in the literature.

(4.7) shows that the desired signal A_i is a function of $p_{i,0}$ and r_i, both of which are random variables. $p_{i,0}$ is related to phase noise while r_i is a random variable that has, for a correlated Rayleigh fading channel, the probability density function (pdf) [28]

$$f(r_i) = \sum_{n=0}^{N-1} \frac{2\lambda_n^{N-2} e^{-2r_i/\lambda_n}}{\prod_{j=0,j\neq n}^{N-1} (\lambda_n - \lambda_j)} \tag{4.8}$$

where $\{\lambda_n\}_{n=0}^{N-1}$ denote the non-zero eigenvalues of the channel covariance matrix whose entries are denoted by $R(n_1,n_2) = \frac{\sigma_h^2}{1-j\{(n_1-n_2)\tau_{\max}/T_b\}}$, with n_1 and n_2 ranging from 0 to $N-1$. $\tau_{\max}$ indicates the maximum channel delay spread.

For small phase noise, the real part of $p_{i,0}$ has a value close to unity and does not vary much with $\phi_i(t)$, while the imaginary part is much smaller with zero mean [22]. Therefore, $E[p_{i,0}] = E\{\mathrm{Re}[p_{i,0}]\}$, which can be used to approximate $\mathrm{Re}[p_{i,0}]$, and yields

$$A_i = 2x_i E[p_{i,0}] r_i \tag{4.9}$$

2. The MAI term I_{i1} is obtained from the same subcarriers of all the other users, i.e., $k \neq i$ and $j = n$;

$$I_{i1} = \sum_{k=1,k\neq i}^{K} \sum_{n=0}^{N-1} x_k(0) c_{k,n} c_{i,n} \left| p_{k,0} h_{i,n}^* h_{k,n} \right| \cos\varphi \tag{4.10}$$

We assume that the transmitted data bits and chips of all users are all mutually independent with zero mean and unity variance, namely, $E[x_k(0)x_i(0)] = \delta(k-i)$ and $E[c_{k,n}c_{i,j}] = \delta(k-i)\delta(n-j)$. The in-phase item $|h_{k,j}|\cos\varphi$ of a Rayleigh random variable $h_{k,j}$ is a Gaussian random variable with zero mean and variance $\sigma_h^2/2$. In terms of central limit theorem, I_{i1} can be approximated as a Gaussian random variable. It is quite straightforward to show that I_{i1} has zero mean, and its variance is represented by

$$\begin{aligned}\sigma_{i1}^2 &= E\left[|I_{i1}|^2\right] \\ &= \frac{1}{2}N\sigma_h^4 \sum_{k=1,k\neq i}^{K} E\left[|p_{k,0}|^2\right] \end{aligned} \tag{4.11}$$

where $E\left[|p_{i,0}|^2\right]$ is given by (4.5).

3. An ICI term, I_{i2}, is obtained from the other subcarriers of all the other users with $k \neq i$ and $j \neq n$;

$$I_{i2} = \sum_{k=1,k\neq i}^{K} \sum_{n=0}^{N-1} \sum_{j=0,j\neq n}^{N-1} x_k(0)\, c_{k,n} c_{i,j} \left| p_{k,n-j} h_{i,j}^* h_{k,j} \right| \cos\varphi \tag{4.12}$$

which, similar to I_{i1}, can be approximated as a Gaussian random variable with zero mean. With large N, by using the following equality [9],

$$\sum_{j=0,j\neq n}^{N-1} E\left[|p_{k,n-j}|^2\right] = 1 - E\left[|p_{i,0}|^2\right] \tag{4.13}$$

we obtain its variance

$$\sigma_{i2}^2 = \frac{1}{2}N\sigma_h^4 \sum_{k=1,k\neq i}^{K} \left\{1 - E\left[|p_{k,0}|^2\right]\right\} \tag{4.14}$$

4. An ICI term, I_{i3}, results from the subcarriers of the same user with $k = i$ and $j \neq n$;

$$I_{i3} = \sum_{n=0}^{N-1} \sum_{j=0,j\neq n}^{N-1} x_i(0)\, c_{i,n} c_{i,j} \left| p_{i,n-j} h_{i,j}^* h_{i,j} \right| \cos\varphi \tag{4.15}$$

which can be approximated as a zero mean Gaussian random variable with its variance,

$$\sigma_{i3}^2 = N\sigma_h^4 \left\{1 - E\left[|p_{i,0}|^2\right]\right\} \tag{4.16}$$

where we use (4.13) as well as the conclusion in [19], that is, for a Rayleigh distributed random variable $|h_{i,j}|$, $E\left[|h_{i,j}|^4\right] = 2\sigma_h^4$.

Conditional on $r_i = \frac{1}{2}\sum_{n=0}^{N-1}|h_{i,n}|^2$, equations (4.7), (4.11), (4.14) and (4.16) yield, for BPSK modulation, the signal to interference plus noise ratio (SINR) for the ith user,

$$\begin{aligned} D_i &= \frac{|A_i|^2}{\sigma_{i1}^2 + \sigma_{i2}^2 + \sigma_{i3}^2 + \sigma_\eta^2} \\ &= \frac{8E^2\left[p_{i,0}\right] r_i^2}{N\sigma_h^4\left\{K + 1 - 2E\left[|p_{i,0}|^2\right]\right\} + 2\sigma_\eta^2} \end{aligned} \tag{4.17}$$

Note that, without phase noise, i.e., $\beta_i = 0$, D_i reduces to $D_i = \frac{8r_i^2}{(K-1)N\sigma_h^4 + 2\sigma_\eta^2}$ with $E\left[p_{i,0}\right] = 1$ and $E\left[|p_{i,0}|^2\right] = 1$. Then, for a correlated fading channel, the BER for the ith user is given by

$$P_{b,i} = \int_{-\infty}^{\infty} \frac{1}{2}\,\mathrm{erf}\,c(\sqrt{D_i}) f\left(r_i\right) dr_i \tag{4.18}$$

which yields using (4.17)

$$P_{b,i} = \sum_{n=0}^{N-1} \frac{\lambda_n^{N-2} a\left\{1 - e^{\frac{1}{4a^2\lambda_n^2}}\,\mathrm{erf}\,c\left(\frac{1}{\sqrt{2}a\lambda_n}\right)\right\}}{2\prod_{j=0, j\neq n}^{N-1}(\lambda_n - \lambda_j)} \tag{4.19}$$

where $a = \left\{\frac{8E^2[p_{i,0}]}{N\sigma_h^4\left\{K+1-2E\left[|p_{i,0}|^2\right]\right\}+2\sigma_\eta^2}\right\}^{\frac{1}{2}}$ is determined by PNLSSRs $\{\beta_i T_b\}_{i=1}^K$. Hence, equation (4.19) shows the effects of phase noise on the average BER performance as a function of $\{\beta_i T_b\}_{i=1}^K$. Small N and K, as well as large $E\left[p_{i,0}\right]$ and $E\left[|p_{i,0}|^2\right]$ (which requires small $\beta_i T_b$) lead to small a, which consequently gives better BER performance. In (4.19), channel correlation, reflected by the eigenvalues of channel matrix, affects the BER performance. Better performance can be achieved with lower correlation levels [28]. Since we simply treated the MAI as Gaussian noise and assumed perfect power control, we couldn't see in (4.19) each single user's interference but all the MAIs from different users as a whole.

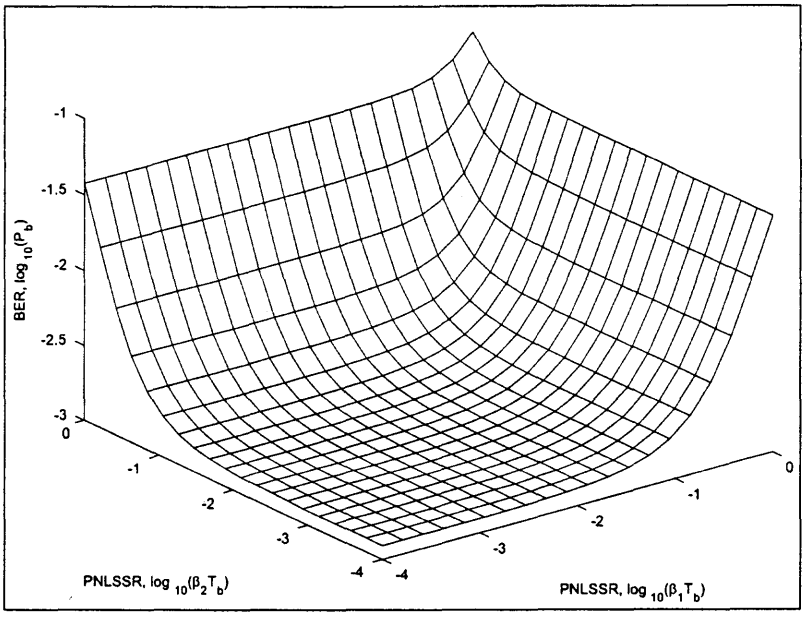

Figure 4.1 BER vs. phase noise linewidth to subcarrier spacing ratio $\beta_1 T_b$ and $\beta_2 T_b$, with K=2 users , N=64 subcarriers, maximum channel delay spread $\tau_{\max} = 0.25T_b$, and SNR=10dB.

The average BER for the receiver, expressed by $P_b = \frac{1}{K}\sum_{i=1}^{K} P_{b,i}$, can thus be written as [30]

$$P_b = \frac{1}{2K}\sum_{i=1}^{K}\sum_{n=0}^{N-1} \frac{\lambda_n^{N-2} a \left\{1 - e^{\frac{1}{4a^2\lambda_n^2}} \operatorname{erf} c\left(\frac{1}{\sqrt{2}a\lambda_n}\right)\right\}}{\prod_{j=0, j\neq n}^{N-1}(\lambda_n - \lambda_j)} \tag{4.20}$$

When β_k's are identical, and $|h_{k,n}|'s$ are independent from user to user, P_b can be simplified as $P_b = P_{b,i}$. Therefore the BER of each user is the same as the average BER of the receiver in the uplink of an MC-CDMA system.

4.2.3 Numerical Results

To illustrate the effects of phase noise on MC-CDMA, the relationship between the BER and the PNLSSR from all transmitters has been depicted in Fig.4.1-4.2 using (4.19) and (4.20).

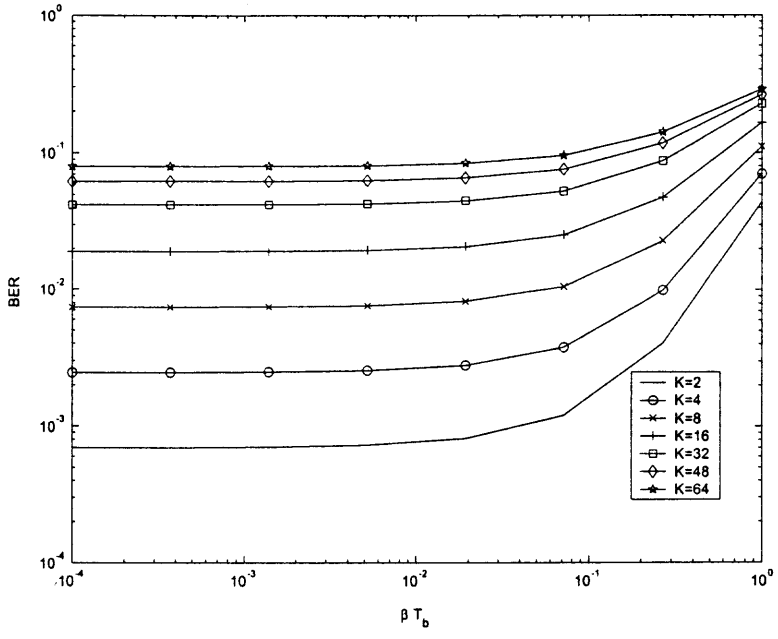

Figure 4.2 BER vs. phase noise linewidth to subcarrier spacing ratio βT_b, where N=64 subcarriers, maximum channel delay spread $\tau_m = 0.1T_b$, and SNR=10dB.

We have shown in (4.20) that the average BER is a function of PNLSSRs $\{\beta_i T_b\}_{i=1}^{K}$. Fig. 4.1 demonstrates how the BER changes with PNLSSRs when there are two active users with different phase noise linewidths. It can be seen that, if any transmitter generates phase noise with high PNLSSR, it always causes severe degradation of uplink MC-CDMA receiver performance, regardless of the performance of other transmitters. As a result, the ICI, indicated by I_2 and I_3 in (4.3), accounts for an important part of interference to the desired signal at the receiver side. This figure suggests that the effects of phase noise can be negligible only if all transmitters are good enough to make their PNLSSRs less than the order of 10^{-2}. Consequently, we have a stable receiver performance for this phase level. Note that the average BER performance versus PNLSSRs for $K > 2$ requires R-dimensional ($R \geq 4$) plot, which is quite hard in practice. That is why we focus on the two-user case in Fig. 4.1.

For many users' ($K \geqslant 2$) case, the phase noise linewidth β_i's for all transmitters are set to the same value β (and therefore the same PNLSSR βT_b) in Fig. 4.2. It has been shown in this figure that, with a fixed number of subcarriers N and the same channel conditions, the system performs worse when number of users K increases. As we know from (4.3) that I_1 and I_2 are MAI-related terms, increasing number of users K makes larger the energy of I_1 and I_2, leading to the worse BER performance. As shown in Fig. 4.2, when K is close or equal to N, number of subcarriers, MAI becomes such a dominant part of interference that BER changes little even with the ICI caused by severe phase noise.

4.3 Multiple Phase Noise Mitigation

The methods for MPN mitigation could be different from system to system, depending on the data structure or parameter settings. Nevertheless, they all have the same principle. Therefore, it is customary to concentrate on the typical OFDM/space division multiple access (OFDM/SDMA) approach, while the conclusions for this system could be readily extended to other systems, such as MC-CDMA.

Space division multiple access (SDMA) is a spectrum efficient technique, which, by implementing a receiver antenna array, provides spatial diversity allowing multiple users to share the same spectrum, and thus significantly increase system capacity. The signals from different users can be effectively separated by using their spatial signatures, i.e., their unique channel transfer functions.

The combined OFDM/SDMA approach has raised a lot of interest recently [31–34], as it appears to be excellent extension of IEEE 802.11a standard by exploiting the advantages of both OFDM and SDMA. A typical case of the OFDM/SDMA systems uses an array of antennas at the base station and single antenna at each user terminal (multiple terminal transmit simultaneously), which results in a greatly improved system capacity but keeps the cost of the user terminals low [31]. Different

types of multi-user detectors (MUD) have been developed for OFDM/SDMA to mitigate the interference among simultaneous users [31, 33, 34]. However, all these methods assume perfect frequency and phase synchronization, and thus ignore the sensitivity of OFDM to random phase noise which is caused by the fluctuation of oscillators both at the transmitter and receiver. Even though various methods have been proposed in the literature [20, 23] to mitigate phase noise, they are suitable with single phase noise. Hence, we propose in this chapter a correction scheme to mitigate the multiple phase noise effects in an OFDM/SDMA approach.

The organization of this section is as follows. In Section 4.3.1, the OFDM/SDMA system model is shown and conventional minimum mean square error (MMSE) MUD is introduced. In Section 4.3.2, we first specify the effects of multiple phase noise on OFDM/SDMA systems, and then propose a multiple phase noise correction (MPNC) scheme in Section 4.3.3 to mitigate the effects of multiple phase noise. Numerical results are presented in Section 4.3.4 to illustrate the effectiveness of the proposed scheme.

4.3.1 OFDM/SDMA System Model

We consider a synchronous uplink OFDM/SDMA system with M active users with its system model shown in Fig. 4.3. Each base station has an array of L antennas ($M \leq L$) while several user terminals simultaneously communicate with base station. To be cost effective, each user terminal has one single antenna. User m out of M active users feeds incoming parallel data into length-N IDFT to obtain the time-domain data sequence. After the insertion of cyclic prefix, data is upconverted and transmitted through multipath fading environment. At the base station, data is received by antenna l ($l = 1, 2, ..., L$) and downconverted. After removing the cyclic prefix and taking length-N DFT, we end up with the kth ($k = 0, 1, ..., N-1$) frequency-domain

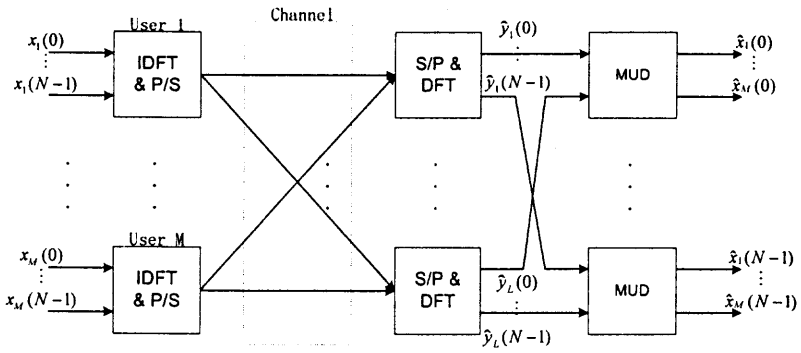

Figure 4.3 OFDM/SDMA system model

subcarrier signal received by the lth antenna

$$y_l(k) = \sum_{m=1}^{M} h_{ml}(k)x_m(k) + n_l(k) \tag{4.21}$$

where $x_m(k)$ and $h_{ml}(k)$ denote the mth user's transmitted signal and the frequency domain channel gain between the mth user and the lth receiver antenna respectively; $n_l(k)$ is the zero mean AWGN noise with variance σ^2. The signal energy is equal to unity, i.e., $E\left[|x_m(k)|^2\right] = 1$. We assume a multipath fading channel which is time invariant within the whole block as shown in [4].

Equation (4.21) can be rewritten using matrices as

$$\mathbf{y}_k = \mathbf{H}_k\mathbf{x}_k + \mathbf{n}_k \tag{4.22}$$

where

$$\mathbf{y}_k = \begin{bmatrix} y_1(k) & y_2(k) & \cdots & y_L(k) \end{bmatrix}^T,$$

with $(\cdot)^T$ denoting transpose operation; $\mathbf{x}_k$ and $\mathbf{n}_k$ take the same form of $\mathbf{y}_k$; while

$$\mathbf{H}_k = \begin{bmatrix} h_{11}(k) & h_{12}(k) & \cdots & h_{1M}(k) \\ h_{21}(k) & h_{22}(k) & \cdots & h_{2M}(k) \\ \vdots & \vdots & \ddots & \vdots \\ h_{L1}(k) & h_{L2}(k) & \cdots & h_{LM}(k) \end{bmatrix}$$

MUD for OFDM/SDMA has previously been discussed and different solutions have been provided in the literature [31,32,34]. In particular, MMSE-MUD has been known to have good performance with lower computational complexity than other schemes. The basic idea of MMSE-MUD is to separate the signals of the simultaneous users by MMSE linear filtering , which implicitly makes a trade-off between multiuser interference and noise amplification [31]. Specifically, with the channel estimate $\tilde{\mathbf{H}}_k$, the MMSE filter is expressed by

$$\mathbf{G} = \tilde{\mathbf{H}}_k^H (\tilde{\mathbf{H}}_k \tilde{\mathbf{H}}_k^H + \sigma^2 \mathbf{I})^{-1}$$

which yields the estimate of $\mathbf{x}_k$ [31]

$$\begin{aligned} \tilde{\mathbf{x}}_k &= \mathbf{G}\mathbf{y}_\mathbf{k} \\ &= \tilde{\mathbf{H}}_k^H (\tilde{\mathbf{H}}_k \tilde{\mathbf{H}}_k^H + \sigma^2 \mathbf{I})^{-1} \mathbf{y}_k \end{aligned} \tag{4.23}$$

4.3.2 The Effects of Multiple Phase Noise

For the uplink OFDM/SDMA systems, multiple user terminals give rise to multiple phase noise which behaves as a random phase factor on each time-domain signal before DFT. To reflect the phase noise effects, the expression of (4.21) is subsequently modified to

$$\begin{aligned} y_l(k) &= \sum_{m=1}^{M} h_{ml}(k) c_m(0) x_m(k) + \\ &\quad \sum_{m=1}^{M} \sum_{n=0, n\neq k}^{N-1} h_{ml}(n) c_m(n-k) x_m(n) + n_l(k) \end{aligned} \tag{4.24}$$

where $c_m(n) = \frac{1}{N}\sum_{k=0}^{N-1} e^{j2\pi kn + j\phi_m(k)}$ with $\phi_m(k)$ denoting the phase noise for the mth user. Since $\phi_m(k)$'s are generated by different users, they are independent of each other. The variance of $\phi_m(k)$ is given by $2\pi\beta_m T$, where β_m and T denote the phase noise linewidth and the OFDM symbol duration respectively. It can be seen from (4.24) that phase noise contributes to:

1. a number of CPEs indicated by $\{c_m(0)\}_{m=1}^{M}$;
2. ICI shown by $\sum_{m=1}^{M}\sum_{n=0,n\neq k}^{N-1} h_{ml}(n)c_m(n-k)x_m(n)$.

The consequences of multiple phase noise are different from that of single phase noise. First, the CPE term $c_m(0)$'s varies according to index m and therefore depend on users. They need to be obtained separately for each user. Second, the ICI from a certain user not only affects himself, but also all the other users due to the simultaneous access.

Referring to (4.22), (4.24) further leads to

$$\mathbf{y}_k = \mathbf{H}_k\mathbf{C}\mathbf{x}_k + \acute{\mathbf{n}}_k \tag{4.25}$$

where $\acute{\mathbf{n}}_k$ is still a $L \times 1$ vector like $\mathbf{n}_k$, but with its lth element denoting the ICI plus AWGN noise term $\sum_{m=1}^{M}\sum_{n=0,n\neq k}^{N-1} h_{ml}(n)I_m(n-k)x_m(n) + n_l(k)$; and $\mathbf{C}$ is a diagonal matrix indicated by $\mathbf{C} = \mathbf{diag}\begin{pmatrix} c_1(0) & c_2(0) & \cdots & c_M(0) \end{pmatrix}$.

4.3.3 Multiple Phase Noise Correction (MPNC)

In the OFDM/SDMA approach where multiple phase noise exist due to the simultaneous access of several user terminals, multiple phase noise correction is required to recover system performance.

We are concerned with medium to small phase noise levels where post-DFT phase noise mitigation is feasible. As described in [11], CPE amounts to over 90% phase noise energy while ICI is relatively small in comparison to CPE. That is, for frequency-domain correction, even though considering both CPE and ICI would yield

better result, CPE correction alone helps save the major performance loss due to phase noise. Furthermore, spatial diversity provided by SDMA also helps the CPE estimator performance. Therefore, multiple CPE estimation and correction, which is different from single-phase-noise case, raises our interest.

As we have known, OFDM/SDMA channel estimation uses the preamble of each transmitted block [31,32]. With frequency-domain channel estimation methods developed in [31], we can get accurate channel estimate represented by $\tilde{\mathbf{H}}_k$. Furthermore, CPE estimation is also necessary to mitigate the effects of multiple phase noise.

To estimate CPE, (4.25) can be rewritten as

$$\mathbf{y}_k = \mathbf{H}_k \mathbf{X}_k \mathbf{c} + \acute{\mathbf{n}}_k \tag{4.26}$$

where $\mathbf{X}_k = diag(\mathbf{x}_k)$ and $\mathbf{c} = \begin{bmatrix} c_1(0) & c_2(0) & \cdots & c_M(0) \end{bmatrix}^T$. Note that $\mathbf{c}$ varies from symbol to symbol due to the random phase noise, and therefore needs to be estimated per symbol basis. With N_p pilot subcarrier signals (the pilot set termed as S_p) , for any $p \in S_p$, the minimization of the cost function $\|\mathbf{y}_p - \mathbf{H}_p \mathbf{X}_p \mathbf{c}\|^2$ leads to the estimate of CPE vector $\mathbf{c}$ [35]

$$\begin{aligned} \hat{\mathbf{c}}_p &= (\mathbf{X}_p^H \tilde{\mathbf{H}}_p^H \tilde{\mathbf{H}}_p \mathbf{X}_p)^{-1} \mathbf{X}_p^H \tilde{\mathbf{H}}_p^H \mathbf{y}_p \\ &= \mathbf{X}_p^{-1} \left(\tilde{\mathbf{H}}_p^H \tilde{\mathbf{H}}_p \right)^{-1} \tilde{\mathbf{H}}_p^H \mathbf{y}_p \end{aligned} \tag{4.27}$$

Equation (4.27) actually gives rise to the least-square (LS) estimate of $\mathbf{c}$. As $\mathbf{c}$ is invariant within an OFDM symbol [11,15], if several pilots are available within a symbol, the estimate represented by (4.27) can be further improved by [35]

$$\hat{\mathbf{c}} = \frac{1}{N_p} \sum_{k \in S_p} \hat{\mathbf{c}}_p \tag{4.28}$$

Note that increasing the number of pilots N_p will give more accurate estimation results. However, larger N_p leads to higher computational complexity and decreases

spectral efficiency. Therefore, to choose a proper value for N_p, there is always a trade-off between performance and spectral/computational efficiency. We will show by simulation that both performance and efficiency can be guaranteed by using only a few pilots.

The estimated CPE is then applied to MMSE-MUD to yield better performance. In particular, in terms of (4.28), the data estimate in (4.23) is modified to [35]

$$\tilde{\mathbf{x}}_k = [diag(\hat{\mathbf{c}})]^{-1} \tilde{\mathbf{H}}_k^H (\tilde{\mathbf{H}}_k \tilde{\mathbf{H}}_k^H + \sigma^2 \mathbf{I})^{-1} \mathbf{y}_k \tag{4.29}$$

Note that in the presence of multiple phase noise, the channel estimation accuracy is affected by the CPE of the preamble. In fact, equation (4.25) shows that, instead of $\mathbf{H}_k$, the channel estimation methods described in [31] and [32] actually gives the estimate of $\mathbf{H}_k \mathbf{C}_1$, where $\mathbf{C}_1$ is the CPE matrix of the preamble. As a result, equation (4.27) and (4.28) actually lead to the estimate of $\mathbf{C}_1^{-1}\mathbf{c}$. Therefore, in the presence of multiple phase noise, its correction provided by the estimate of (4.29) is quite necessary as:

1. it corrects the phase rotation error for all subcarrier signals within a specific symbol;

2. it compensates for the deviation of channel estimate introduced by CPE of the preamble $\mathbf{C}_1$.

From this standpoint, CPE estimation not only corrects phase noise rotation, but also helps to correct the increased channel estimation errors due to phase noise.

4.3.4 Numerical Results

The proposed MPNC scheme is evaluated in this section for Rayleigh fading channels by Monte Carlo trials. The OFDM data of each user are constructed based on the IEEE 802.11a standard. However, channel coding is not used in our simulations since we focus on symbol error rate (SER). The base station has four antennas to separate

up to four users by SDMA. Each user occupies 20MHz bandwidth which consists of 64 subcarriers. QPSK modulation is used in the simulation. The preamble of each data block is designated for channel estimation. The number of pilots for MPNC is not fixed (e.g., four pilots per data symbol in IEEE802.11a standard [4]), but was changed in some of our simulations to evaluate its effect on performance and find its most suitable value. The length of cyclic prefix is always larger than channel delay spread. The simulation parameters is summarized in Table 4.1.

Table 4.1 Simulation parameters for phase noise correction in OFDM/SDMA systems

Parameter	Value
bandwidth for each user	20 MHz
number of subcarriers	$N = 64$
modulation method	QPSK
number of antennas	$L = 4$
number of simultaneous users	$M = 4$

Fig. 4.4 shows the SER performance of MPNC in comparison to no-phase-noise and no-phase-noise-correction cases. Four pilots are used in this simulation, i.e., $N_p = 4$. We can see that multiple phase noise results in large impairment of system performance such that phase noise correction must be considered. On the other hand, the proposed MPNC scheme results in the performance close to no-phase-noise case. It gives approximately 0-2 dB performance loss compared with no-phase noise case, when the number of users is less than the number of receiver antennas. However, performance loss increases if all users simultaneously communicate with the base station, e.g., there is about 5dB loss for the four-user case in Fig. 4.4. This implies that more users introduces more multiuser interference, which affects the accuracy of CPE estimation.

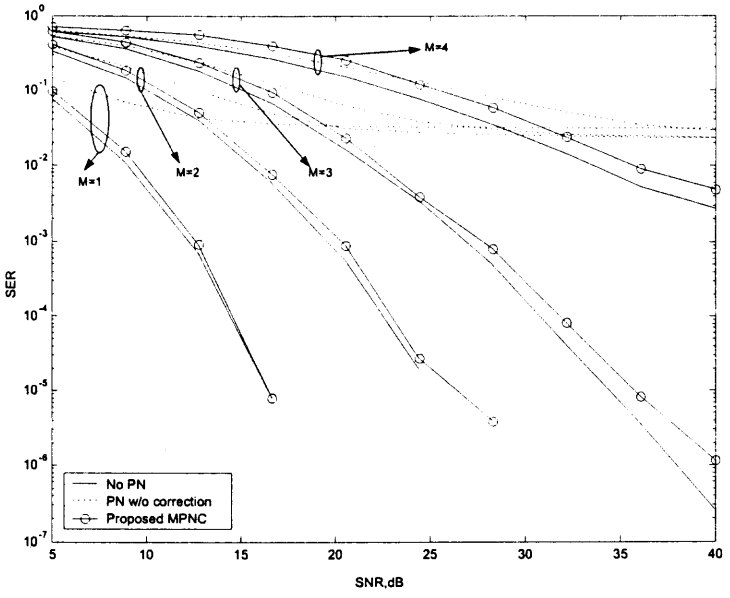

Figure 4.4 SER versus SNR, 1-4 simultaneous users with PN variance 10^{-2}, pilot number $N_p = 4$

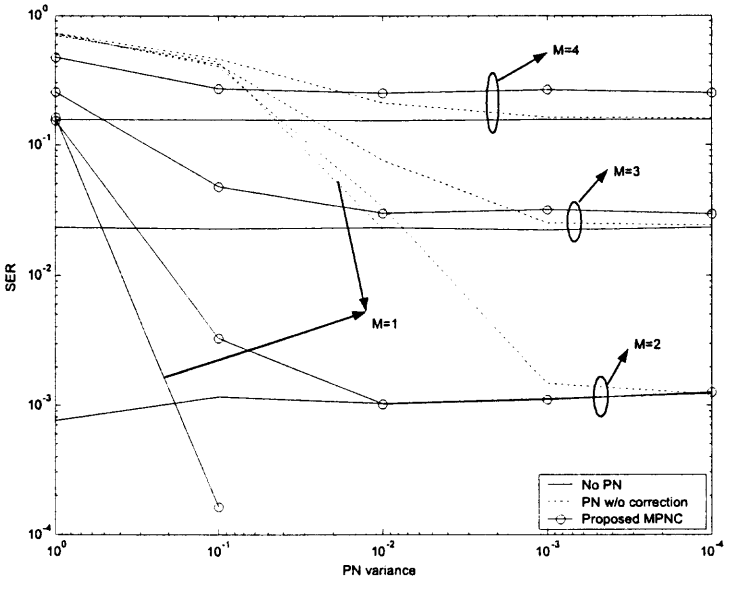

Figure 4.5 SER versus PN variance levels, 1-4 simultaneous users with SNR= 20dB, pilot number $N_p = 4$

Fig. 4.5 demonstrates how the performance of the proposed scheme changes with phase noise levels. It shows that when phase noise variance is greater than 10^{-3}, the OFDM/SDMA receiver, without phase noise mitigation, suffers remarkable performance degradation. However, the proposed MPNC provides significant performance improvement over no-phase-noise-correction case. This is quite adequate as the aim of the proposed scheme is to correct medium to small phase noise, i.e., for phase noise variance less than 10^{-1}.

For the phase noise variance range $[10^{-3}, 10^{-1})$, the illustrated SER performance is satisfactory when working in the combined OFDM/SDMA approach. In fact, this working range $[10^{-3}, 10^{-1})$ of MPNC fits the practical consideration of phase noise levels in any OFDM systems.

When phase noise variance is less than 10^{-3}, we notice an the error floor for both three-user and four-user cases due to multiple user interference. Whereas, as phase noise under this situation is so small, one can hardly see the effects of multiple phase noise. Hence, the performance of the no-phase-noise-correction case approaches that of no-phase-noise case. In other words, when phase noise variance is less than 10^{-3}, it is so small that there even necessary to take the proposed MPNC or any other schemes to correct multiple phase noise for this phase noise variance range.

Fig. 4.6-4.7 illustrate how the number of pilots N_p affects the performance of the MPNC scheme when the number of users is 1/2 and 3/4 respectively. It is quite straightforward that more pilots give rise to a better performance. However, we would like to know how many pilots we need to guarantee a certain performance level while keeping the computational complexity as low as possible. As can be seen in these two figures, the performance differences are quite noticeable for the value of N_p changing from 1 to 8, but hard to tell when N_p is greater than or equal to 8. This is true for one to four users. Therefore, $N_p = 8$ gives a good trade-off between good

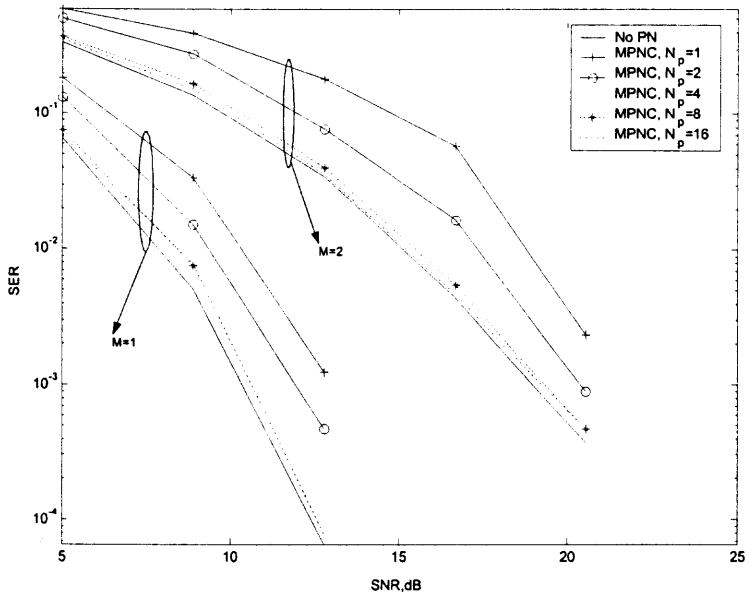

Figure 4.6 SER versus SNR, 1-2 simultaneous users with PN variance 10^{-2}

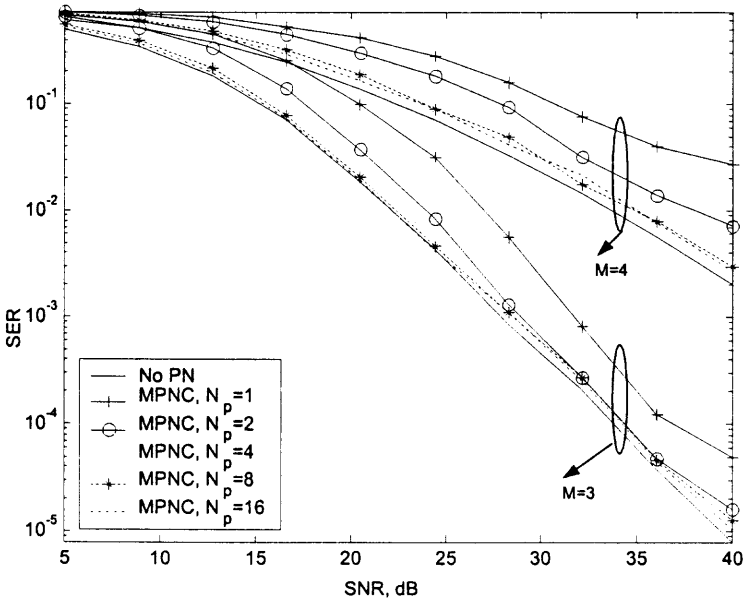

Figure 4.7 SER versus SNR, 3-4 simultaneous users with PN variance 10^{-2}

performance and low computational complexity. 12.5% spectrum is occupied for the pilot allocation.

4.4 Conclusions

The BER performance of an uplink MC-CDMA system has been analyzed in the presence of multiple phase noise and correlated Rayleigh fading environments. Both multiple access interference (MAI) and inter-carrier interference (ICI) are considered in this chapter. The BER expression has been determined to depict system performance. For a multiple access environment, if any transmitter has the phase noise linewidth greater than 10^{-2}, the ICI becomes so noticeable at the receiver side that the MC-CDMA system performance suffers severe degradation due to ICI. However, multiple access causes the major interference to a MC-CDMA system with the phase noise linewidth of all transmitters below 10^{-2}. As the number of users increases, the MAI accounts for more interference, leading to the worse BER performance. In summary, a small number of subcarriers and users, as well as small PNLSSRs for all transmitters, are preferred for good receiver performance.

While several methods have been developed in the literature to correct single phase noise, they do not apply for systems with multiple phase noise, such as OFDM/SDMA. In this chapter, a new multiple phase noise correction scheme has been proposed to mitigate the effects of multiple phase noise originated from multiple user terminals that simultaneously communicate in the uplink OFDM/SDMA systems. This scheme aims to compensate for CPE, the major effect of phase noise for medium to low phase noise levels where phase noise correction is possible. The proposed scheme effectively mitigates the effects of multiple phase noise and significantly improves the performance of OFDM/SDMA systems. With few pilots involved per user, the proposed scheme presents quite a satisfactory performance. Numerical results show the effectiveness of MPNC when dealing with multiple phase noise in the uplink

OFDM/SDMA systems. Moreover, the MPNC scheme is applicable and stable within a wide range of phase noise levels, which shows its potential in practical applications.

CHAPTER 5

GENERALIZED PHASE NOISE MITIGATION APPROACHES

5.1 Introduction

As we discussed earlier, phase noise mitigation could be done in the time domain or in the frequency domain respectively. The frequency domain approach proves to be more practical and we have proposed several mitigation methods.

In the presence of phase noise, each received subcarrier signal (excluding AWGN noise) is actually the weighted sum of all transmitted signals multiplied by the corresponding channel response in the frequency domain. Moreover, CPE and ICI are both functions of those weighting coefficients, so that, once we obtain those weighting coefficients, phase noise can be readily mitigated. Based on this observation, two general approaches are proposed to estimate these phase noise parameters. It proves that the conventional approaches, either in the time domain, or in the frequency domain, can be readily obtained from our new methods with some simple approximation or orthogonal transform. After the phase noise parameters are estimated, different implementation methods are further discussed for phase noise mitigation. Numerical results are also provided to illustrate the effectiveness of the proposed schemes.

This chapter is organized as follows. The new approaches for phase noise mitigation are proposed in Section 5.2, and performance analysis is presented in Section 5.3. Section 5.4 gives the numerical results to demonstrate the effectiveness of the proposed schemes compared with others. Section 5.5 concludes this chapter.

5.2 Phase Noise Mitigation

5.2.1 Phase Noise Vector Estimation

Frequency Domain Parameters As discussed in the previous chapter, equation (3.18), which gives

$$\mathrm{y} = \mathbf{W}\mathrm{c} + \mathbf{n} \tag{5.1}$$

depicts the frequency-domain vector **c** resulting from time-domain phase noise. Furthermore, it is shown that

$$\mathbf{W} = \begin{pmatrix} a_0 & a_1 & \cdots & a_{N-1} \\ a_1 & a_2 & \cdots & a_0 \\ \vdots & \vdots & \ddots & \vdots \\ a_{N-1} & a_0 & \cdots & a_{N-2} \end{pmatrix} \tag{5.2}$$

with $a_k = x_m(k)h(k)$. The frequency domain approach of phase noise mitigation is to find the vector **c** and compensate for it.

Time Domain Parameters Equation (1.11) can be rewritten in matrix form as

$$\mathrm{c} = \frac{1}{\sqrt{N}}\mathbf{F}^H\mathrm{t} \tag{5.3}$$

where $\mathrm{t} = \left[e^{j\phi(0)}, e^{j\phi(1)}, ..., e^{j\phi(N-1)}\right]^T$, and **F** is the DFT matrix denoted by

$$F = \frac{1}{\sqrt{N}} \begin{pmatrix} 1 & 1 & \cdots & 1 \\ 1 & e^{-j2\pi/N} & \cdots & e^{-j2\pi(N-1)/N} \\ \vdots & \vdots & \ddots & \vdots \\ 1 & e^{-j2\pi(N-1)/N} & \cdots & e^{-j2\pi(N-1)(N-1)/N} \end{pmatrix} \tag{5.4}$$

Equation (5.3) is equivalent to

$$\mathrm{t} = \sqrt{N}\mathbf{F}\mathrm{c} \tag{5.5}$$

Equation (5.5) shows that, vector **t** is simply the FFT output of the desired vector **c**. Therefore, once we obtain the frequency domain vector **c** using some

estimator, we can get the time domain vector $\mathbf{t}$. This indicates that these two vectors are equivalent from the estimation point of view. Hereinafter, we will focus on different estimation techniques in the frequency domain, since the extension of those methods to the time domain is quite straightforward using (5.5).

5.2.2 Maximum Likelihood Estimation (MLE)

For a Gaussian random variable shown in (5.1), the maximum likelihood estimation (MLE) is a method that asymptotically achieves Cramer-Rao lower bound (CRLB) [27]. This phase noise estimation method was first introduced by us in [36] for phase noise estimation and was termed as simultaneous CPE and ICI correction (SCIC) in Section 3.4, wherein the MLE of frequency-domain vector $\mathbf{c}$ is derived as,

$$\check{\mathbf{c}}_{ml} = \mathbf{W}^{-1}\mathbf{y} \tag{5.6}$$

If we consider a subset of c, say, only the first element c_0, (5.6) reduces to CPEC introduced in [2

For the time domain approach, (5.5) simply gives

$$\check{\mathbf{t}}_{ml}=\sqrt{N}\mathbf{F}\check{\mathbf{c}}_{ml} \tag{5.7}$$

Note that the time domain approach proposed in [24] actually leads to the same estimate as (5.7) when the number of pilots equals the number of subcarriers N. In other words, (5.6) and the approach in [24] indicate the same estimator from the frequency domain and time domain point of view, respectively.

5.2.3 Linear Minimum Mean Square Error Estimation (LMMSEE)

MLE does not include the effect of AWGN noise in the estimator. For the received signals in (5.1), the linear minimum mean square error estimation (LMMSEE), which

considers AWGN noise, gives [27]

$$\breve{\mathrm{c}}_{ml} = \mathbf{R}_{cy}\mathbf{R}_{yy}^{-1}\mathbf{y} \tag{5.8}$$

It is readily shown that

$$\mathbf{R}_{cy} = E\left[\mathrm{c}\mathbf{y}^H\right] = \mathbf{R}_c\mathbf{W}^H \tag{5.9}$$

and

$$\mathbf{R}_y = E\left[\mathbf{y}\mathbf{y}^H\right] = \mathbf{W}\mathbf{R}_c\mathbf{W}^H + \sigma^2\mathbf{I} \tag{5.10}$$

with $\mathbf{R}_c = E\left[\mathbf{c}\mathbf{c}^H\right]$. In terms of (1.7), we denote $\mathbf{R}_c$ by

$$[\mathbf{R}_c]_{mn} = e^{-\pi\beta T|m-n|/N}, \text{ with } m, n \in [1, N]$$

Substituting (5.9) and (5.10) into (5.8) yields

$$\breve{\mathrm{c}}_{lmmse} = \mathbf{R}_c\left[\mathbf{R}_c + \sigma^2\left(\mathbf{W}^H\mathbf{W}\right)^{-1}\right]^{-1}\mathbf{W}^{-1}\mathbf{y} \tag{5.11}$$

Likewise, (5.5) give the time-domain estimator

$$\breve{\mathrm{t}}_{lmmse} = \sqrt{N}\mathbf{F}\breve{\mathrm{c}}_{lmmse} \tag{5.12}$$

As can be seen in (5.12), the LMMSEE requires the statistics of phase noise as well as AWGN noise. In other words, the LMMSEE depends on phase noise linewidth β, AWGN noise variance σ^2. Similarly, PNS algorithm in [20] is just a special case of the estimator in (5.11) by only estimating the first element of c, c_0, and approximating the ICI as noise.

Remark 1 *We show that conventional frequency-domain approaches are the special cases of our methods. Rewrite (5.1) as*

$$\mathbf{y} = u_0 c_0 + \acute{\mathbf{n}} \tag{5.13}$$

where $\acute{\mathbf{n}} = \begin{pmatrix} w_1 & \cdots & w_{N-1} \end{pmatrix} \cdot \mathbf{c}^1 + \mathbf{n}$, *with* $\mathbf{c}^1$ *denoting the vector* $\mathbf{c}$ *without the first element. This data expression implies that ICI is approximated as a Gaussian random variable. This is true for small phase noise and large number of subcarrier* N*. In this case, the CPE factor* c_0 *is the major consequence of phase noise. Therefore, it may be sufficient to estimate* c_0 *using the ML method [23], or using the MMSE method for better performance [20]. This suggests that conventional frequency domain methods, such as those in [23] and [20], are just the simplifications of the methods proposed in the paper by estimating a subset of the weighting coefficient vector. The advantage of these simplified approaches is the reduction of computational complexity.*

Remark 2 *Conventional time-domain approaches, such as the one proposed in [24] give the corresponding time-domain expression of our estimated vector by applying IDFT to both sides of (5.6) or (5.11), as shown in (5.7) or (5.12). However, it is worth mentioning that [24] claims that, using orthogonal transforms, e.g., DFT or DCT, the* N*-element phase noise vector* t *in the time domain could be obtained from* L *parameters, which are estimated using* M $(L \leq M \leq N)$ *pilot signals. Nevertheless, it is readily understood that there is no guarantee that such a orthogonal transform, from* $L \times 1$ *vector to* $N \times 1$ *vector with* $L \leq N$*, does always exist, when both vectors are deterministic. In other words, some approximation may be necessary to achieve such a transform in some situations. Therefore,* L *can not be much less than* N *in order to make the approximation applicable. On the other hand, since the condition* $L \leq M \leq N$ *must be satisfied, a large number of pilots* M *is necessary which significantly decreases spectral efficiency, especially when random phase noise is presented which requires symbol-by-symbol phase noise mitigation.*

Alternatively, our approaches have high spectral efficiency by taking advantage of decision feedback. Moreover, unlike [24] where only the performance of AWGN channel is verified, we explicitly deals with fading channels.

5.2.4 Complexity Reduction

The MLE and LMMSEE methods require the inversion of the matrix $\mathbf{W}$, which, in general, needs the major computations in the magnitude N^3. We extend circulant matrix theory in [37] and define $\mathbf{W}$ as a shift-backward circulant matrix, which means each row of $\mathbf{W}$ is the left circular shift of the previous row, and uniquely determined by its first row $\mathbf{w}_0 = \begin{pmatrix} a_0 & a_1 & \cdots & a_{N-1} \end{pmatrix}$.

It is shown that $\mathbf{W}$ can be decomposed as (see Appendix C)

$$\mathbf{W} = \mathbf{F}^H \mathbf{V} \mathbf{F} \mathbf{P} \tag{5.14}$$

where $\mathbf{F}$ is the DFT matrix and $\mathbf{V}$ is a diagonal matrix defined in (C.8). The inversion of $\mathbf{W}$ is then given by

$$\mathbf{W}^{-1} = \mathbf{P}^{-1} \mathbf{F}^H \mathbf{V}^{-1} \mathbf{F} = \mathbf{P} \mathbf{F}^H \mathbf{V}^{-1} \mathbf{F} \tag{5.15}$$

where we used $\mathbf{P}^{-1} = \mathbf{P}$ with respect to its definition in (C.3). Substituting (5.15) into the MLE (5.6) and the LMMSEE (5.11) gives rise to

$$\check{\mathbf{c}}_{ml} = \mathbf{P} \mathbf{F}^H \mathbf{V}^{-1} \mathbf{F} \mathbf{y} \tag{5.16}$$

On the other hand, Matrix Inversion Lemma gives

$$\left(\mathbf{P}^{-1} + \mathbf{A}^H \mathbf{B} \mathbf{A}\right)^{-1} = \mathbf{P} - \mathbf{P} \mathbf{A}^H \left(\mathbf{A} \mathbf{P} \mathbf{A}^H + \mathbf{B}^{-1}\right)^{-1} \mathbf{A} \mathbf{P} \tag{5.17}$$

it is shown that

$$\begin{aligned} & \mathbf{R}_c \left[\mathbf{R}_c + \sigma^2 \left(\mathbf{W}^H \mathbf{W}\right)^{-1}\right]^{-1} \\ =& \mathbf{I} - \mathbf{W}^{-1} \left[\left(\mathbf{W}^{-1}\right)^H \mathbf{R}_c^{-1} \mathbf{W}^{-1} + \sigma^{-2} \mathbf{I}\right]^{-1} \left(\mathbf{W}^{-1}\right)^H \mathbf{R}_c^{-1} \\ =& \mathbf{I} - \left[\mathbf{I} + \sigma^{-2} \mathbf{R}_c \mathbf{W}^H \mathbf{W}\right]^{-1} \end{aligned} \tag{5.18}$$

Substituting (5.14), (5.15) and (5.18) into (5.11) gives rise to

$$\begin{aligned} \check{\mathrm{c}}_{lmmse} &= \left\{\mathbf{I} - \left[\mathbf{I} + \sigma^{-2}\mathbf{R}_c\mathbf{W}^H\mathbf{W}\right]^{-1}\right\}\mathbf{W}^{-1}\mathbf{y}\mathbf{w} \\ &= \left\{\mathbf{I} - \left[\mathbf{I} + \sigma^{-2}\mathbf{R}_c\mathbf{P}\mathbf{F}^H\mathbf{V}^H\mathbf{V}\mathbf{F}\mathbf{P}\right]^{-1}\right\} \cdot \mathbf{P}\mathbf{F}^H\mathbf{V}^{-1}\mathbf{F}\mathbf{y} \end{aligned} \tag{5.19}$$

Note that,

1. The inversion of the diagonal matrix $\mathbf{V}$ is quite simple;
2. $\mathbf{P}$ is a simple permutation matrix;
3. Fourier transform matrix $\mathbf{F}^H$ or $\mathbf{F}$ can be implemented with fast algorithm;

Therefore, the computational complexity is significantly reduced with respect to the inversion of $\mathbf{W}$. It is worth mentioning that, the LMMSE needs the matrix inversion of the term $\mathbf{R}_c + \sigma^2\mathbf{P}\mathbf{F}^H\left(\mathbf{V}^H\mathbf{V}\right)^{-1}\mathbf{F}\mathbf{P}$.Even though the computational complexity may be further reduced using its symmetric structure, it's still more complex than the MLE.

5.2.5 Phase Noise Mitigation

Phase noise parameters have been estimated using either MLE or LMMSE approach. Therefore, we need to consider the implementations of these estimates. Two methods are proposed in this section for phase noise mitigation: decorrelator and interference canceler.

Decorrelator Rewrite (5.1) as

$$\mathrm{y} = \mathbf{C}\mathrm{w}_0 + \mathrm{n} = \mathbf{C}\mathbf{H}\mathbf{x} + \mathrm{n} \tag{5.20}$$

with $\mathbf{H} = diag\left(h\left(0\right), h\left(1\right), ..., h\left(N-1\right)\right)$, $\mathbf{x} = \left[x\left(0\right), x\left(1\right), ..., x\left(N-1\right)\right]^T$, and accordingly

$$\mathbf{C} = \begin{pmatrix} c_0 & c_1 & \cdots & c_{N-1} \\ c_{N-1} & c_0 & \cdots & c_{N-2} \\ \vdots & \vdots & \ddots & \vdots \\ c_1 & \cdots & c_{N-1} & c_0 \end{pmatrix} \tag{5.21}$$

Similar to $\mathbf{W}$, $\mathbf{C}$ is a circulant matrix determined by the estimated phase noise vector $\mathbf{c}$ given in (5.6) or (5.11). each row of $\mathbf{C}$ has the identical elements as the previous row, but with one-element circular shift to the right. Then, applying the decorrelation method to (5.20), the estimated data is given by

$$\hat{\mathrm{x}} = \mathbf{H}^{-1}\mathbf{C}^{-1}\mathbf{y} \tag{5.22}$$

The inversion of the $N \times N$ matrix $\mathbf{C}^{-1}$ requires the computational complexity of $O\left(N^3\right)$. This may not be acceptable in many cases. Whereas, we notice that the circulant matrix $\mathbf{C}$ can be readily diagonalized by [37]

$$\mathbf{C} = \mathbf{F}^H \wedge \mathbf{F} \tag{5.23}$$

where $\wedge$ is a diagonal matrix $\wedge = \mathbf{diag}\left[f\left(\mathbf{c}, 1\right), f\left(\mathbf{c}, e^{j\frac{2\pi}{N}}\right), ..., f\left(\mathbf{c}, e^{j\frac{2\pi(N-1)}{N}}\right)\right]$ with the polynomial function $f\left(\mathbf{c}, x\right)$ given in (C.7).

It's interesting to see that, in fact, the diagonal elements of $\wedge$ are just the IDFT of $\mathbf{c}$, i.e., $\wedge = \sqrt{N}\mathbf{diag}\left(\mathbf{F}^H\mathbf{c}\right)$.

Therefore, in terms of (5.23), (5.22) yields

$$\hat{\mathrm{x}} = \mathbf{H}^{-1}\mathbf{F}^H \wedge^{-1} \mathbf{F}\mathbf{y} \tag{5.24}$$

Equation (5.24) only involves the matrix multiplication and DFT computations. It's quite straightforward to see that the computational complexity are significantly reduced.

Interference Canceler As shown in (5.13), the received data can be expressed by

$$\begin{aligned} \mathbf{y} &= \mathrm{w}_0 c_0 + \mathbf{W}^1 \mathbf{c}^1 + \mathbf{n} \\ &= c_0 \mathbf{H}\mathbf{x} + \mathbf{W}^1 \mathbf{c}^1 + \mathbf{n} \end{aligned} \tag{5.25}$$

where $\mathbf{W}^1$ denotes the matrix $\mathbf{W}$ without the first column vector. Then, the estimated data is given by

$$\hat{\mathrm{x}} = \mathbf{H}^{-1} \check{c}_0^{-1} \left[\mathrm{y} - \mathbf{W}^1 \check{\mathbf{c}}^1 \right] \tag{5.26}$$

The methods has less computational complexity than the decorrelator, due to the fact that it does not require the inversion of matrix or even DFT.

5.2.6 Practical Considerations

Both ML and LMMSE techniques proposed in the paper requires *a priori* knowledge of matrix $\mathbf{W}$, which is determined by the transmitted signals and channel gains in the frequency domain. In other words, it is necessary to know:

1. Channel gains in the frequency domain;

2. All transmitted signals within an OFDM symbol.

In a high rate OFDM system, usually channel varies little within a data block. Therefore, all subcarriers of the preamble of each block is used for channel estimation as in [4]. Pilot assisted channel estimation is therefore feasible [25,26]. These channel estimates are accurate enough for our purpose.

Transmitted signals can be obtained from the tentative data, i.e., the initial estimate of data signals. These initial estimates can be accomplished by applying one of conventional CPE correction methods [20,23], and channel equalization to the received signals in the frequency domain.

Finally, the estimated channel and the tentative data apply to (5.6) and (5.11), leading to phase noise mitigation.

5.3 Performance Analysis

In this section, the performance of different estimation methods on system performance is discussed. the frequency-domain approach is of concern since the extension to the time domain is quite straightforward.

5.3.1 General Comparisons

1. It's well known that LMMSEE has a better performance than MLE by minimizing the mean square error of the estimation result. However, LMMSEE requires *a prior* knowledge of phase noise linewidth β and AWGN noise variance σ^2. Without them, MLE should be a better choice;

2. Both methods require the inversion of matrix which requires the computational complexity $O\left(N^3\right)$, but some mathematical methods, such as fast Fourier transform (FFT) algorithm, can be used to reduce the complexity. On the other hand, LMMSEE is more complex than MLE by requiring the extra computations for $\mathbf{I}-\left[\mathbf{I}+\sigma^{-2}\mathbf{R}_c\mathbf{P}\mathbf{F}^H\mathbf{V}^H\mathbf{V}\mathbf{F}\mathbf{P}\right]^{-1}$.we notice that, although phase noise $\phi_m\left(n\right)$ is non-stationary, the resulting random variable $e^{j\phi_m(n)}$, as shown in (1.7), is stationary, so is $\mathbf{R}_c$. Hence, once we know phase noise linewidth β, DFT length N and OFDM symbol period T, $\mathbf{R}_c$ can be pre-computed and stored for the processing of data.

3. For high signal to noise ratios (SNRs), i.e., $\sigma^2 \rightarrow 0$, (5.11) gives that $\check{\mathbf{c}}_{lmmse} \rightarrow \left\{\mathbf{I}-\left[\mathbf{I}+\sigma^{-2}\mathbf{R}_c\mathbf{P}\mathbf{F}^H\mathbf{V}^H\mathbf{V}\mathbf{F}\mathbf{P}\right]^{-1}\right\}\mathbf{W}^{-1}\mathbf{y}=\mathbf{W}^{-1}\mathbf{y}$, which is the same as (5.6). This implies that, for high SNRs, the performance of these two methods will stay close.

5.3.2 Computational Complexity

We first keep in mind that each complex multiplication is equivalent to four real multiplications plus two real additions, and each complex addition is equivalent to two real additions.

MLE This technique needs the inversion of $\mathbf{W}$, which requires computational complexity $O(N^3)$. By taking advantage of the properties of the circulant matrix, we successfully factorize $\mathbf{W}$ into four matrices with one being diagonal and the rest being unitary (some are DFT matrices). Since the inversion of a diagonal matrix is very straightforward, and the inversion of unitary matrices in (5.16) is also simple ($\mathbf{P}^{-1} = \mathbf{P}$, and $\mathbf{F}^{-1} = \mathbf{F}^H$), then the complexity reduction should be significant. To be specific, the following features are helpful in reducing complexity:

1. $\mathbf{P}$ is a simple permutation matrix which doesn't require complex multiplications or additions;

2. $\mathbf{F}^H$ or $\mathbf{F}$ can be implemented with fast algorithm;

3. $\mathbf{V}$ is a diagonal matrix with its elements related to the DFT of vector $\mathbf{w}_0$, or more specifically, $\{a_k\}_{k=0}^{N-1}$.

Complex multiplications and complex additions required for (5.16) are computed as approximately $3N^2$ and $3N^2 - 2N$, respectively. Considering that $\mathbf{F}$ is a DFT matrix and using FFT algorithm, the complexity is further reduced to $\frac{3N}{2}\log_2 N + N$ complex multiplications and $3N\log_2 N$ complex additions.

LMMSEE Equation (5.19) requires the extra computation of $\mathbf{I} - \left[\mathbf{I} + \sigma^{-2}\mathbf{R}_c\mathbf{P}\mathbf{F}^H\mathbf{V}^\mathbf{H}\mathbf{V}\mathbf{F}\mathbf{P}\right]^{-1}$ in comparison to (5.6).

1. $\mathbf{FP}$ involves permutation only. $\mathbf{V}\cdot(\mathbf{FP})$ requires N^2 complex multiplications and no extra calculations for $\mathbf{P}\mathbf{F}^H\mathbf{V}^\mathbf{H}$. Note also that the elements of $\mathbf{V}$ will be

available after finishing the computation of $\mathbf{PF}^H\mathbf{V}^{-1}\mathbf{Fy}$ in (5.19) and therefore no additional computations are needed;

2. The multiplication of $\mathbf{PF}^H\mathbf{V^H}$ with $\mathbf{VFP}$, when FFT algorithm is applied, needs $\frac{N^2}{2}\log_2 N$ complex multiplications and $N^2\log_2 N$ complex additions;

3. The multiplication of $\sigma^{-2}\mathbf{R}_c$ with $\mathbf{PF}^H\mathbf{V^HVFP}$ requires $N^3/2$ complex multiplications and $N^3/2$ complex additions;

4. The addition of $\mathbf{I}$ with $\sigma^{-2}\mathbf{R}_c\mathbf{PF}^H\mathbf{V^HVF}$ requires extra N complex additions;

5. The inversion of $\mathbf{R}_c\left(\mathbf{W}^H\mathbf{W}\right)+\sigma^2\mathbf{I}$ requires N^3 complex multiplications and N^3 complex additions respectively;

6. The addition of $\mathbf{I}$ with $\left[\mathbf{I}+\sigma^{-2}\mathbf{R}_c\mathbf{PF}^H\mathbf{V^HVFP}\right]^{-1}$ requires N complex additions;

7. The multiplication of $\mathbf{I}-\left[\mathbf{I}+\sigma^{-2}\mathbf{R}_c\mathbf{PF}^H\mathbf{V^HVFP}\right]^{-1}$ with $\mathbf{W}^{-1}\mathbf{y}$ requires N^2 complex multiplications and N^2 complex additions respectively.

In summary, LMMSE requires approximately extra $\frac{3N^3+N^2\log_2 N+2N^2}{2}$ complex multiplications and $\frac{3N^3}{2}+N^2\log_2 N+N^2+2N$ complex additions, which are much more than $\frac{3N}{2}\log_2 N+N$ complex multiplications and $3N\log_2 N$ complex additions required by MLE. This turns out to be a relatively large complexity increase in many applications.

5.3.3 Mean Square Error

For both MLE and LMMSEE, it is readily understood that LMMSEE would yield better performance and the mean square errors (MSEs) of these two methods could be found in [27]. It is of interest to compare the performance of different implementation techniques for phase noise mitigations, i.e., decorrelator and interference canceler, with the same estimation errors.

It is assumed that the estimate has the form $\hat{\mathbf{c}} = \mathbf{c} + \mathbf{e}$, where $\mathbf{e}$ denotes the estimation error which is Gaussian distributed with zero mean and the normalized variance σ_e^2. Then we have $\curlywedge = \mathbf{diag}\left(f_{\breve{\mathbf{c}}}(1), f_{\breve{\mathbf{c}}}\left(e^{j\frac{2\pi}{N}}\right), ..., f_{\breve{\mathbf{c}}}\left(e^{j\frac{2\pi(N-1)}{N}}\right)\right)$, while $\wedge = \mathbf{diag}\left(f_{\mathbf{c}}(1), f_{\mathbf{c}}\left(e^{j\frac{2\pi}{N}}\right), ..., f_{\mathbf{c}}\left(e^{j\frac{2\pi(N-1)}{N}}\right)\right)$.

Decorrelator From (5.20) and (5.24), it is readily shown that

$$\begin{aligned} & E\left[||\mathbf{x}-\hat{\mathbf{x}}||^2\right] \\ = \; & E\left[\left|\left|\mathbf{x}-\mathbf{H}^{-1}\mathbf{F}^H\curlywedge^{-1}\mathbf{F}\left(\mathbf{CHx}+\mathbf{n}\right)\right|\right|^2\right] \\ = \; & E\left[\left|\left|\mathbf{H}^{-1}\mathbf{F}^H\mathbf{BFHx}-\mathbf{H}^{-1}\mathbf{F}^{\mathbf{H}}\curlywedge^{-1}\mathbf{Fn}\right|\right|^2\right] \end{aligned} \tag{5.27}$$

where $\mathbf{\Lambda}_B = \mathbf{diag}\left(b_{\breve{\mathbf{c}}}(1), b_{\breve{\mathbf{c}}}\left(e^{j\frac{2\pi}{N}}\right), ..., b_{\breve{\mathbf{c}}}\left(e^{j\frac{2\pi(N-1)}{N}}\right)\right)$ with $b_{\breve{\mathbf{c}}}(x) = \frac{\sum_{i=0}^{N-1} e_i x^i}{\sum_{i=0}^{N-1} \breve{c}_i x^i} = \frac{\sum_{i=0}^{N-1} e_i x^i}{\sum_{i=0}^{N-1} (c_i+e_i) x^i}$. Equation (5.27) further gives

$$\begin{aligned} & E\left[||\mathbf{x}-\hat{\mathbf{x}}||^2\right] \\ = \; & E\left[\left|\left|\mathbf{H}^{-1}\mathbf{F}^H\mathbf{\Lambda}_b\mathbf{FHx}-\mathbf{H}^{-1}\mathbf{F}^{\mathbf{H}}\curlywedge^{-1}\mathbf{Fn}\right|\right|^2\right] \\ = \; & \varepsilon_x^2 \cdot tr\left[\mathbf{D}^{-1}\mathbf{\Lambda}_B\mathbf{D}\mathbf{D}^H\mathbf{\Lambda}_B^H\left(\mathbf{D}^{-1}\right)^H\right] \\ & +\sigma^2 \cdot tr\left[\mathbf{H}^{-1}\left(\mathbf{F}^H\left(\curlywedge\curlywedge^H\right)^{-1}\mathbf{F}\right)\left(\mathbf{H}^{-1}\right)^H\right] \\ = \; & \varepsilon_x^2 \cdot \sum_{i=0}^{N-1}\sum_{k=0}^{N-1}\left|\left[\mathbf{D}^{-1}\mathbf{\Lambda}_B\mathbf{D}\right]_{ik}\right|^2 \\ & +\sigma^2 \cdot \sum_{i=0}^{N-1}\left\{\left|f_{\breve{\mathbf{c}}}\left(e^{j\frac{2\pi}{N}i}\right)\right|^{-2}\right\}\sum_{k=0}^{N-1}\left\{|h_k|^{-2}\right\} \end{aligned} \tag{5.28}$$

where $tr(\cdot)$ denotes the trace of the matrix; $\mathbf{D}$ is defined as $\mathbf{D} = \mathbf{FH}$.

Interference canceler In light of (5.1) and (5.26), the MSE is given by

$$\begin{aligned} & E\left[||\mathbf{x}-\hat{\mathbf{x}}||^2\right] \\ = \; & E\left[\left|\left|\mathbf{x}-\mathbf{H}^{-1}\breve{c}_0^{-1}\left[\mathbf{W}\mathbf{c}+\mathbf{n}-\mathbf{W}^1\breve{\mathbf{c}}^1\right]\right|\right|^2\right] \\ = \; & E\left[\left|\left|\breve{c}_0^{-1}\mathbf{H}^{-1}\mathbf{E}\mathbf{H}\mathbf{x}-\breve{c}_0^{-1}\mathbf{H}^{-1}\mathbf{n}\right|\right|^2\right] \\ = \; & \varepsilon_x\left|\breve{c}_0^{-1}\right|^2\cdot tr\left[\mathbf{H}^{-1}\mathbf{E}\mathbf{H}\mathbf{H}^H\mathbf{E}\left(\mathbf{H}^{-1}\right)^H\right] \\ & +\left|\breve{c}_0^{-1}\right|^2\sigma^2\cdot tr\left[\mathbf{H}^{-1}\left(\mathbf{H}^{-1}\right)^H\right] \end{aligned} \tag{5.29}$$

where ε_x is the signal energy as defined in Chapter 1; matrix $\mathbf{E}$ is a circulant matrix determined by the error vector $\mathbf{e}$, and has the same form of (5.21). Following the diagonalization method described in (5.23), $\mathbf{E}$ is given by

$$\mathbf{E}=\mathbf{F}^H\mathbf{\Lambda}_E\mathbf{F} \tag{5.30}$$

which, when substituted into (5.29), yields

$$\begin{aligned} & E\left[||\mathbf{x}-\hat{\mathbf{x}}||^2\right] \\ = \; & \varepsilon_x\left|\breve{c}_0^{-1}\right|^2\cdot tr\left[\mathbf{D}^{-1}\mathbf{\Lambda}_E\mathbf{D}\mathbf{D}^H\mathbf{\Lambda}_E^H\left(\mathbf{D}^{-1}\right)^H\right] \\ & +\sigma^2\left|\breve{c}_0^{-1}\right|^2\cdot tr\left[\mathbf{H}^{-1}\left(\mathbf{H}^{-1}\right)^H\right] \\ = \; & \varepsilon_x\left|\breve{c}_0^{-1}\right|^2\cdot\sum_{i=0}^{N-1}\sum_{k=0}^{N-1}\left|\left[\mathbf{D}^{-1}\mathbf{\Lambda}_E\mathbf{D}\right]_{ik}\right|^2 \\ & +\sigma^2\left|\breve{c}_0^{-1}\right|^2\cdot\sum_{k=0}^{N-1}\left\{|h_k|^{-2}\right\} \end{aligned} \tag{5.31}$$

Note that when CPE accounts for the majority part of phase noise power, or, $\frac{|c_0|^2}{\sum_{i=0}^{N-1}|c_i|^2}\rightarrow 1$, it can be readily seen that both MSEs in (5.31) and (5.28) can be approximated as

$$\begin{aligned} E\left[||\mathbf{x}-\hat{\mathbf{x}}||^2\right] &= \sigma_x^2\cdot\sum_{i=0}^{N-1}\sum_{k=0}^{N-1}\left|\left[\mathbf{D}^{-1}\mathbf{\Lambda}_E\mathbf{D}\right]_{ik}\right|^2 \\ &+\sigma^2\cdot\sum_{k=0}^{N-1}\left\{|h_k|^{-2}\right\} \end{aligned} \tag{5.32}$$

(5.28) holds for small to median phase noise level with its variance less than 10^{-1}, which are the working range of these two estimation approaches. Therefore, two mitigation techniques yield the same performance in practice with the same estimation result. On the other hand, we notice that interference canceler is more cost effective than decorrelator when complexity is of concern since decorrelator requires the inversion of matrix.

5.4 Numerical Results

The proposed approaches are evaluated in this section for Rayleigh fading channels by Monte Carlo trials. The OFDM data are constructed based on the IEEE 802.11a standard. The preamble of each data block is specifically for channel estimation. Channel coding is not used in our simulations since we focus on the symbol error rate (SER) of an uncoded OFDM system. 16QAM modulation is always the case if not specifically indicated in the simulation. The length of cyclic prefix is assumed larger than channel delay spread throughout the simulations. The simulation parameters are summarized in Table 5.1.

Table 5.1 Simulation parameters for generalized phase noise mitigation approaches

Parameter	Value
bandwidth for each user	20 MHz
number of subcarriers	$N = 64$
number of pilots	$N_P = 4$
Modulation method	16QAM

Fig. 5.1-5.2 demonstrate the computational complexity needed for two phase noise estimation methods, MLE and LMMSE. We see from this figure that, in order to get the best performance from LMMSE, we need to trade computational complexity

for that. As a result, LMMSE has the highest complexity among all schemes, even a little worse than the conventional SCIC scheme give in [36].

Fig. 5.3 shows that when using the MLE method, what are the values of the estimated CPE and ICI in comparison to the actual values. It clearly demonstrates that phase noise mitigation is applicable only if phase noise variance is less than 10^{-1}. For large phase noise with its variance above 10^{-1}, mitigation may not be effective since the estimation errors become large. Note that the MLE method has the same performance as SCIC, therefore their estimation results have the same accuracy.

Fig. 5.4-5.5 show the SER performance of the generalized MLE and LMMSE approaches with phase noise variance equal to 10^{-2}. It is shown that the proposed approaches outperform conventional CPEC technique for both decorrelator and interference canceler cases. For the LMMSE approach, a performance gain of 1-2 dB is observed in comparison to the MLE approach. This is straightforward as the LMMSE uses the phase noise statistics to minimize the overall estimation errors. Also, comparing Fig. 5.4 with Fig. 5.5, we can find that there is no obvious difference between decorrelator and interference canceler. This fits our previous theoretical analysis with respect to these two mitigation methods.

Fig. 5.6 illustrates the MSEs for both MLE and LMMSE using decorrelator. Note that the similar curves are expected with interference canceler. Therefore, no extra figures were drawn for the case of interference canceler. This figure suggests the better performance with LMMSE approach as expected.

5.5 Conclusions

Based on the same parametric model of OFDM signals for SCIC method, a received frequency domain subcarrier signal is expressed as exactly the sum of all subcarrier signals weighted by a parameter vector. In terms of this, we have proposed two generalized approaches, using both the maximum likelihood (ML) and linear minimum

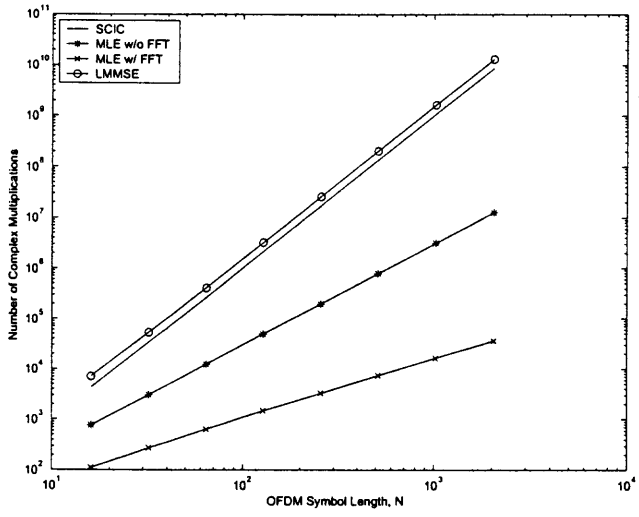

Figure 5.1 Complex multiplications needed for MLE and LMMSE

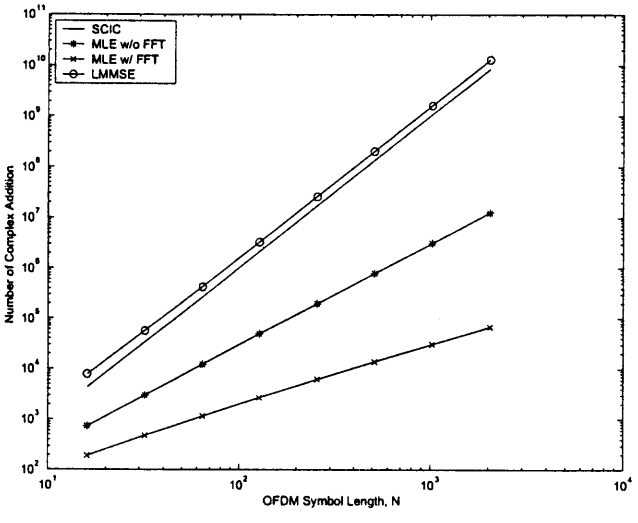

Figure 5.2 Complex additions needed for MLE and LMMSE

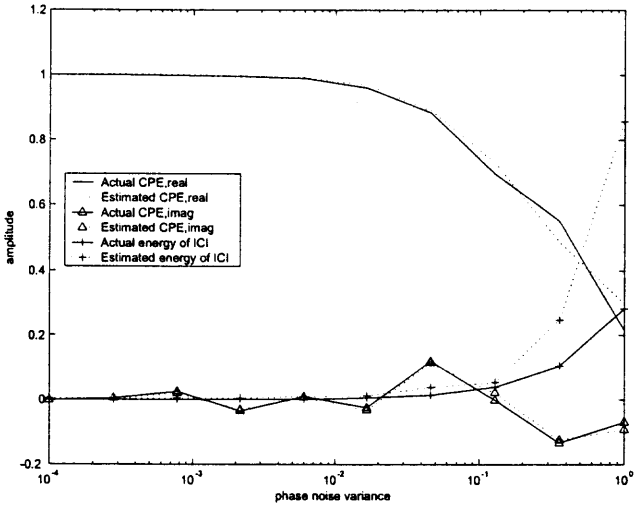

Figure 5.3 Estimated CPE and ICI versus their actual values with MLE approach

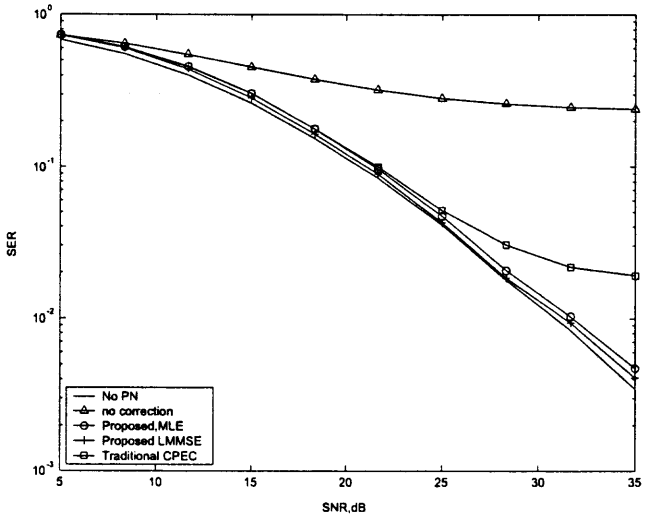

Figure 5.4 The SER performance of the proposed approaches using decorrelator versus CPEC, with phase noise variance equal to 10^{-2}, and the number of pilots equal to 4.

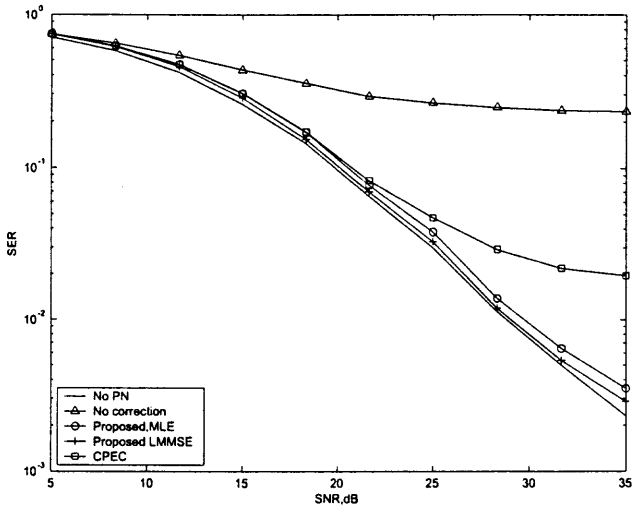

Figure 5.5 The SER performance of the proposed approaches using interference canceler versus CPEC, with phase noise variance equal to 10^{-2}, and the number of pilots equal to 4.

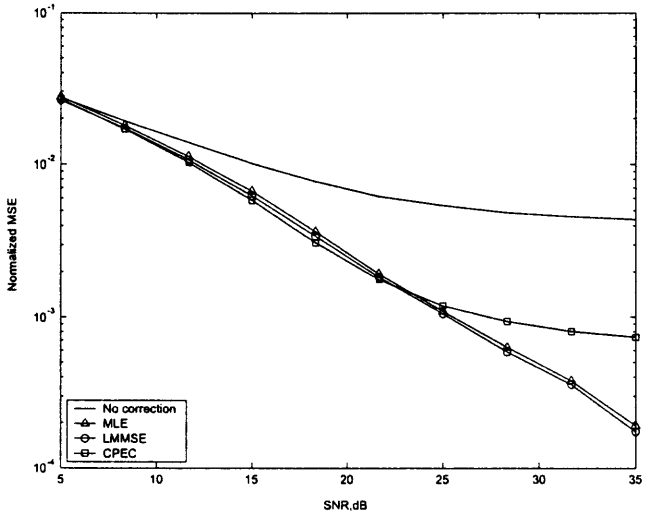

Figure 5.6 Mean square error of LMMSE and MLE, using decorrelator.

mean square error (LMMSE) techniques, to estimate this weighting vector. Phase noise is therefore mitigated based on the subsequent estimates. Some mathematical algorithm has also been proposed which effectively reduces the computational complexity of these methods. It shows that conventional methods can be readily derived from our approaches with some approximation or orthogonal transform. In this regard, the conventional methods in the literature are just special cases of what we have proposed in the paper. The data structure of this new model has further been analyzed and the corresponding solutions have been provided to reduce computational complexity for implementation purpose. Furthermore, it is indicated that we could use several methods, including decorrelator and interference canceler, to mitigate phase noise after the estimation results are obtained, and we could expect the same performance from these two methods while interference canceler is more computationally efficient.

In order to analyze the difference between these estimation and mitigation methods, theoretical analysis has been provided which was further verified by the computer simulations. It is shown that the proposed approaches use a more general and accurate model to estimate and mitigate phase noise. Therefore, better results are expected with these approaches in comparison to conventional ones.

CHAPTER 6

PHASE NOISE MITIGATION FOR MIMO-OFDM

6.1 Introduction

Multiple Input Multiple Output (MIMO) technique has emerged as one of the most significant technical breakthroughs in wireless communications [38] [39] [40]. One key feature of MIMO systems, with multiple transmit and receive antennas, is the ability to turn multipath propagation, which was conventionally detrimental to wireless transmission, into a benefit for the user. MIMO systems can offer, through space diversity [41] [42] [43] or space multiplexing [44], substantial improvements over conventional systems with respect to either bit error rate (BER) performance or capacity (transmission data rate).

Furthermore, the combined MIMO-OFDM approach has recently raised a lot of interest as it appears to be quite suitable for future wireless broadband networks by taking advantage of both OFDM and MIMO techniques. Therefore, similar to OFDM, MIMO-OFDM might also suffer severe performance degradation from phase noise. Even though various methods have been proposed to mitigate small phase noise, they are specifically designed for single-antenna systems. To the best of the authors' knowledge, there has not been, in the literature, any method proposed for MIMO-OFDM phase noise mitigation. Motivated by this fact, we propose a new scheme to mitigate phase noise for MIMO-OFDM.

The organization of this paper is as follows. In Section 6.2, the OFDM-MIMO system model is introduced. In Section 6.3, we first specify the effects of phase noise on MIMO-OFDM systems, and then propose a new scheme to eliminate the effects of phase noise on MIMO-OFDM. Numerical results are presented in Section 6.4 to illustrate the effectiveness of the proposed scheme. Section 6.5 concludes this paper.

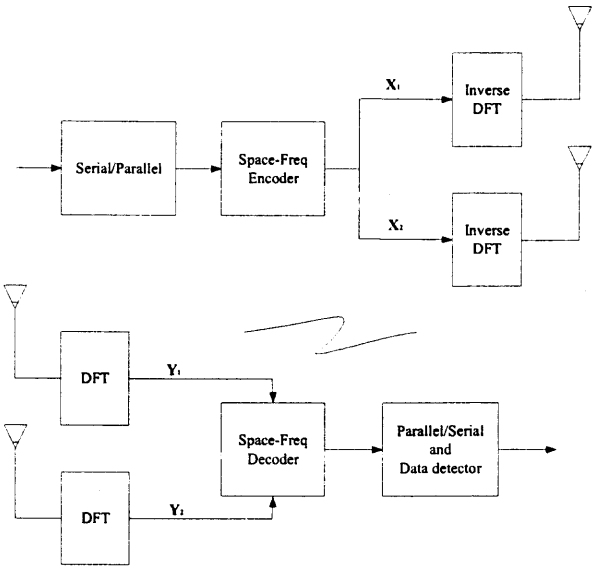

Figure 6.1 Block diagram of the MIMO-OFDM system with 2 Tx antennas and 2 Rx antennas.

6.2 MIMO-OFDM System Model

In a single-user MIMO-OFDM system with M transmit antennas and L receive antennas, data are first space-time/space-frequency coded, and then fed into M inverse DFT units each connected to one transmit antenna. After the insertion of cyclic prefix, data is upconverted and transmitted through multipath fading environment. At the base station, data is received by antenna l ($l = 1, 2, ..., L$) and downconverted. After removing the cyclic prefix and taking length-N DFT, data are forwarded to decoding unit for detection.

A simply transmit diversity scheme was described [41] using orthogonal space-time coding and later was extended into the space-frequency domain for MISO-OFDM with 2×1 ($M = 2, L = 1$) antennas [45]. In this paper, implementing the same space-frequency diversity technique in [45], we consider the case of MIMO-OFDM with 2×2 ($M = 2, L = 2$) antennas transmitting BPSK/QPSK modulated signals. The system diagram is shown in Fig. 6.1.

At the transmitter side, during the rth OFDM symbol period, the incoming data stream is coded into two substreams for two transmit antennas, namely, $\mathbf{X}_m^1$ and $\mathbf{X}_m^2$, with

$$\mathbf{X}_r^1 = \left[x_r(0), -x_r^*(1), ..., x_r(N-2), -x_r^*(N-1)\right]^T \quad (6.1)$$

$$\mathbf{X}_r^2 = \left[x_r(1), x_r^*(0), ..., x_r(N-1), x_r^*(N-2)\right]^T \quad (6.2)$$

which implements the transmit diversity technique in [41] and [45].

At the receiver side, after DFT, we have two received symbols from two receive antennas, namely, $\mathbf{Y}_r^1$ and $\mathbf{Y}_r^2$, respectively, with

$$\mathbf{Y}_r^l = \left[y_r^l(0), y_r^l(1), ..., y_r^l(N-1)\right]^T, \ l = 1, 2 \quad (6.3)$$

where

$$y_r^l(k) = \sum_{m=1}^{2} h_{ml}(k)\mathbf{X}_r^m(k) + n_l(k) \quad (6.4)$$

with $k = 0, 1, ..., N-1$; $\mathbf{X}_r^m(k)$ and $h_{ml}(k)$ denote the $(k+1)$th element of vector $\mathbf{X}_r^m$ as defined in (6.1) and the frequency-domain channel gain between the mth transmit antenna and the lth receiver antenna respectively; $n_l(k)$ is the zero mean AWGN noise with variance σ^2. In order to exploit transmit diversity using combining technique, the space-frequency transmit diversity technique [45] requires that the fading channel between adjacent subcarriers does not change much. This condition holds in cases when channel coherent bandwidth is relatively large compared with transmission bandwidth. Also, fading channel is assumed to be time invariant within an OFDM symbol. The latter means small Doppler shift which is usually the case especially with wide band MIMO-OFDM systems.

Without loss of generality, the kth ($k = 0, 1$) frequency-domain subcarrier signals are studied. The space-frequency decoding of the $(0, 1)$th frequency-domain subcarrier

signals is simply given by maximum ratio combining (MRC) technique. In other words, the decision criteria towards data detection are given by

$$\begin{aligned}\hat{x}_r(0) &= y_1(0)\,h_{11}^*(0) + y_1^*(1)\,h_{21}(0) \\ &\quad + y_2(0)\,h_{12}^*(0) + y_2^*(1)\,h_{22}(0) \\ &= x_r(0)\sum_{m=1}^{2}\sum_{l=1}^{2}|h_{11}(0)|^2 \\ &\quad + h_{11}^*(0)\,n_1(0) + h_{21}(0)\,n_1(1) \\ &\quad + h_{12}^*(0)\,n_2(0) + h_{22}(0)\,n_2(1) \end{aligned} \tag{6.5}$$

$$\begin{aligned}\hat{x}_r(1) &= y_1(0)\,h_{21}^*(0) - y_1^*(1)\,h_{11}(0) \\ &\quad + y_2(0)\,h_{22}^*(0) - y_2^*(1)\,h_{12}(0) \\ &= x_r(1)\sum_{m=1}^{2}\sum_{l=1}^{2}|h_{11}(0)|^2 \\ &\quad + h_{21}^*(0)\,n_1(0) - h_{11}(0)\,n_1(1) \\ &\quad + h_{22}^*(0)\,n_2(0) - h_{12}(0)\,n_2(1) \end{aligned} \tag{6.6}$$

where the space diversities provided by both transmit and receive antennas are exploited by MRC. Note that, although the conclusions of (6.5) and (6.6) hold for $(0,1)$th subcarrier signals, the extension to the $(2n, 2n+1)$th subcarrier signals is quite straightforward (with n ranging from 0 to $\frac{N}{2}-1$). Therefore, we omit the details.

6.3 A New Phase Noise Mitigation Scheme for MIMO-OFDM

6.3.1 The Effects of Phase Noise

The imperfect phase synchronization of both transmitter and receiver oscillators causes random phase noise, which can be described as a continuous Brownian motion process with zero mean and variance $2\pi\beta t$, where β denotes the phase noise linewidth, i.e., frequency spacing between 3-dB points of its Lorentzian power spectral density

function [9] [11]. Phase noise destroys the orthogonalities among subcarrier signals and causes system degradation. In the presence of phase noise, the expression of (6.4) is subsequently modified to

$$\begin{aligned} y_l(k) &= \sum_{m=1}^{2} c(0)h_{ml}(k)\mathbf{X}_r^m(k) + \\ &\quad \sum_{m=1}^{2}\sum_{n=0,n\neq k}^{N-1} c(n-k)h_{ml}(n)\mathbf{X}_r^m(n) + n_l(k) \\ &= \sum_{m=1}^{2} c(0)h_{ml}(k)\mathbf{X}_r^m(k) + \acute{n}_l(k) \end{aligned} \tag{6.7}$$

6.3.2 Phase Noise Mitigation

In order to handle phase noise for MIMO-OFDM systems, a new scheme is developed in this paper to deal with this noise. Considering the high complexity of MIMO systems, the new scheme aims to improve the performance in a simple yet effective way. Note that MIMO-OFDM channel estimation with accurate results have been discussed in the literatures [46] [47], therefore, without loss of generality, channel is assumed known at the receiver.

Assume there are N_p pilot subcarrier signals (the pilot set is termed as S_p) for phase noise mitigation. which are evenly distributed within an OFDM symbol for the better estimation performance. We use a phase noise mitigation criterion to minimize the overall square error between received signals and their true values at these pilot positions, i.e.,

$$\min_{c(0)} \left\| \sum_{k\in S_p}\sum_{l=1}^{2} \left(y_l(k) - \sum_{m=1}^{2} c(0)h_{ml}(k)\mathbf{X}_r^m(k) \right) \right\|^2 \tag{6.8}$$

After some algebraic manipulations, (6.8) gives rise to the solution for $c(0)$, namely

$$\hat{c}(0) = \frac{\sum_{k\in S_p}\sum_{l=1}^{2} y_l(k)\left[\sum_{m=1}^{2} h_{ml}^*(k)\left(\mathbf{X}_r^m(k)\right)^*\right]}{\sum_{k\in S_p}\sum_{l=1}^{2}\left|\left|\sum_{m=1}^{2} h_{ml}(k)\mathbf{X}_r^m(k)\right|\right|^2} \tag{6.9}$$

Note that the estimator of $c(0)$ in (6.9) becomes more accurate with larger number of pilots N_p, but will lower spectral efficiency and make computational complexity higher. In other words, there is a tradeoff between performance and efficiency of computation and spectrum. It will be shown later that, due to space diversity provided in MIMO systems, significant performance gain will be achieved with few pilots for the proposed scheme. This makes this approach quite attractive in practice.

After the estimation of CPE, the decision results in (6.5) and (6.6) are modified to

$$\begin{aligned}\hat{x}_r(0) &= x_r(0)\left|c(0)\right|^2\sum_{m=1}^{2}\sum_{l=1}^{2}\left|h_{11}(0)\right|^2 \\ &\quad +c^*(0)\left[h_{11}^*(0)\,n_1(0)+h_{21}(0)\,n_1(1)\right] \\ &\quad +c^*(0)\left[h_{12}^*(0)\,n_2(0)+h_{22}(0)\,n_2(1)\right]\end{aligned} \tag{6.10}$$

$$\begin{aligned}\hat{x}_r(1) &= x_r(1)\left|c(0)\right|^2\sum_{m=1}^{2}\sum_{l=1}^{2}\left|h_{11}(0)\right|^2 \\ &\quad +c^*(0)\left[h_{21}^*(0)\,n_1(0)-h_{11}(0)\,n_1(1)\right] \\ &\quad +c^*(0)\left[h_{22}^*(0)\,n_2(0)-h_{12}(0)\,n_2(1)\right]\end{aligned} \tag{6.11}$$

6.4 Numerical Results

The proposed scheme is evaluated in this section for Rayleigh fading channels by Monte Carlo trials. The OFDM data block is based on the IEEE 802.11a standard, with 64 subcarriers for each OFDM symbol. We apply the space-frequency diversity

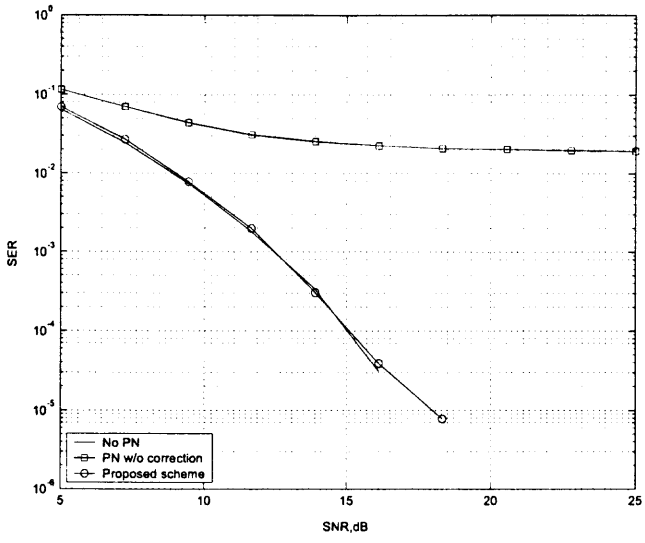

Figure 6.2 SER performance versus SNR, 2 Tx antennas and 2 Rx antennas, with phase noise variance of 10^{-2}, number of pilots N_p equal to 4.

technique in [45] to our simulations, wherein QPSK modulation is used. The length of cyclic prefix is taken to be larger than channel delay spread.

Fig. 6.2 shows the SER performance of the proposed scheme in comparison to no-mitigation and no-phase-noise case. In this figure, even at small phase noise variance level of 10^{-2}, there is an obvious error floor on the SER performance of MIMO-OFDM systems when there is no correction. This error floor makes useless the advantages of space and frequency diversities of MIMO and OFDM techniques, and the performance is not acceptable in all SNRs. On the other hand, the proposed scheme provides, as shown in Fig. 6.2, significant performance gain though with only 4 out of 64 subcarriers as pilots, and the performance stays close to no-phase-noise case.

The working range of the proposed scheme is examined in Fig. 6.3 which depicts the SER performance of the proposed scheme as a function of phase noise level. As we discussed earlier, only small phase noise mitigation is needed as it is very common in practice. Therefore, it is concluded from Fig. 6.3 that, the proposed scheme

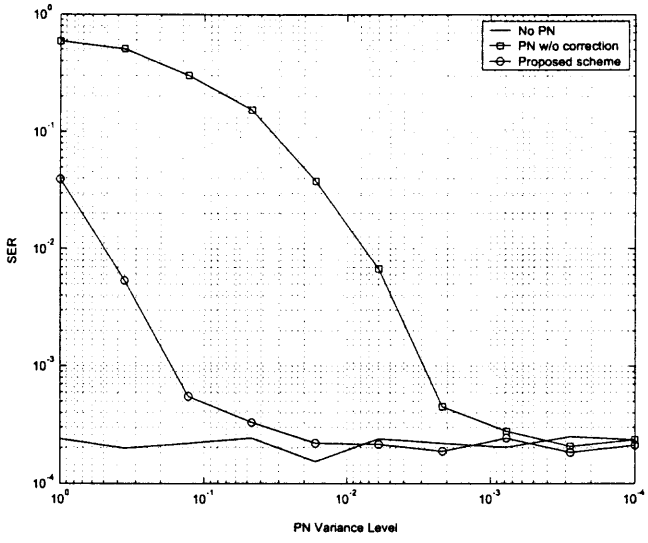

Figure 6.3 SER performance versus phase noise variance levels, 2 Tx antennas and 2 Rx antennas with SNR equal to 20dB, number of pilots N_p equal to 4

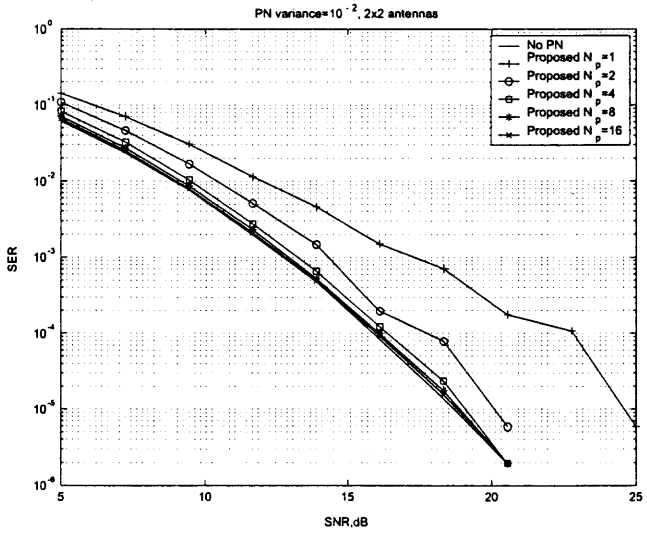

Figure 6.4 SER performance of the proposed scheme when number of pilots changes, with 2 Tx antenna and 2 Rx antennas at the phase noise level of 10^{-2} (phase noise variance)

would be sufficient. It is not difficult to see how worse the performance is without mitigation as phase noise becomes larger. However, the proposed scheme performs well in recovering the phase-noise-corrupted signals with small phase noise variance of 10^{-1} or less. This figure also illustrates that, with phase noise variance of 10^{-3} or less (a very accurate oscillator), sufficient performance of MIMO-OFDM systems is guaranteed with extra mitigation.

The number of pilots needed is also important as it depicts compromise between performance and efficiency. Fig. 6.4 demonstrates how the performance of the proposed scheme is related to number of pilots. We conclude that,

1. Number of pilots $N_p = 1$ suggests performance loss up to 6dB (say, SER=10^{-4}), which, in many case, is certainly intolerable;

2. Increasing number of pilots by only one, i.e., $N_p = 2$, brings 5dB extra performance improvement over the case with $N_p = 1$. This performance improvement is quite necessary for practical systems;

3. Increasing number of pilots to $N_p = 4$, adds up to 2dB performance improvement (say, SER=10^{-4}) over the case with $N_p = 2$;

4. Increasing number of pilots to $N_p = 8$, brings less than 1dB performance improvement over the case with $N_p = 4$;

5. With number of pilots $N_p = 16$ or 32, performance improvement is barely shown over the case with $N_p = 8$. Therefore, using number of pilots greater than 8 is not justified.

In summary, Fig. 6.4 implies that, for a 64-subcarrier OFDM-system with 2 transmit and 2 receive antennas, choosing number of pilot equal to 4 gives sufficient performance with very high spectral efficiency (4/64=6.25% transmission bandwidth for pilots) and relatively low computational complexity.

6.5 Conclusions

MIMO-OFDM, has become attractive for future high rate wireless communications over multipath fading environment since it takes advantages of space-frequency diversity provided by MIMO and OFDM techniques, and exhibits robustness against channel frequency selectivity. However, OFDM is very sensitive to phase noise, as it has been shown in the literature that even small phase noise causes severe performance degradation of OFDM.

Motivated by past work for phase noise mitigation in single-antenna OFDM systems, a new scheme is developed in this paper to deal with phase noise effects on MIMO-OFDM. The proposed scheme provides significant performance gains over a conventional system without such mitigation. Numerical results have shown the effectiveness of the proposed when dealing with phase noise. Furthermore, the proposed scheme requires very small number of pilots to guarantee a sufficient performance gain, and also provides a quite simple structure, which makes it very attractive for practical implementation

CHAPTER 7

SUMMARY

OFDM, which has been very attractive for future high rate wireless communications, is very robust to channel multipath fading effect while providing high transmission data rate with high spectral efficiency. One drawback of OFDM is its sensitivity to phase noise, a random process caused by the fluctuation of the receiver and transmitter oscillators. Phase noise causes leakage of DFT which subsequently destroys the orthogonalities among subcarrier signals, leading to the significant performance degradation.

We have presented the OFDM performance analysis in the presence of phase noise in both single-user and multiple access environments. For single-user case, we provide exact closed-form expression of signal to interference plus noise ratio (SINR), while for multi-user case, a closed-form BER expression has been derived with BPSK modulation. With the understandings of phase noise effects, several methods, such as phase noise suppression (PNS) and simultaneous CPE and ICI correction (SCIC), have also been proposed to mitigate both single and multiple phase noise. Numerical results are provided to demonstrate the effectiveness of the proposed methods. To further extend our work, we proposed two general approaches to estimate phase noise parameters. It proves that the conventional approaches, either in the time domain, or in the frequency domain, can be readily obtained from our new methods with some simple approximation or orthogonal transform. Furthermore, a particular algorithm has been proposed which significantly reduces the computational complexity of the proposed methods. After the phase noise parameters are estimated, we further discuss different implementation methods for phase noise mitigation. Numerical results are also provided to illustrate the effectiveness of the proposed schemes.

Similar to OFDM, an OFDM with multiple antennas, i.e., Multiple Input Multiple Output (MIMO)-OFDM might also suffer severe performance degradation from phase noise, and what have been proposed may not be applicable to MIMO-OFDM. Therefore, we propose a new scheme to mitigate phase noise for MIMO-OFDM. The proposed scheme provides significant performance gains over a conventional system without phase noise mitigation. Numerical results have shown the effectiveness of phase noise mitigation when dealing with phase noise. Furthermore, the proposed scheme requires a very small number of pilots and thus provides high spectrum efficiency. Hence, adequate performance is achieved with a quite simple structure which makes it very attractive for practical implementations.

In summary, we have not only analyzed the performance of OFDM systems in the presence of phase noise, but also proposed the corresponding solutions to the impairments of phase noise on OFDM systems. We have considered OFDM systems with both single-access and multiple access mechanisms. We further consider the phase noise mitigation in multiple-antenna systems, i.e., MIMO-OFDM systems. Some mathematical algorithms have been developed in our dissertation work to reduce the complexities of the proposed methods, the proposed methods successfully achieve outstanding performance with relatively low complexity, and are thus suitable for practical applications.

APPENDIX A

ENERGY OF PHASE NOISE COMPONENTS $C_M(P)$

The derivation of the energy of $c_m(p)$ is quite crucial for the exact SINR expression. From (2.3), the energy of $c_m(p)$ can be written as

$$E\left[|c_m(p)|^2\right] = \frac{1}{N^2} E\left\{\left|\sum_{n=0}^{N-1} e^{j\left[\frac{2\pi pn}{N}+\phi_m(n)\right]}\right|^2\right\} \tag{A.1}$$

In addition, in view of (1.3), the discrete phase noise model is rewritten as

$$\begin{aligned} & \phi_m(n) \\ = & \sum_{i=-N_g}^{m(N+N_g)+n} u(i) \\ = & \sum_{i=-N_g}^{m(N+N_g)-1} u(i) + \sum_{i=0}^{n} u\left[m(N+N_g)+i\right] \\ = & D + \sum_{i=0}^{n} v(i) \end{aligned} \tag{A.2}$$

where $v(n)$ and D are defined by $v(n) = u\left[m(N+N_g)+n\right]$ and $D = \sum_{i=-N_g}^{m(N+N_g)-1} u(i)$, respectively. Substituting (A.2) into (A.1) yields

$$
\begin{aligned}
& E\left[|c_m(p)|^2\right] \\
= & \frac{1}{N^2} E\left\{ \left| \sum_{n=0}^{N-1} e^{j\left[\frac{2\pi pn}{N} + D + \sum_{i=0}^{n} v(i)\right]} \right|^2 \right\} \\
= & \frac{1}{N^2} E\left\{ \left| \sum_{n=0}^{N-1} e^{j\left[\frac{2\pi pn}{N} + \sum_{i=0}^{n} v(i)\right]} \right|^2 \right\} \\
= & \frac{1}{N^2} E\left\{ \sum_{n=0}^{N-1} e^{j\left[\frac{2\pi pn}{N} + \sum_{i=0}^{n} v(i)\right]} \sum_{l=0}^{N-1} e^{-j\left[\frac{2\pi pl}{N} + \sum_{i=0}^{l} v(i)\right]} \right\} \\
= & \frac{1}{N^2} \left\{ E\left\{ \sum_{n=0}^{N-1} \sum_{l=0, l\neq n}^{N-1} e^{j\left[\frac{2\pi p(n-l)}{N} + sgn(n-l) \sum_{i=0}^{|n-l|-1} v(i)\right]} \right\} + N \right\} \\
= & \frac{1}{N^2} \left\{ \sum_{n=0}^{N-1} \sum_{l=0, l\neq n}^{N-1} \left\{ e^{j\frac{2\pi p(n-l)}{N}} E\left[e^{jq_{n,l}}\right] \right\} + N \right\}
\end{aligned}
\tag{A.3}
$$

where $q_{n,l}$ is defined as $sgn(n-l) \sum_{i=0}^{|n-l|-1} v(i)$. We notice that $E\left[|c_m(p)|^2\right]$ is independent of time index m as well as the parameter D of (A.2). Since $\{v(i)\}_{i=0}^{|n-l|-1}$ are mutually independent Gaussian random variables with zero mean and covariance σ_u^2, then $\{sgn(n-l)v(i)\}_{i=0}^{|n-l|}$ are also mutually independent Gaussian random variables with the same mean and variance as $\{v(i)\}_{i=0}^{|n-l|-1}$; and the sum of $|n-l|$ such Gaussian random variables, namely, $q_{n,l} = sgn(n-l) \sum_{i=0}^{|n-l|-1} v(i)$, is Gaussian with the characteristic function given by [19]

$$
\begin{aligned}
& \Psi_v(jx) = E\left[e^{jxq_{n,l}}\right] \\
= & \prod_{i=0}^{|n-l|-1} e^{-x^2\sigma_u^2/2} \\
= & e^{-|n-l|x^2\sigma_u^2/2}
\end{aligned}
\tag{A.4}
$$

Equation (A.4), which gives the solution to the term $E\left[e^{jq_{n,l}}\right]$ in (A.3), therefore gives rise to

$$
\begin{aligned}
& E\left[|c_m(p)|^2\right] \\
= & \frac{1}{N^2}\left\{\sum_{n=0}^{N-1}\sum_{l=0}^{N-1}\left\{e^{j\frac{2\pi p(n-l)}{N}}\Psi_v(jx)|_{x=1}\right\}+N\right\} \\
= & \frac{1}{N^2}\left\{\sum_{n=0}^{N-1}\sum_{l=0}^{N-1}\left\{e^{j\frac{2\pi p(n-l)}{N}}e^{-|n-l|\sigma_u^2/2}\right\}+N\right\}
\end{aligned} \tag{A.5}
$$

Now we have $d_p = e^{j\frac{2\pi p}{N}-\frac{\sigma_u^2}{2}}$ as the function of p. Since $\sigma_u^2 = 2\pi\beta T/N = 2\pi\beta/R$, with $R = N/T$ indicating the transmission data rate, then $d_p = e^{j\frac{2\pi p}{N}-\frac{\pi\beta}{R}}$. Substituting d_p into (A.5) yields

$$
\begin{aligned}
& E\left[|c_m(p)|^2\right] \\
= & \frac{1}{N^2}\left\{\sum_{n=1}^{N-1}\sum_{l=0}^{n-1}d_p^{n-l}+\sum_{n=0}^{N-2}\sum_{l=n+1}^{N-1}\left(d_p^*\right)^{l-n}+N\right\} \\
= & \frac{1}{N^2}\left\{\sum_{n=1}^{N-1}nd_p^{N-n}+\sum_{n=1}^{N-1}n\left(d_p^*\right)^{N-n}+N\right\} \\
= & \frac{1}{N^2}\left\{\sum_{n=1}^{N}nd_p^{N-n}+\sum_{n=1}^{N}n\left(d_p^*\right)^{N-n}-N\right\} \\
= & \frac{1}{N^2}\left\{2\,\mathrm{Re}\left(\sum_{n=1}^{N}nd_p^{N-n}\right)-N\right\}
\end{aligned} \tag{A.6}
$$

where $\mathrm{Re}(\cdot)$ indicates the real part of a complex variable. It can be shown that $\sum_{n=1}^{N}nd_p^{N-n} = \frac{d_p^{N+1}-(N+1)d_p+N}{(d_p-1)^2}$, which, when substituted into (A.6), gives the closed-form expression of the energy of the phase noise components $c_m(p)$, namely

$$
\begin{aligned}
& E\left[|c_m(p)|^2\right] \\
= & \frac{1}{N^2}\left\{2\,\mathrm{Re}\left(\frac{d_p^{N+1}-(N+1)d_p+N}{(d_p-1)^2}\right)-N\right\}
\end{aligned} \tag{A.7}
$$

APPENDIX B

SMALL PHASE NOISE APPROXIMATION

For $p = 0$, d_p equals $e^{-\frac{\sigma_u^2}{2}}$, but $\sigma_u^2 = 2\pi\beta T/N$, hence, the assumption that the phase noise variance is much less than unity, or $2\pi\beta T << 1$, yields

$$e^{-\frac{\sigma_u^2}{2}} \approx \sum_{k=0}^{3} \frac{1}{k!}\left(-\frac{\sigma_u^2}{2}\right)^k \tag{B.1}$$

and

$$e^{-\frac{(N+1)\sigma_u^2}{2}} \approx \sum_{k=0}^{3} \frac{1}{k!}\left(-\frac{(N+1)\sigma_u^2}{2}\right)^k \tag{B.2}$$

Using (B.1) and (B.2), it is shown that (A.7) becomes

$$\begin{aligned}
& E\left[|c_m(0)|^2\right] \\
= \; & \frac{1}{N^2}\left\{2\left[\frac{d_0^{N+1} - (N+1)d_0 + N}{(d_0-1)^2}\right] - N\right\} \\
\approx \; & \frac{1}{N^2}\left\{\frac{\sum_{k=0}^{3}\frac{1}{k!}\left(-\frac{(N+1)\sigma_u^2}{2}\right)^k - \sum_{k=0}^{3}\frac{N+1}{k!}\left(-\frac{\sigma_u^2}{2}\right)^k + N}{(\sum_{k=0}^{3}\frac{1}{k!}\left(-\frac{\sigma_u^2}{2}\right)^k - 1)^2}\right\} - \frac{1}{N} \\
= \; & 1 - \frac{(N+1)(N+2)}{6N}\sigma_u^2
\end{aligned} \tag{B.3}$$

For large subcarrier number N, (B.3) can be further simplified as

$$\begin{aligned}
E\left[|c_m(0)|^2\right] &\approx 1 - \frac{N\sigma_u^2}{6} \\
&= 1 - \frac{\pi\beta T}{3} \\
&= 1 - \frac{\pi\beta N}{3R}
\end{aligned} \tag{B.4}$$

Note that β is defined in [9] as one-sided phase noise linewidth whereas in Section 1.2.2 of our paper β denotes two-sided linewidth. Taking this into consideration, the result of (B.4) is exactly the same as that derived in [9].

For small phase noise β and large number of subcarriers N, by approximating $E\left[|c_m(p)|^2\right]$ by $|c_m(p)|^2$, we obtain

$$\begin{aligned}
&\sum_{p=0}^{N-1} E\left[|c_m(p)|^2\right] \\
\approx\ &\sum_{p=0}^{N-1} |c_m(p)|^2 \\
=\ &\frac{1}{N^2}\sum_{p=0}^{N-1}\sum_{n_1=0}^{N-1}\sum_{n_2=0}^{N-1}\left\{e^{j[\phi_m(n_1)-\phi_m(n_2)]}e^{j\frac{2\pi p(n_1-n_2)}{N}}\right\} \\
=\ &\frac{1}{N^2}\sum_{n_1=0}^{N-1}\sum_{n_2=0}^{N-1}\left\{\frac{1-e^{j2\pi(n_1-n_2)}}{1-e^{j2\pi(n_1-n_2)/N}}e^{j[\phi_m(n_1)-\phi_m(n_2)]}\right\}
\end{aligned} \tag{B.5}$$

Substituting

$$\frac{1-e^{j2\pi(n_1-n_2)}}{1-e^{j2\pi(n_1-n_2)/N}} = N\cdot\delta(n_1-n_2)$$

into (B.5) yields

$$\sum_{p=0}^{N-1} E\left[|c_m(p)|^2\right] = 1 \tag{B.6}$$

It's interesting to conclude that the sum of the energy of $c_m(p)$,due to phase noise, equals unity, which gives exactly the same conclusion drawn in [9]. Finally we get by using (2.2), (B.6) and (B.4) that

$$
\begin{aligned}
& E[|ICI_m(k)|^2] \\
= \; & \varepsilon_x \left\{1 - E\left[|c_m(0)|^2\right]\right\} \\
= \; & \frac{\pi\beta N\varepsilon_x}{3R}
\end{aligned}
\tag{B.7}
$$

APPENDIX C

DIAGONALIZATION OF A SHIFT-BACKWARD MATRIX

It can be readily learned from (5.1) that, the shift-backward circulant matrix $\mathbf{W}$ is uniquely determined by its first row elements

$$\mathbf{W} = \sum_{i=0}^{N-1} a_i \mathbf{\Gamma}_i \tag{C.1}$$

where matrix $\mathbf{\Gamma}_i$ is defined by

$$\mathbf{\Gamma}_i = \begin{pmatrix} 0 & \cdots & 1_{(1,i+1)} & \cdots & 0 \\ \vdots & \diagup & 0 & 0 & \vdots \\ 1_{(i+1,1)} & 0 & \diagup & 0 & 1_{(N-i-1,N)} \\ \vdots & 0 & 0 & \diagup & \vdots \\ 0 & \cdots & 1_{(N,N-i-1)} & \cdots & 0 \end{pmatrix} \tag{C.2}$$

with the (row,column) positions of all non-zero entries marked by the subscripts. Specifically, for $i = 0$, $\mathbf{\Gamma}_i$ becomes the identity matrix, i.e., $\mathbf{\Gamma}_0 = \mathbf{I}$. In view of the structure of matrix $\mathbf{\Gamma}_i$, it is clear that

$$\mathbf{\Gamma}_i = \underbrace{\begin{pmatrix} 0 & \cdots & 0 & 0 & 1 \\ 1 & 0 & \diagdown & \diagdown & 0 \\ 0 & \diagdown & \diagdown & \diagdown & 0 \\ \vdots & \diagdown & \diagdown & 0 & \vdots \\ 0 & \cdots & 0 & 1 & 0 \end{pmatrix}}_{\mathbf{A}}^{i+1} \underbrace{\begin{pmatrix} 0 & \cdots & 0 & 1 \\ \vdots & \diagup & \diagup & 0 \\ 0 & \diagup & \diagup & \vdots \\ 1 & 0 & \cdots & 0 \end{pmatrix}}_{\mathbf{P}} \tag{C.3}$$

Substituting (C.3) into (C.1) yields

$$\mathbf{W} = \left(\sum_{i=0}^{N-1} a_i \mathbf{A}^{i+1} \right) \mathbf{P} \tag{C.4}$$

A is a unitary matrix which indicates the operation of backward shift permutation. It is readily shown that **A** can be diagonalized by

$$\mathbf{A} = \mathbf{F}^H \mathbf{U} \mathbf{F} \tag{C.5}$$

where **F** is the DFT matrix defined by (5.4) and $\mathbf{U} = diag\left(1, e^{j\frac{2\pi}{N}}, ..., e^{j\frac{2\pi(N-1)}{N}}\right)$ .Substituting (C.5) into (C.4) gives rise to

$$\mathbf{W} = \mathbf{F}^H \mathbf{V} \mathbf{F} \mathbf{P} \tag{C.6}$$

With the vector $\mathbf{y} = [y_0, y_1, ..., y_{N-1}]^T$, we define the polynomial function

$$f_{\mathbf{y}}(x) = \sum_{i=0}^{N-1} y_i x^i \tag{C.7}$$

which gives rise to the matrix **V** in (C.6), namely

$$\mathbf{V} = diag\left[g_0, g_1, ..., g_{N-1}\right] \tag{C.8}$$

where $g_k = e^{-j\frac{2\pi}{N}k} f_{\mathbf{w}_0}\left(e^{-j\frac{2\pi}{N}k}\right)$. Equivalently, (C.8) can then be expressed in a matrix form

$$\mathbf{V} = \sqrt{N} diag\left(\mathbf{U}\mathbf{F}\mathbf{w}_0\right) \tag{C.9}$$

BIBLIOGRAPHY

[1] J. Bingham, "Multicarrier modulation for data transmission: an idea for whose time has come," *IEEE Commun. Mag.*, vol. 28, pp. 5 –14, May 1990.

[2] H. Sari, G. Karam, and I. Jeanclaude, "Transmission techniques for digital terrestrial TV broadcasting," *IEEE Commun. Mag.*, vol. 33, pp. 100 –109, Feb. 1995.

[3] ETSI TS 101 475 V1.3.1 (2001-12), *Broadband radio access networks (BRAN); HIPERLAN type 2; physical (PHY) layer.* http://www.etsi.org, Dec. 2001.

[4] IEEE Std 802.11a-1999, *Supplement to IEEE standard for information technology - telecommunications and information exchange between systems - local and metroplitan area networks - specific requirements. Part 11: wireless LAN medium access control (MAC) and physical layer (PHY) specifications: high-speed physcial layer in the 5GHz band.* http://www.ieee.org, Dec. 1999.

[5] P. H. Moose, "A technique for orthogonal frequency division multiplexing frequency offset correction," *IEEE Trans. Commun.*, vol. 42, pp. 2908 –2914, Oct. 1994.

[6] H. Sari, G. Karam, and I. Jeanclaude, "Channel equalization and carrier synchronization in OFDM systems," in *1993 Tirrenia Int. Workshop on Digital Communications*, (Tirrenia, Italy), Sep. 1993.

[7] M. A. Visser and Y. Bar-Ness, "OFDM frequency offset correction using an adaptive decorrelator," in *Proc. PIMRC'98*, Boston, MA, pp. 816 –820, Sep. 1998.

[8] M. A. Visser, P. Zong, and Y. Bar-Ness, "A novel method for blind frequency offset correction in OFDM systems," in *Proc. CISS'32*, Princeton, NJ, pp. 483 –488, Mar. 1998.

[9] T. Pollet, M. Bladel, and M. Moeneclaey, "BER sensitivity of OFDM systems to carrier frequency offset and Wiener phase noise," *IEEE Trans. Commun.*, vol. 43, pp. 191 –193, Feb. 1995.

[10] M. S. El-Tanany, Y. Wu, and L. Hazy, "Analytical modeling and simulation of phase noise interference in OFDM-based digital television terrestrial broadcasting systems," *IEEE Trans. Broadcast.*, vol. 47, pp. 20 –31, Mar. 2001.

[11] L. Tomba, "On the effect of wiener phase noise in OFDM systems," *IEEE Trans. Commun.*, vol. 46, pp. 580 –583, May 1998.

[12] J. Scott, "The effects of phase noise in COFDM," *EBU Technical Review*, Summer 1998.

[13] A. G. Armada and M. Calvo, "Phase noise and sub-carrier spacing effects on the performance of an OFDM communication system," *IEEE Commun. Lett.*, vol. 2, pp. 11 –13, Jan. 1998.

[14] A. G. Armada, "Understanding the effects of phase noise in orthogonal frequency division multiplexing (OFDM)," *IEEE Trans. Broadcast.*, vol. 47, pp. 153 –159, Jun. 2001.

[15] S. Wu and Y. Bar-Ness, "Performance analysis on the effect of phase noise in OFDM systems," in *Proc. ISSSTA'02*, Prague, Czech, pp. 133 –138, Sep. 2002.

[16] G. J. Foschini and G. Vannucci, "Characterizing filtered light waves corrupted by phase noise," *IEEE Trans. Inform. Theory*, vol. 34, pp. 1437 –1448, Nov. 1988.

[17] A. Demir, A. Mehrotra, and J. Roychowdhury, "Phase noise in oscillators: a unifying theory and numerical methods for characterization," *IEEE Trans. Fundamental Theory and Applications.*, vol. 47, pp. 655 –674, May 2000.

[18] K. Nikitopoulos and A. Polydoros, "Compensation schemes for phase noise and residual frequency offset in OFDM systems," in *Proc. GLOBECOM'01*, San Antonio, TX, pp. 331 –333, Nov. 2001.

[19] J. G. Proakis, *Digital Communications.* McGraw-Hill Inc., 3rd ed., 1995.

[20] S. Wu and Y. Bar-Ness, "A phase noise suppression algorithm for OFDM based WLANs," *IEEE Commun. Lett.*, vol. 6, pp. 535 –537, Dec. 2002.

[21] S. Wu and Y. Bar-Ness, "OFDM systems in the presence of phase noise: consequences and solutions," *Submitted to IEEE Trans. Commun.*, Dec. 2002.

[22] L. Tomba and W. A. Krzymien, "Sensitivity of the MC-CDMA access scheme to carrier phase noise and frequency offset," *IEEE Trans. Veh. Technol.*, vol. 48, pp. 1657 –1665, Sep. 1999.

[23] P. Robertson and S. Kaiser, "Analysis of the effects of phase noise in orthogonal frequency division multiplexing (OFDM) systems," in *Proc. ICC'95*, Seattle, WA, pp. 1652 –1657, 1995.

[24] R. A. Casas, S. L. Biracree, and A. E. Youtz, "Time domain phase noise correction for OFDM signals," *IEEE Trans. Broadcast.*, vol. 48, pp. 230 –236, Sep. 2002.

[25] O. Edfors, M. Sandell, J. V. D. Beek, S. K. Wilson, and P. O. Borjesson, "OFDM channel estimation by singular value decomposition," *IEEE Trans. Commun.*, vol. 46, pp. 931 –939, Jul. 1998.

[26] Y. Li, L. J. C. Jr., and N. R. Sollenberger, "Robust channel estimation for OFDM systems with rapid dispersive fading channels," *IEEE Trans. Commun.*, vol. 46, pp. 902 –915, Jul. 1998.

[27] S. C. Kay, *Fundamentals of Statistical Signal Processing: Estimation Theory.* NJ, Prentice Hall, 1993.

[28] T. Kim, Y. Kim, and et al, "Performance of an MC-CDMA system with frequency offsets in correlated fading," in *Proc. ICC'2000*, pp. 1095 –1099, Jun. 2000.

[29] S. Hara and R. Prasad, "Overview of multicarrier CDMA," *IEEE Commun. Mag.*, vol. 35, pp. 126 –133, Dec. 1997.

[30] S. Wu and Y. Bar-Ness, "MC-CDMA performance with multiple phase noise over an uplink correlated rayleigh fading channel," in *IST mobile and wireless communications summit 2003*, Aveiro, Portugal, pp. 180 –183, June 2003.

[31] P. Vandenameele and et al, "A combined OFDM/SDMA approach," *IEEE J. Select. Areas Commun.*, vol. 18, pp. 2312 –2321, Nov. 2002.

[32] C. Garnier and et al, "Performance of an OFDM-SDMA based system in a time-varying multi-path channel," in *Proc. VTC'01 Fall*, Atlantic City, NJ, pp. 1686 –1690, Oct. 2001.

[33] P. Vandenameele and et al, "A novel class of uplink OFDM/SDMA algorithms for WLAN," in *Proc. Globecom'99*, Rio de Janeiro, Brazil, pp. 6 –10, Dec. 1999.

[34] J. Li, K. B. Letaief, R. S. Cheng, and Z. Cao, "Multi-stage low complexity maximum likelihood detection for OFDM/SDMA wireless LANs," in *Proc. ICC'01*, Helsinki, Finland, pp. 1152 –1156, Jun. 2001.

[35] S. Wu and Y. Bar-Ness, "Multiple phase noise correction for OFDM/SDMA," in *Proc. Globecom'03*, San Francisco, CA, pp. 1311 –1315, Dec. 2003.

[36] S. Wu and Y. Bar-Ness, "A new phase noise mitigation method in OFDM systems with simultaneous CPE and ICI correction," in *Proc. MCSS'03*, Oberpfaffenhofen, Germany, Sep. 2003.

[37] P. J. Davis, *Circulant Matrices.* New York, John Wiley and Sons, 1979.

[38] D. Gesbert and et al, "From theory to practice: an overview of MIMO space-time coded wireless systems," *IEEE J. Select. Areas Commun.*, vol. 21, pp. 281 –297, Apr. 2003.

[39] G. L. Stuber and et al, "Broadband MIMO-OFDM wireless communications," *Proceeding of the IEEE*, vol. 92, pp. 271 –294, Feb. 2004.

[40] A. V. Zelst and T. C. W. Schenk, "Implementation of a MIMO OFDM-based wireless LAN system," *IEEE Trans. Signal Processing*, vol. 52, pp. 483 –494, Feb. 2004.

[41] S. Alamouti, "A simple transmitter diversity scheme for wireless communications," *IEEE J. Select. Areas Commun.*, vol. 16, pp. 1451 –1458, Oct. 1998.

[42] V. Tarokh and A. Seshadri, "Space-time codes for high data rate wireless communication: Performance criterion and code construction," *IEEE Trans. Inform. Theory*, vol. 44, pp. 744 –765, March 1998.

[43] V. Tarokh, H. Jafarkhani, and A. R. Calderbank, "Space-time block codes from orthogonal designs," *IEEE Trans. Inform. Theory*, vol. 45, pp. 1456 –1476, July 1999.

[44] G. J. Foschini and M. J. Gans, "On limits of wireless communications in a fading environment when using multiple antennas," *Wireless Personal Communications*, vol. 6, pp. 311 –335, Mar. 1998.

[45] K. F. Lee and D. B. Williams, "A space-frequency transmitter diversity technique for OFDM systems," in *Proc. GLOBECOM'00*, San Francisco, CA, pp. 1473 -ÍC1477, Nov. 2000.

[46] J. H. W. Y. (G.) Li and N. R. Sollenberger, "MIMO-OFDM for wireless communications: signal detection with enhanced channel estimation," *IEEE Trans. Commun.*, vol. 50, pp. 1471 –1477, Sept. 2002.

[47] Y. G. Li and H.-J. Wang, "Channel estimation for MIMO-OFDM wireless communications," in *Proc. PIMRC'03*, Beijing, China, pp. 2891 -ÍC2895, Sept. 2003.